2019

EXAMINING ASPEN EXPANSION FROM BEFORE AND AFTER PRESCRIBED BURNING IN A NATIVE FESCUE GRASSLAND THROUGH GEOSPATIAL TECHNIQUES

Christopher Anderson
Michigan Technological University, clanders@mtu.edu

EXAMINING ASPEN EXPANSION FROM BEFORE AND AFTER PRESCRIBED BURNING IN A NATIVE FESCUE GRASSLAND THROUGH GEOSPATIAL TECHNIQUES

By

Christopher L. Anderson

A THESIS

Submitted in partial fulfillment of the requirements for the degree of

MASTER OF SCIENCE

In Applied Ecology

MICHIGAN TECHNOLOGICAL UNIVERSITY

2019

This thesis has been approved in partial fulfillment of the requirements for the Degree of MASTER OF SCIENCE in Applied Ecology.

School of Forest Resources and Environmental Science

Thesis Co-Advisor:	*Curtis Edson*
Thesis Co-Advisor:	*Cristina Eisenberg*
Committee Member:	*John Vucetich*
School Dean:	*Andrew J.Storer*

Table of Contents

List of figures

List of tables

Acknowledgments

There have been many people who have provided tremendous help, guidance, advice, and support throughout this thesis processes, including but not limited to, the collecting and processing of data and all other related activities. Most of all I would like to thank my advisors, Dr. Curtis Edson and Dr. Cristina Eisenberg, without them this would not have been possible. Curtis has worked with me patiently through my many geospatial questions, is always ready to lend a hand and has bestowed on me what it means to have the mindset of a pioneer in the geospatial field. Cristina has been a steady mentor throughout my academic career. I have trusted her council on many occasions. On many occurrences, she has provided great insight that inspired me into a broader means of ecological thought. Both Cristina and Curtis have provided tremendous support throughout the many vicissitudes of life.

Many groups of people have provided support for this research, including associates of Michigan Technological University; my committee member Dr. John Vucetich, thank you for your support throughout this process and discussing the ecological picture for this project. Mike Hyslop and Dr. Ann Maclean have proved valuable geospatial insight on many occasions. Robert Richard, Alex Rice, and Parth Bhatt have been trusty office mates who are always willing to lend a hand. Many members of the Waterton Lakes National Park Staff have provided ecological and ecosystem insight. Barb Johnston has been a constant support throughout the research and possesses invaluable knowledge of the park's ecosystem; my understanding of the park ecosystem has generally increased just form having a conversation with her. Scott Murphy has provided insight into his knowledge of wildfire and prescribed burning, and Rob Sissons of local plant ecology, particularly grass identification. Dr. Adam Collingwood has been an ever-present and gracious resource for many topics related to Waterton, but especially the geospatial aspects of Waterton. Retired Parks Canada employee Rob Watt has also been a trusted source of local ecosystem knowledge and has added to my overall ecological aptitude. This research would also not be possible without the Waterton Earthwatch field staff and

the many volunteers that assisted with data collection, a special thanks goes to Elliot Fox; he provided support on multiple fronts.

The support of my family and friends has been of tremendous value; I don't know what I what do without them. Thank you to all of them. Most of all I thank my parents, they are wonderful people who have always been there for me and provided tremendous support throughout the thesis process.

List of abbreviations

WLNP: Waterton Lakes National Park.

GNSS: Global navigation satellite system

UAS: Unmanned aerial system

CCE: Crown of the Continent Ecosystem

TEK: Traditional ecological knowledge

GSD: Ground sample distances

UAV: Unmanned aerial vehicle

SPOT: Satellite Pour l'Observation de la Terre

NIR: Near-infrared

RGB: Red, green, blue

GIS: Geographic information system

DSLR: Digital single lens reflex

PCA: Principal components analysis

PPK: Post-processed kinematic

IMU: Inertial measurement unit

GC: Ground control points

RTK: Real Time Kinematic

UTM: Universal Transverse Mercator System

TBC: Trimble Business Center

CHM: Canopy height model

DTM: Digital terrain model

DEM: Digital elevation model

KE: Knowledge Engineer

Abstract

Native fescue (*Fescue* spp.) grasslands of the Intermountain West have become increasingly scarce due to the advent of modern agriculture, the loss of Indigenous people's land management practices, modern wildfire management and the extirpation of bison (*Bison bison bison*). Native grassland is a biodiversity hot-spot, is significant for carbon sequestration, and essential to many species of flora and fauna that occur in the ecosystem. Our study site, on the Rocky Mountain Front in Waterton Lakes National Park, Alberta Canada, consists of 30 discrete aspen stands (*Populous tremuloides*) which are encroaching on this declining shortgrass fescue grassland. Parks Canada is attempting to suppress aspen expansion and improve fescue prairie through ecological restoration by instituting prescribed burns and elk (*Cervus elaphus*) browse. Prescribed burns will decrease woody vegetation through adult aspen stem mortality while stimulating regeneration, which is subsequently browsed by elk. The park has a wolf pack (*Canis lupus*) that preys primarily on the elk, thereby affecting aspen stem recruitment spatially. These dynamics create a natural laboratory for examining the interaction of fire, elk and wolves that impact the aspen/grassland dynamics. We measured the aspen stand structure before and after a prescribed burn set in spring of 2017 to determine the change in aspen stand area from before to after the burn. We measured aspen stands before the prescribed burn during the summer of 2016 via GNSS handheld mapping units. We collected post-burn measurements in summer 2017 via unmanned aerial system (UAS). We also conducted ground measurements for a subset of aspen stands in 2017 to ground-truth the aerial photography data. We used knowledge Engineer (KE) in Erdas Imagine for classifying the UAS imagery and then created polygons in ArcGIS to analyze the data from before and after prescribed burning. We also digitized all aspen stand layers from the UAS imagery through the heads-up digitization technique and used these data to compare the aspen stands from before to after prescribed burning. Aspen stand area did not decline at a statistically significant level for any layers we measured: canopy, regeneration, and shrub expansion before and after prescribed burning. We did see an observational decline in the total aspen canopy area.

1 Introduction

Native grasslands in the Intermountain West are under pressure from multiple sources and have been in decline since the 1800s (Samson and Knopf 1994). We measured the response of aspen (*Populus tremuloides*) in Waterton Lakes National Park, Alberta, Canada (WLNP) before and after a prescribed burn in a native fescue (*Fescue* spp.) grassland. We collected data with a global navigation satellite system (GNSS) receiver before the prescribed burn and collected post-prescribed burn data via unmanned aerial system (UAS) and compared the processed geospatial products for analysis. Our analysis focused on change detection for aspen stand area and stand structure from pre- to post-prescribed burn. We completed post-prescribed burn examination with two types of analyses. We manually digitized aspen stands at stratified class levels from the raster data, which were created from the UAS imagery, and classified aspen stand layers using geospatial software. We compared both methods to the GNSS collected data at the same classes (pre-prescribed burn).

WLNP is in Alberta on the U.S. Canadian border, north of Montana (Figure 1), in a region known as the Crown of the Continent Ecosystem (CCE) of the northern Rocky Mountains. The CCE is one of the most ecologically intact temperate ecosystems in North America. It contains a diverse landscape of mountains, valleys, prairie, forests, alpine meadows, and lakes, and encompasses 2.5 million hectares (ha) of protected land (Pedynowski 2003, Eisenberg et al. 2019). The ecosystem is also home to all mammal species present in the early 1800s, including elk (*Cervus elaphus*), wolves (*Canis lupus*) and grizzly bears (*Ursus arctos*), except for free-ranging plains bison (*Bison bison bison*) and woodland caribou (*Rangifer tarandus caribou*). The study site is a remnant native fescue grassland on the ecotone of the prairie and the Rocky Mountains, which contains discreet trembling aspen stands of varying sizes spread throughout (Levesque 2005). This ecologically important landscape contains much of the remaining native shortgrass fescue prairie in Southwest Alberta and remains intact amongst many biotic and abiotic stressors (Eisenberg et al. 2019). The dominant native grass species in the study site are Parry's oatgrass (*Danthonia parryi*), foothills rough fescue (*Festuca campestris*), Idaho fescue

(*Festuca idahoensis*), bluebunch wheatgrass (*Pseudoroegneria spicata*), and needlegrass (*Nassella* spp.) (Seager et al. 2013, Eisenberg et al. 2019). The 750-ha study site, called by WLNP the "Eskerine Complex," consists of a series of winding slopes, ridgetops, and lowlands that were created as the glaciers melted (Livingstone et al. 2015). The Eskerine Complex also contains shrubs that exist within the aspen and as independent patches far from any aspen. These shrub species, such as serviceberry (*Amelanchier alnifolia*) and cherry (*Prunus spp.*), provide nourishment in the form of berries for bears, songbirds and many other species living in the ecosystem.

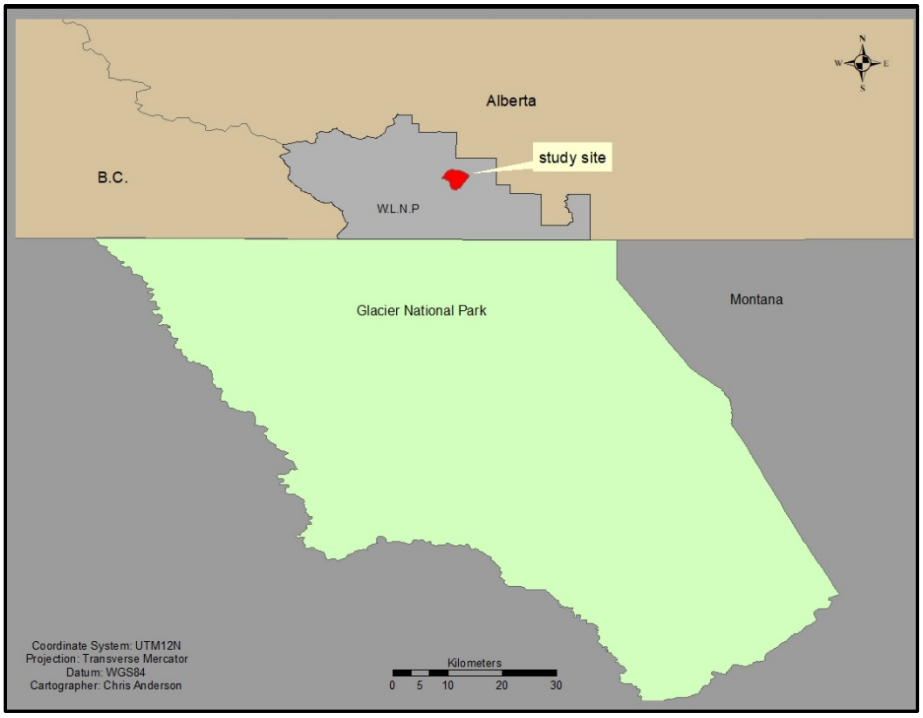

Figure 1. Waterton Lakes National Park and study site location.

The Eskerine Complex is in an elk winter range that contains a high number of elk, estimated to be 1000 animals (Eisenberg et al. 2017). The study area is on the edge of the prairie that was home to vast bison herds, as well as the current inhabitants, badgers (*Taxidea taxus*), ground squirrels (*Urocitellus* spp.), songbirds, avian predators, and many other species. This habitat type, discreet aspen stands within a grassland, is of high conservation priority because it provides an environment that is suitable for many species, including herbaceous plants, shrubs, small mammals and an endangered

butterfly, the half-moon hair streak (*Satyrium semiluna*) (Levesque 2005, Johnston 2018). Indeed, this grassland is so ecologically and culturally valuable, that WLNP is a Biosphere Reserve and a World Heritage Site. The fescue grassland is also a significant climate change buffer, as it sequesters a substantial amount of carbon into its root system, and associated organisms, biomass that also transfer carbon to the ground through decomposition. Temperate grasslands can store as much as 98% of their carbon below ground, which has a slow rate of turnover compared to above ground carbon (Jones and Donnelly 2004).

Southern Alberta grasslands have been in decline since the late 1800s due to the advent of modern agriculture, the loss of wildfire and fire set by Indigenous people, extirpation of wild-free-ranging bison (Samson and Knopf 1994, Romme et al. 2001), and in Southwestern Alberta, related aspen stand expansion. Much of the prairie in Southwestern Alberta was plowed to make way for crops and cattle as European settlements moved west (Simonson and Johnson 2005) to the point that no more than 5% of native North American prairie remains (Knapp et al. 1999). Wildfire and fire set by Indigenous people were historically frequent in the North American prairies (Barrett 1996), but modern land management practices have suppressed the historic fire regime for roughly 100 years (Singer 1979, Levesque 2005). Many processes are dependent upon regular burning in this fire-evolved ecosystem. Fire increases productivity and creates a spatial mosaic of wildlife habitat. Indigenous human communities also historically set fires in this ecosystem regularly to sustain desired conditions for hunting and gathering (Roos et al. 2018, Eisenberg et al. 2019). Indigenous people burned woody vegetation to attract bison by stimulating vigorous grass sprouting and growth.

Bison were a keystone species on the prairie and impacted the aspen/grassland community as well (Campbell et al. 1994). Bison would inhibit the growth of woody vegetation, such as shrubs and aspen, by thrashing stems with their horns and by wallowing and trampling. The bison also maintained the grassland through foraging, and affected species composition through their natural life processes; prairie species arrangement is influenced by bison urine and carrion decomposition (Knapp et al. 1999).

According to pollen and historical records, the American Northern Plains were primarily covered by grass, and aspen became abundant by the early 1930s, after bison and wolf extirpation of the 1880s (Campbell et al. 1994). Aspen generally does not pollinate before they are 10 - 20 years of age (Shepperd 2001), which means that aspen expansion started in the 1860s. Before aspen began expanding its range the species may have been suppressed by the high number of bison on the landscape (Campbell et al. 1994); bison were abundant, numbering in the hundreds of thousands of individuals in our study site (Flores 1991).

During the last century, aspen lost a significant portion of its historical range in the Intermountain West (DeByle and Winokur 1985). Aspen decline is attributed to climate change, agricultural practices, fire exclusion, conifer encroachment, and loss of historical ungulate predators, (Romme et al. 2001, Brown et al. 2006). Amid this decline, aspen remained the tree species with the widest range in North America (Turner et al. 1998, Brown et al. 2006). Currently in WLNP, in contrast with aspen dynamics elsewhere in much of Western North America, aspen is expanding into the fescue grasslands (Kashian et al. 2007, Hogg et al. 2008). Aspen expansion occurs through seed dispersal and vegetative reproduction (root-sprouting from the existing organism, termed "regeneration"). In WLNP vegetative propagation is the noteworthy form of the two methods of reproduction because aspen generally does not produce seed annually, or in the first several years of life (Romme et al. 2001, Kashian et al. 2007). Seed sprouting of aspen has not been observed in this ecosystem despite decades of intensive surveys.

Aspen stands are clonal, typically consisting of a single organism that root-sprouts, and in which all stems are connected through the root system. The organism regenerates suckers within the stand and from the edge of the pre-existing stand through an expanding root system (DeByle and Winokur 1985, Shepperd 2001). Young aspen roots have been known to expand as much as 15 m in 10 weeks (Perala 1980), and the stand will continue to expand until an abiotic or biotic factor blocks the expansion (Romme et al. 2001). Since aspen is a fire-evolved species, there are mixed results when aspen is consumed by fire (Bartos et al. 1994). Aboveground woody biomass is killed, while the organism

responds by growing more stems. Because of the patchy nature of prescribed burns, post-prescribed burn, aspen stands structure ranges from a stand with a few dead stems among many living mature stems, to a stand where all adult stems have succumbed to mortality, and the ground has a dense covering of aspen saplings (Frey et al. 2003).

Species interactions also play a significant role in an aspen stems ability to grow into the canopy. These trophic interactions explain the way energy moves through an ecosystem. There are top-down and bottom-up effects. Bottom-up effects include abiotic factors such as sunlight, moisture, and nutrients that affect the primary productivity of the ecosystem. Top-down effects are initiated by organisms that reside at higher levels of the ecosystem's trophic structure, i.e., an apex predator. They have a direct effect on the level below them, e.g., the apex predator's primary prey species, which causes an indirect impact on the level below it. This trickle-down effect is called a trophic cascade (Paine 1980, Estes et al. 2011). The trophic interactions influencing aspen stand structure in parts of Western North America are the indirect effects of wolf predation of elk on aspen. Wolves prey upon elk, which in turn affects elk density and behavior and how elk use the ecosystem. Elk become more alert (termed "vigilance," the amount of time elk spend with their heads up above their shoulder) when wolves are present compared to when they are not present (Creel and Winnie 2005, Eisenberg et al. 2014) In the absence of a predator, elk are less vigilant and can loiter and feed without the fear of predation. In the presence of wolves elk are more vigilant and avoid areas of high risk for predation, such as aspen stands where it is more difficult to escape predation (Brown et al. 1999, Laundré et al. 2001), and move more frequently, thus reducing aspen browse. This altered feeding behavior of elk causes a change in aspen regeneration, recruitment, and overall stand dynamics, as the altered feeding behavior effects the ability of aspen to grow above the browse height of elk (termed recruitment). Interactions among species affect the way wildlife use the ecosystem (DeByle and Winokur 1985, Eisenberg et al. 2013), as different species prefer different types of habitat.

Parks Canada is executing an ecological restoration plan for the Eskerine Complex that implements prescribed burning and incorporates elk herbivory. *Ecological restoration* is

defined as the process of assisting the recovery of an ecosystem that has been degraded, damaged, or destroyed (Martin 2017). The parks intention is to suppress aspen expansion and improve habitat through natural processes, thus, returning the foothills parkland ecoregion to a condition comparable to its historical state. The park executed prescribed burns in the Eskerine Complex in 2006, 2014 and 2017; and before the Kenow wildfire in 2017, wildfire had not been present in Waterton since 1906 (Barrett 1996, Eisenberg et al. 2017, 2019). Hypothetically, prescribed burns will decrease woody vegetation through adult stem mortality while stimulating aspen regeneration, which is subsequently browsed by elk over the winter season. Elk primarily consume aspen in the winter after the grass (their ideal food) has been foraged and is exhausted (Skovlin et al. 2002). Aspen can provide as much as 60% of an elk's nourishment while they are on their winter range (Hobbs et al. 1981). However, there may be obstacles to the park's ecological restoration plan, in WLNP high consumption of aspen by elk has not been detected via microhystological analysis of elk fecal pellets (Eisenberg and Hibbs 2019, unpublished data). Other studies (Baker 2009) have shown a decrease of aspen browsing by elk when wolves are present. In WLNP, wolves may be causing a complex top-down interaction between themselves elk and aspen that the park did not consider. There is also a possibility that the aspen contain secondary metabolites as a defense compound to deter herbivores from browsing (Lindroth and St. Clair 2013). When elk do feed on aspen they primally eat the apical bud, which can stop the stem from growing into the canopy (DeByle and Winokur 1985). Furthermore, prescribed burning may slow aspen expansion (Frey et al. 2003), as several studies have shown that aspen suckering can decrease after repeated burns. The result is a habitat comprised of more open grassland and smaller aspen stands which vary in age and spatial structure. The stands will contain gaps, openings, and other features such as snags (dead standing mature aspen) and deadfall that provides critical wildlife habitat (DeByle and Winokur 1985, Lee 1998). Aspen stand variation and patch dynamics are exceptionally important for many migratory bird species (Hollenbeck and Ripple 2007).

Fire ecology and trophic cascades in the CCE are the focus of the overarching study that began in 2006, on which our geospatial analysis is based. The broader investigation began as a trophic cascade and fire ecology study completed by Dr. Cristina Eisenberg as part of her Ph.D. dissertation. The study's ecological scope and techniques implemented continue to expand since its inception, and now include Traditional Ecological Knowledge (TEK), and the geospatial components. The research design and sampling for this trophic cascade research were based on traditional forestry methods, encompassing data collected on aspen expansion, the composition and density of the understory and overstory, elk browsing of aspen, and other aspen stand related dynamics such as grass surveys within the aspen and the open grassland. We also measured shrubs (species and proportion of cover and height) in the aspen stands, as shrub response is a significant measure of trophic cascades and fire response. The geospatial analysis was added in 2016 when we mapped the aspen stands in the Eskerine Complex with GNSS; creating a baseline map for the UAS analysis. After the prescribed burn in 2017, we collected UAS imagery for the entire study area, and mapping data on a subset of stands with the GNSS to ground-truth the UAS data.

All forms of data collection are currently providing information to answer our study questions and to assist WLNP management in their rangeland management (ecological restoration) decision-making process. Specifically, we want to know, is the combination of prescribed burning and elk browse decreasing woody vegetation (adult aspen and shrubs) and increasing grassland area?

Related Questions

- Is aspen recruitment decreasing?
- Is there any change in aspen stand area from before to after prescribed burning (Is aspen stand area decreasing)?
- Has prescribed burning affected the structure of the aspen stand?
- How well can we define the edge of each aspen stand via UAS?

We applied a combination of techniques (GNSS and UAS) to answer the area and geospatial questions. In researching if, or to what extent, the area of each aspen stand changed post-prescribed burn, we stratified the aspen stands on three levels: canopy, regeneration, and shrub avulsion. We defined the *canopy layer* as all stems that recruited into the canopy, in this case, all aspen that were out of an elk's reach (≥ 2.5 m) (White et al. 2003, Seager et al. 2013). We defined the *regeneration layer* as the outer extent of all understory aspen (< 2.5 m) within a specific stand that existed between the canopy and the outer edge of the regenerating aspen. We defined the *shrub avulsion layer* as the extent to which the shrubs expanded outward from the aspen stand. After we completed the data processing, we compared the area of pre-prescribed burn measurements to post-prescribed burn measurements to measure aspen stand expansion and analyze UAS data for accuracy.

1.1 Geospatial Background

The collection of ecological data through remote sensing and the resulting classification of land cover are important components of natural resource management (Thompson et al. 2007, Oumer et al. 2017). Remote sensing is the collection of data on an object without contacting the object (Lillesand et al. 2015). Basic examples of remote sensing are pictures taken with any camera or just making a visual observation without contacting the object that is observed. The critical components of this data acquisition, sensors, cameras, robotics, and post-processing software, have advanced to the point where remote sensing is a capable platform for natural resource mapping, and in some cases species determination (Laliberte et al. 2011, Gini et al. 2014). The data produced from remotely sensed data contribute to available environmental inventory and gives managers another means in their decision-making process. The early forms of remote sensing began with hot air balloons and kites before airplanes were utilized (Wich and Koh 2018). Satellite-based remote sensing data originated from the Landsat systems. Landsat 1 was the original earth view satellite to collect imagery, launched on July 23, 1972, and remained in operation through January 1978. Landsat 8, launched in 2013, is the most recent Landsat satellite and its imagery is the most widely used of the seven Landsat

generations to orbit the earth, Landsat 6 failed to launch. The original Landsat systems, and Satellite Pour l'Observation de la Terre (SPOT), an early French earth view satellite, produce imagery with spatial resolutions of 5 – 79 m. The more advanced generations of remote sensing satellites, GeoEye and WorldView produce imagery with spatial resolutions of 0.5 to 1 m. These advanced technologies produce imagery that rivals traditional airplane photography of 0.1 to 0.5 m (Whitehead and Hugenholtz 2014) and are expected to improve.

The use of the earth view platform is extensive and well documented within several forestry applications such as deforestation, fire ecology (Pope et al. 2015), and conservation management (Tang et al. 2010). In general, satellite-based imagery that is highly accessible has a relatively low spatial resolution, with ground sample distances (GSD) of 10 - 30 m, depending on what spectral band the researcher is accessing. The Imagery is also limited by several factors that are out of the investigator's control, such as, cloud cover, and timing of data collection for local phenology. This lack of timely data collection on the area of interest can cause a significant problem when data is needed on a fine spatial scale; the necessary satellite imagery might not be available (Tang and Shao 2015). The low spatial resolution of the imagery also presents obstacles, such as linking large scale remote sensing data to fine-scale ground data (Kerr and Ostrovsky 2003). The use of a human-piloted aircraft is more efficient as it can be flown on demand, but is limited by operational costs, such as fuel, pilot, maintenance, and the scheduling of airtime; that can become a hindrance rather quickly (Tang and Shao 2015).

The UAS is an alternative for collecting data for monitoring and management of natural resources in a more cost-effective way. The terms UAS, UAV (unmanned aerial vehicle), remotely piloted aircraft (RPA) and drone, all have specific associations, UAV and drone refer to the aerial vehicle component, but are generally used synonymously. A UAS is comprised of an aircraft (commonly called a drone) without a pilot on board, a controller that allows the pilot to communicate with the aircraft, a sensor, and in some cases a launching platform. The UAS is an environmental monitoring tool, which may be applied to ecological restoration. After the initial equipment purchase, data collection via UAS

has a low operational cost with flexibility in both spatial and temporal resolution. Another advantage is a lower risk of injury to the field crew. Operating a UAS is relatively easy by a small crew (it is possible to operate with one person) over a relatively short period, and many landscape obstacles are easily avoided (Zhang et al. 2016). A battery operated UAS has no fuel costs but is limited by the researcher's time availability, access to equipment, battery life, and flight restrictions. UAS flights can be repeated as many times as needed or are feasible for a specific project. The UAS can also survey a more extensive area more rapidly than a field crew, and access study sites that are problematic for any other remote sensing tool to enter (Anderson and Gaston 2013). The digital images are also saved for perpetuity, essentially freezing the moment of data collection in time.

The UAS is a new technology that is expanding rapidly, as uses are continually being experimented with and developed. The systems currently available can produce imagery with a spatial resolution higher than one cm, immensely expanding the range of remote sensing possibilities versus satellite systems. UAS sensors are continually being developed to take full advantage of the electromagnetic spectrum. Forest ecology has played an integral role in developing the UAS for data collection. Initial observations focused on the acquisition of data for common forestry measurements such as canopy area, gap locations, and forest area (Koh and Wich 2012). Currently, detection possibilities vary widely; researchers are producing imagery of insect outbreaks, phenological cycles, wildlife poaching activities, active wildfires, and other detailed forestry data (Wulder et al. 2006, Schiffman 2014, Tang and Shao 2015).

Before 2012, there were very few UAS-based remote sensing studies, and they were not well known. Examples of pioneering UAS forest ecology studies include a forest gap study and a conservation project that utilized short flight time intervals for identifying illegal crop plantings. Investigators in the gap study used 2.5 cm GSD (visible spectrum) imagery to identify one-meter square gaps at two locations, about 1000 m apart, in a selectively logged German forest. They were then able to enter the forest and asses the gaps for bio-diversity (Getzin et al. 2012). An example of spatially timed data (on

demand) collection is demonstrated in a Sumatran project which pioneered the use of drones for conservation and biodiversity studies; Koh and Wich (2012) named their UAS "The Conservation Drone." The drone imagery had a 10 cm GSD and was used to survey preservation land for the detection of illegal land use. The images revealed illegal crops of maize and palm oil in a nature reserve. After detection, they referenced the images with Google Earth and directed rangers to the area. The project also used the drone to detect the presence of wildlife such as elephants and orangutans, demonstrating UAS in wildlife assessment applications.

Contrasting satellite and UAS imagery with georeferenced ground data was a necessary step in developing the UAS technology for data collection, as the process substantiates the data collection platform. Spence and Mengistu (2016) Used four fence posts to georeference images collected for a project focused on identifying an intermittent stream. The resolution of the UAS imagery is 2 cm, and post locations are known from a previous study. The researchers obtained satellite imagery via the 2014 SPOT-5 satellite with 10 m resolution (Spence and Mengistu 2016). The team collected 39 GPS locations for native grasses and aspen stands along the intermittent stream to ground-truth the data. These locations were used to compare the actual stream bed with what is identified as a stream bed from the photos. Both supervised, and unsupervised classification procedures could not adequately identify an intermittent stream in the SPOT-5 imagery. The stream was consistently categorized as grasses or trees, presumably because the area was wet and due to averaging of the vegetation and water pixels, it was classified as vegetation. The team located the stream in the UAS imagery with a very high success rate. The differing successes were attributed to the narrowness of the channel, which resulted in consistent misclassification of the stream as grassland and dry upland trees on the SPOT-5 imagery (Spence and Mengistu 2016). This intermittent stream location study exemplifies how data collected with a UAS can be more accurate and precise compared to satellite-derived imagery due to spatial resolution and is more robust when fine-scale information is needed.

The next step in UAS-based research development was to narrow the scope of the investigation conducted; as study designs on a finer scale are vital for gaining knowledge as to the extent of what research can be conducted (Tang and Shao 2015). A way to complete this task is to conduct comparative studies based on imagery that is substantiated with data collected in the field via GNSS. Michez et al. 2016 conducted a study locating invasive species in a riparian zone. Data collection took place when the species of interest were in bloom; therefore phenology aided with identification. The researchers created a map of the study area that identified the locations of three species from the UAS imagery. The team completed an accuracy assessment to confirm the invasive plant's locations identified in the aerial images that produced a satisfactory operational result for one species (92%). A previous study achieved an accuracy of 77% for the same species. (Michez et al. 2016a). They credited the high success rate of this species with the timing of the survey, as its phenology is slightly different from the surrounding plants. The unsatisfactory result for the other two species was also credited to timing as these two invasive plants were growing with similar native varieties and could not be separated spectrally. The unsatisfactory detections had an accuracy below 69%. The study result is also an example of why local phenology is a significant variable to consider when planning image collection.

The viability of instituting UAS data as a primary resource for data collection in long-term studies will be a catalyst in pushing the scientific boundaries of the UAS in the future. Many studies based on traditional field data collection can be challenging to implement on a yearly basis as field crews become exhausted and funds are depleted (Tang and Shao 2015). The UAS is a promising tool to overcome these challenges and adds to the range of conceivable data collection due to its temporal flexibility (Anderson and Gaston 2013). The combination of periodic field surveys with UAS based remote sensing data is predicted to be a robust data collection duo in years to come (Tang and Shao 2015).

1.2 Data Collection Methods Introduction

Our Geospatial data collection methods stem from the trophic cascade methods of the overarching project (Eisenberg et al. 2014). We implemented two forms of geospatial measurements, mapping grade GNSS units and UAS to measure 30 discreet aspen stands that are scattered throughout the 750-ha Eskerine Complex (Figure 2).

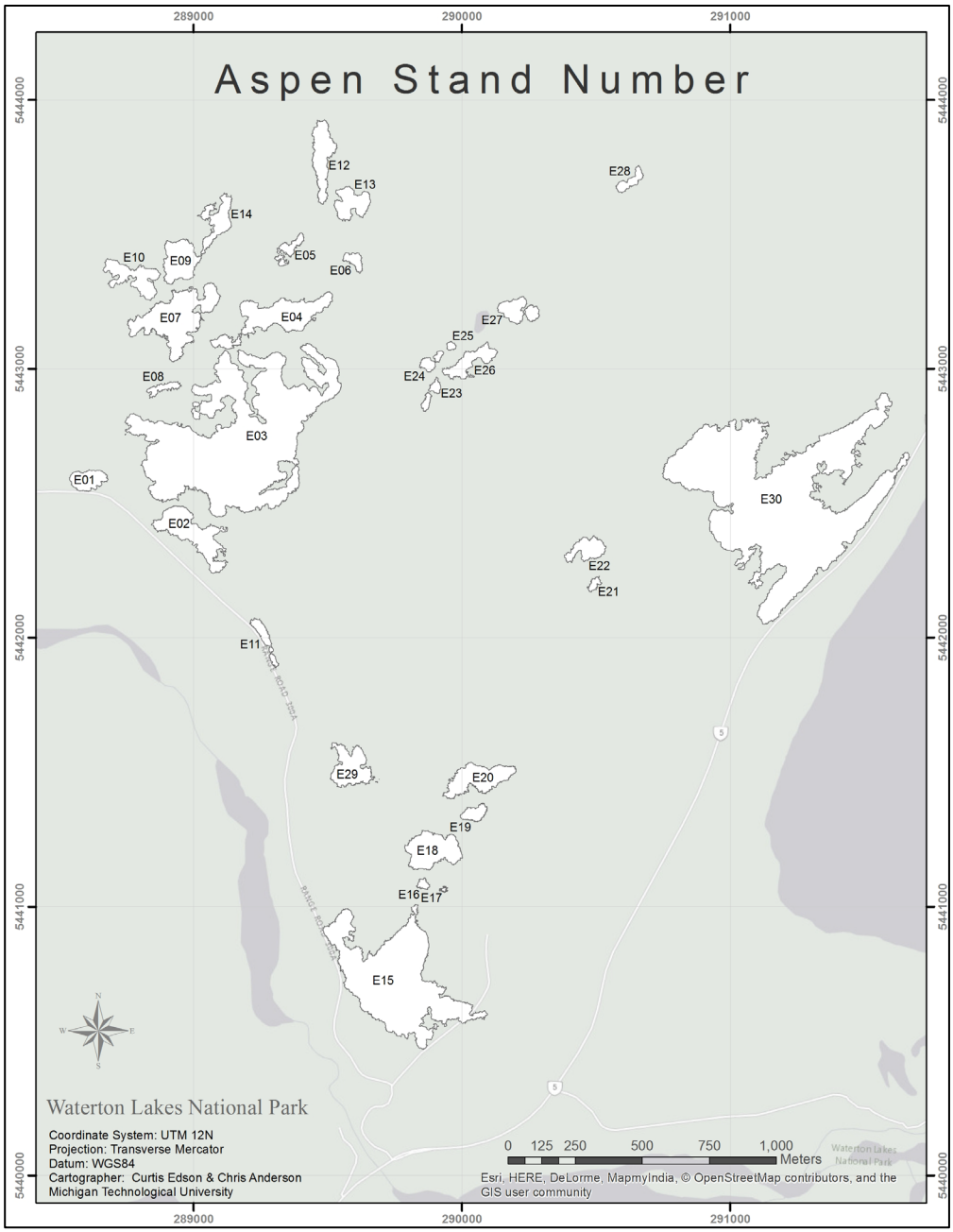

Figure 2. Study site aspen stand locations with stand number.

The aspen stands vary in size from < 1 ha to 30 ha. For the investigation of local aspen stand dynamics, we stratified the aspen stands into three layers: canopy, regeneration, and shrub avulsion. The shrub avulsion is a layer including all shrubs that extend outward from an aspen stand but not including the shrubs within the stand. The analyses focus on assessing the change in aspen stand area on each layer from pre- to post-prescribed burn. These data will provide an opportunity to evaluate aspen growth one-year post-prescribed burn, and provide a baseline for further investigation, as aspen ecological response to fire takes several years to develop (Romme et al. 2011). Shrub avulsion is important because shrubs expand from the edge of the aspen stands, adding to the overall associated stand area that is encroaching on grassland. For management purposes, the shrubs have increased the area of the aspen stand expansion into the grassland.

Our ground-based GNSS mapping began in July of 2016 when we mapped each category (canopy, regeneration, and shrubs) in all 30 aspen stands. WLNP implemented a prescribed burn in the spring of 2017. We began data collection via UAS in July of 2017 to synchronize data collection phonologically with post-prescribed burns peak aspen growth. We collected UAS imagery on the 750-ha study area in near-infrared (NIR) and visible spectrum red, green, blue (RGB), resulting in complete data sets of the Eskerine Complex in both spectrums. We also mapped a subset of randomly chosen aspen stands with ground GNSS in the summer of 2017 to assess the spatial accuracy of the UAS imagery classification.

The global navigation satellite system is a collection of satellite constellations in medium earth orbit of which the locations are known. These constellations include GPS (US), GLONASS (Russia), Beido (China), and Galileo (European Union). The ground-based mapping and the UAS imagery, utilize the GNSS technology. The receiver captures signals from the satellites. This receiver (also called a rover) measures the time it takes for the signal to reach it from several satellites to gain its position. The rover must connect with a minimum of four satellites to calculate its geographic location. Errors can

occur with the signal due to atmospheric conditions, clock bias and other factors (the clocks on the receiver may not be as accurate as of the atomic clock on the satellite) (Lillesand et al. 2015). The errors are corrected through differential corrections by base station(s) comparison. Points collected simultaneously by a precisely located base station receiver are used to correct rover positions either real time (real time kinematic – RTK) or by post-processing. Both the ground-based mapping GNSS and the UAS receivers used in this study can receive GPS, GLONASS, BeiDou, and Galileo satellite signals.

1.2.1 Aspen Stand Mapping Methods (Ground-Based GNSS)

We measured the aspen expansion/contraction of discrete aspen stands into a fescue grassland, in a study area managed with prescribed burning and under browsing pressure by elk. We used these measurements to determine stand area for analysis of stand dynamics in response to prescribed burning and herbivory. Our study site lies in the foothills parkland ecoregion in WLNP, Alberta, and consists of a grassland matrix that contains discrete aspen stands. We defined an *aspen stand* as three or more aspen not more than 20 m from each other. We mapped three vegetation categories: 1) canopy; 2) regeneration; and 3) shrubs. The field crew used a handheld Trimble Geo7x mapping grade GNSS to record the aspen stand polygons.

Mapping the Canopy: The canopy consisted of all aspen stems ≥2.5 m in height (Eisenberg 2014). We chose a minimum canopy height of 2.5 m because this is the height beyond which elk typically can browse the aspen (White et al. 2003). We reference aspen < 2.5 m ht. as saplings. Aspen saplings that have grown to 2.5 m are therefore highly likely to develop into mature aspen. Many stands consisted of several polygons and were therefore collected as a multi-part feature, these features consist of a set of disconnected polygons that share one attribute which is the single stand. When a gap existed between a stem or group of stems, (as defined below) and another aspen, this aspen received a polygon but was a part of the same feature as the discrete stand in which it is located (the polygon limit). We define a *gap* between aspen as a distance ≥ 5 m, as per typical mature aspen stand dynamics (DeByle and Winokur 1985).

We collected the mapping data with a minimum of two technicians: usually with >2 spotters and a GNSS operator using the following procedures. Before the canopy-mapping layer began, the spotter double flagged the recording start with pin flags. The GNSS recorder followed behind the spotter collecting a polygon feature, while the spotter walked the perimeter. The operator paused as decisions and measurements were made based on the canopy and polygon limits. Aspen height measurements were sometimes necessary to determine which height class specific aspen fit in. We walked the perimeter of the polygon until we reached the two pin flags at the start point. When the first polygon was completed, the crew moved on to map all other polygons that needed to be completed within the stand. All polygons within the stand were recorded as the same layer in the GNSS receiver and collected at a rate of one point (node) per second. The polygons belonging to the same stand were joined later in a geographic information system (GIS) as one feature class to calculate statistics. If a single tree was encountered within the stand and separate from other polygons, we collected the tree's canopy dimensions as an individual polygon.

Mapping the regeneration layer: We defined *regeneration* as all aspen sprouts and saplings that have not reached the canopy. We used a threshold of < 2.5 m above the ground to define where the canopy height begins (Eisenberg 2014). Therefore, on a landscape scale and horizontal axis, we defined the regeneration layer as consisting of all immature aspen that existed between the canopy and the outer edge of all aspen in this size class. The same method was used for mapping the regeneration as the canopy class, but we identified aspen regeneration.

Mapping the shrub layer: We measured the perimeter of all shrubs extending from the aspen stands. Shrubs that qualified for mapping were continuous from the edge of the aspen or occurred within 2 m of the aspen. We chose 2 m as our expansion distance because few of our shrubs, such as, snowberry, (*Symphoricarpos* spp.), red osier dogwood (*Cornus sericea*), shrubby cinquefoil (*Dasiphora fruticose*), kinnikinnick (*Arctostaphylos uva-ursi*), possessed rhizomes and therefore did not extend underground from the edge of the aspen stand where they were found (Baker 2009).

We mapped as shrubs any area contiguous to the aspen stand where shrubs constituted an ecologically significant cover type extending away from the stand. We defined significant cover as 25% or more of shrubs, (25% will show the invasion of shrubs into the grasslands). The 25% shrub limit consisted of more than the grassland shrub species alone, which include wild rose (*Rosa* spp.), shrubby cinquefoil, and kinnikinnick. While conducting surveys in the short fescue prairie in the spring/summer of 2016 in Waterton, we found that these species were common in the grassland and were not associated with aspen stand expansion. We completed many of the grass surveys in places > 100 m from aspen. The shrub expansion limit was no more than 20 m from the aspen. Occasionally dominant shrub cover continued into the grassland. At this point, the expanding shrubs have joined with shrub patches that existed independently of aspen stands or have joined the shrubs from a neighboring stand; when this event occurred, we cut off the shrub mapping at the 20 m limit.

While walking the shrub layer, the spotter and the operator walked the outer edge of all aspen in the stand. When dominant shrub cover was spotted that extended outside of the aspens' outer edge, the team walked around them, and then returned to the aspen after the technician mapped the shrubs. This procedure allowed us to measure shrub expansion from the aspen edge in a GIS.

1.2.2 UAS Data Collection Methods

We measured the aspen stands, post-prescribed burn, with a fixed-wing UAS. The UAS imagery had two purposes; to assess the area of each aspen stand post-prescribed burn and assess how accurately the edge of a post-prescribed burned aspen stand could be defined with this method. In addition to these objectives, the UAS imagery allowed us to assess a stands interior for further analysis of stand dynamics, such as gaps in the aspen, which the perimeter GNSS method does not reveal. We measured the study site with a Trimble UX5 and UX5HP aircraft equipped with Sony Cameras. The UAS is comprised of 3 main components, the launcher, the aircraft with the sensor, and the controls. The launcher is an elevated rail and tension cord that acts as a catapult for the aircraft. The

aircraft is the data collection vehicle, and the mission controls software is based in a Trimble tablet that communicates with the aircraft and contains the flight controls and flight block parameters. The parameters (the dimensions and location of each block) were pre-planned using Trimble Aerial Imaging software, a program designed for this specific purpose. The UAS is fully automated from launch to landing, which means that after the researcher designs a flight plan for data collection and programs the aircraft to follow these instructions, the aircraft was flown in a back and forth, overlapping pattern predetermined in the mission planning segment and communicated to the aircraft via FM modem. We programmed the image overlap and side-lap to 80%, which means that each image has an 80% overlap on all four sides, and we used the highest spatial resolution available for each aircraft. We divided the study area into flight blocks based on battery life limitations; the number of flights was equal to the number of blocks.

Advantages of using a UAS with integrated GNSS and inertial measurement unit (IMU) system is the rapid response navigation data such as altitude, acceleration position coordinates and the roll pitch and yaw of the aircraft; these attributes are used for initial approximations of the orientation and associated GNSS coordinates of each image that is collected during processing. The IMU measures force and angular rate using an accelerometer and gyroscope. The UX5 and UX5HP record the aircraft route information, but the GNSS on the UX5HP is more precise and gives a better estimate of the image positions. The precise locations help the image processing software line up the imagery during data processing. The combination of the IMU and GNSS provide an accurate location of each image

Figure 3. Aircraft resting on launcher in the Eskerine Complex.

1.2.2.1 *Aircraft and Camera Specification*

We used the UX5 to capture color imagery (RGB). It was equipped with a 24 MP Sony a5100 digital single lens reflex (DSLR) camera, with a 15 mm lens that allowed data collection as fine as 2 cm spatial resolution. We used the UX5HP to capture NIR. It was equipped with a Trimble GNSS receiver with post-processed kinematic (PPK) technology, 36 MP full frame Sony A7R DSLR camera, with 35 mm lens that allowed data collection with a spatial resolution as high as 1 cm. The camera used for NIR data collection produced more red saturation in the imagery than other RGB and NIR forms of imagery, such as satellite-derived data. Both aircraft had a wingspan of 1 meter, and the flying heights above the takeoff location where we launched from were between 75 and 122 m (Transport Canada and US Federal Aviation Administration flying height restriction).

1.2.2.2 *Mission Planning*

We used Trimble Aerial Imaging software to create a flight plan that consisted of flight blocks for data collection before the imagery collection began (Figure 4). The flight blocks were based on a per flight time capability of the aircraft and divided the entire area

into overlapping blocks. The manufactures specified battery life for each aircraft was different (UX5 – 50 min., UX5HP – 35 min.), but the flight time for each flight also varied depending on wind speed and how far the aircraft needed to fly before entering the flight block. Therefore, each flight block's flight time was less than the specified battery life values for each block (the tablet notified us of the battery life range for each flight, between 0 – 100%). The collection of the RGB data required 20 flight blocks (2 cm resolution), and the NIR data collection required 27 fight blocks (1 cm resolution). We set the direction of travel for each flight based on the manufacturer's recommendation, which was to fly perpendicular to wind direction and the prevailing wind of the study area when possible (generally Southwest to Northeast). We also set Imagery specifications so that each flight pass has an 80% overlap and side lap to ensure the image quality of the final mosaic, and the necessary overlap for 3D modeling of digital elevation models (DEM) and digital surface models (DSM). Hypothetically, the final mosaic will be of a higher quality as the image overlap for each image taken is increased; a larger overlap of adjacent images provides more points for the software to match with one another in each image.

Ground control points: Placing Ground control points (GCPs) in the flight blocks is an important step before data collection takes place, especially for the UX5, which does not have the high-grade PPK GNSS receiver. GCPs are fixed points in the study area with known coordinates used for aero triangulating the UAS imagery during photogrammetric processing; each image collected has a GNSS coordinate associated with it. We used three different types of ground control points, traditional black and white mylar aerial targets, pink flagging tape pinned to the ground in an X or star pattern, or rocks with "easily" distinguishable features. We placed a minimum of three GCPs in each flight block, and where feasible one in each corner for a total of four. When we used three GCPs, we placed one in the center of a block and one at each end. Most of the flight blocks were long and narrow, and generally, their locations were based on take-off and landing locations. The locations were important because we needed to maintain communication with the aircraft. We collected coordinates for each GCP location with a

Trimble R8, Real Time Kinematic (RTK) GNSS receiver in the Universal Transverse Mercator System (UTM) coordinate system zone 12 and WGS84 datum. RTK utilizes a base receiver stationed at a known location and a rover that communicates location corrections through an FM radio link; the two components are connected to the same satellite constellation. We established the local base station location using a Trimble R8S survey grade GNSS receiver in a static location for 5.2 hours and then corrected the locations using the US National Geodetic Survey (NGS) Online Position User Service (OPUS). The OPUS solution used three base stations for correction. We placed the base GNSS receiver at a high point in the study area to increase the FM communication range to the rover. The rover was placed on a tripod and left in place over the center of each GCP for a minimum of two minutes to log its location. We collected 109 ground control points throughout the Eskerine Complex (Figure 5).

Data Collection Flights: The Eskerine Complex is a 750 ha roadless area with very few access points. There are roads on two sides which we used to access three areas for suitable launching and landing of the aircraft. A suitable mission control site needs to have a launch area that is clear of trees (vertical obstacles), has a clear line of sight to the aircraft throughout the flight, at or above the mission's high point, a landing area that is ~ 100 by 50 m and clear of debris as the aircraft belly lands. Three sites were necessary for the study since it was not possible for the UAS to collect data for the entire study area from one location due to accessibility, line of sight, and FM communication. Furthermore, because the study area is in Canada, we are subject to Transportation Canada UAS rules and restrictions which do not allow the aircraft to pass above vehicle traffic, or any person who is not a member of the project. Due to these stipulations, we collected data for blocks adjacent to roads shortly after sunrise when vehicle traffic was least likely. We attempted to fly all interior blocks when sunlight was overhead to avoid shadows in the imagery, but due to time constraints, we flew several at low light.

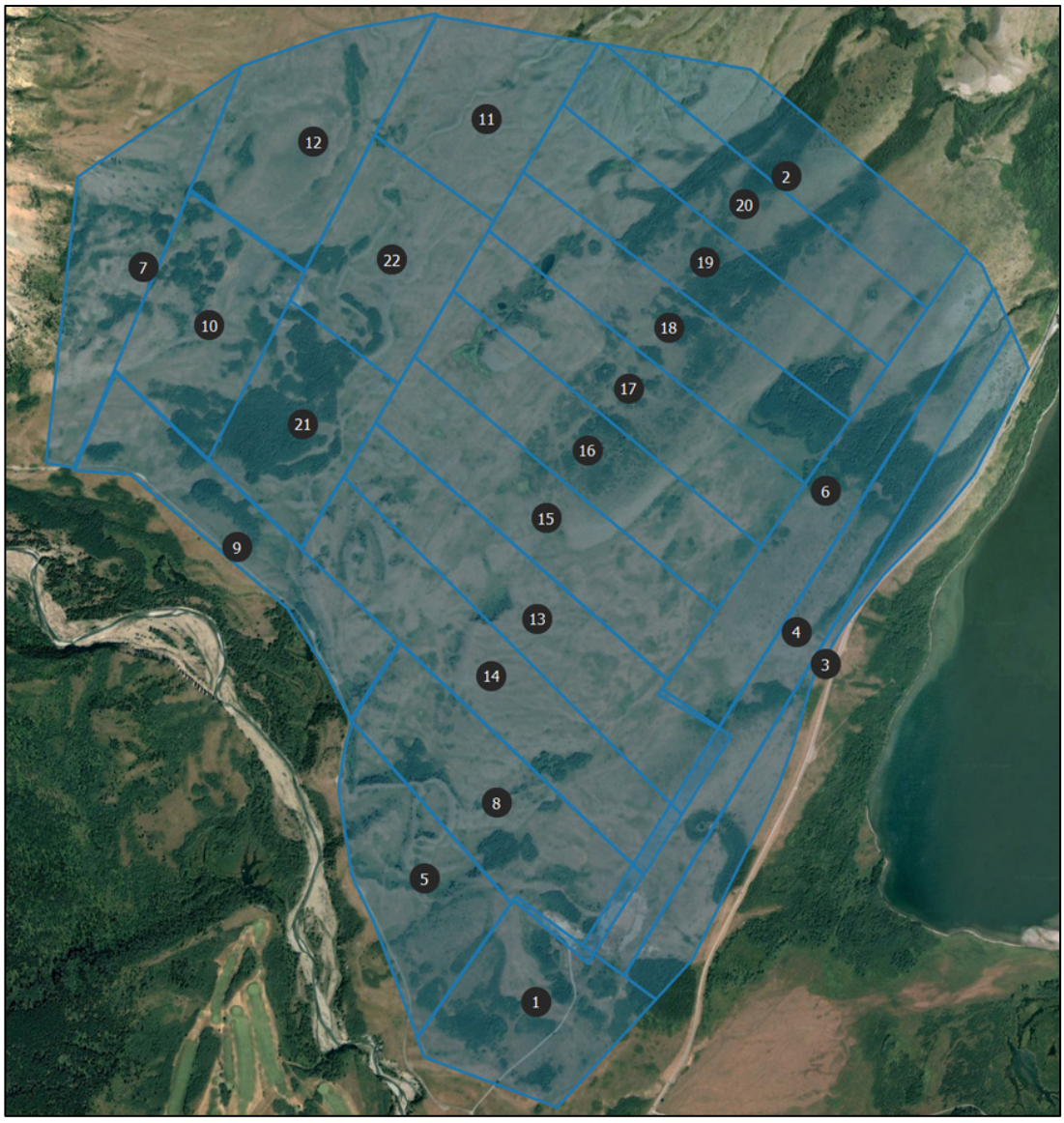

Figure 4. The flight blocks for the UX5, RGB flights. Each numbered block receives a flight

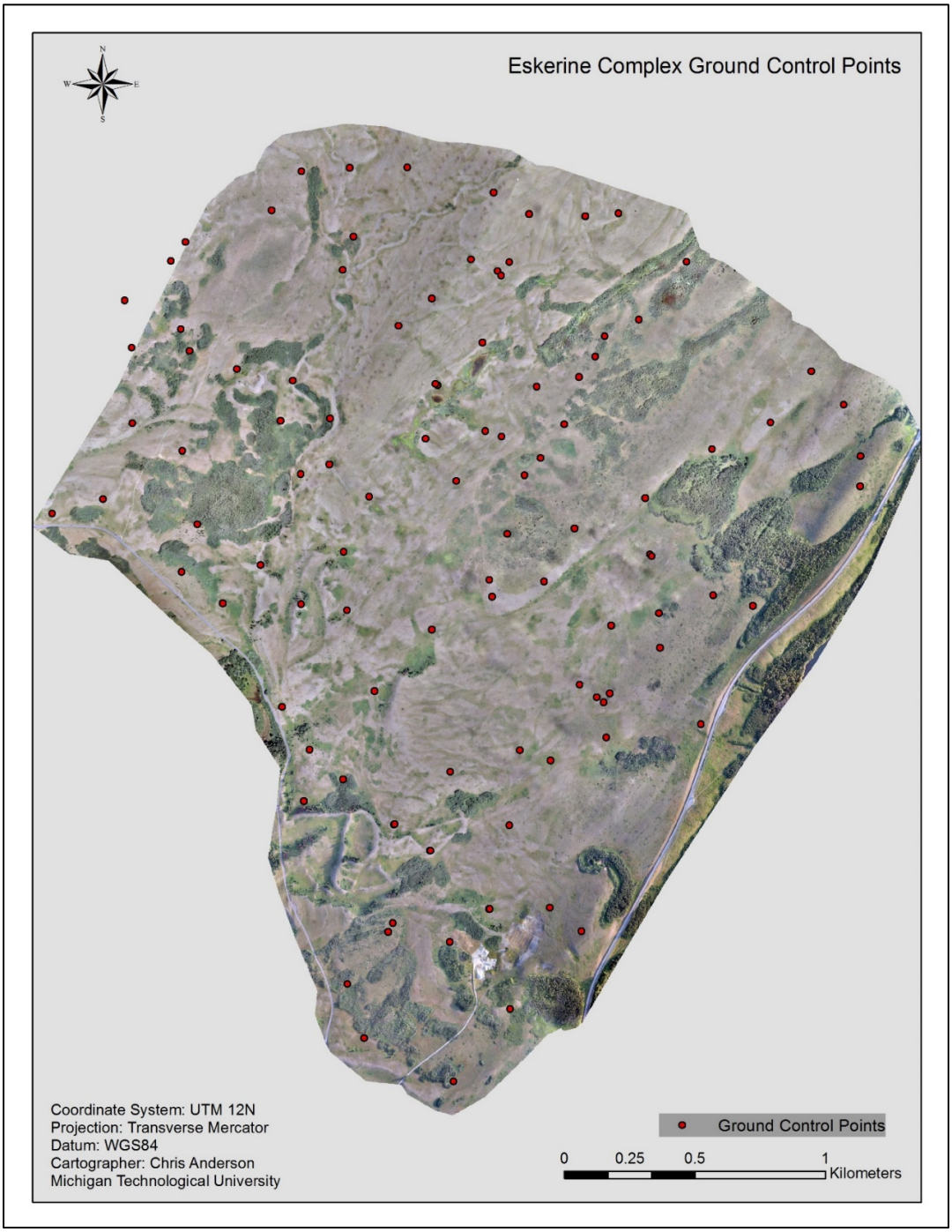

Figure 5. Ground control points placed for UAS mapping

2 Data Processing and Classification Introduction

The data processing segment was comprised of many components, and each area of data collection took several weeks or months to process, depending on computer hardware capabilities. Processed data included the full set of GNSS mapping of the Eskerine Complex for 2016 and the subset data mapped in 2017; and the UAS mapping data (RGB and NIR) for 2017. Both data collection methods (GNSS and UAS) had several processing segments. The GNSS processing included post-processing of all polygon points collected and editing on each of the stratified aspen stand layers: canopy, regeneration, and shrubs. The UAS processing included several steps for the creation of the orthomosaic for each flight block, followed by the mosaicking of all flight blocks for the entire study area into one image. Upon completion of the mosaic several digital image processing steps were used. which included landcover classification. We conducted several variations of supervised and unsupervised classifications, and manually digitized polygons through image analysis of the regeneration, canopy and shrub layers for the 2017 GNSS mapping data.

Data processing computing requirements and cost for a specific project should be researched before the project is begun. Simply put, the ideal computer for data processing is the most powerful computer available. The data processing for this project has been a two-year progression; it began on a Dell computer with 16 GB of RAM, a 3.6 GHz Quad-Core I7 processor and various detached hard drivers. The 16 GB dell was unable to consistently handle the necessary processing load. Due in part to the difficulties encountered during data processing of this project, two more powerful data processing computers were purchased for the remote sensing lab for the specific purpose of processing geospatial big data. The new computers are equipped with 64GB of RAM, and a 2.20 GHz Quad-Core 2x Xeon processor. The greatest benefit of the new computers is their ability to process large data sets without failing or simply stopping for an unexplained reason. Each image processing software has its own processing specifications; the minimum specifications for processing high-resolution data are 32 GB of RAM, a 2.80 GHz Quad-Core processor, a 100 GB hard drive and a powerful graphics

card (www.Trimble.com 2017). On a large-scale project, the hard drive space would need to be increased exponentially as several image processing programs require an excessive amount of temporary storage. The software programs utilized for this project were Esri ArcGIS, Erdas Imagine, Trimble Business Center, Trimble UASMaster, Trimble Pathfinder, and AgiSoft Metashape Professional.

2.1 GNSS Ground Mapping Data Processing

The same steps were followed to complete data processing on 2016 pre-prescribed burn, and 2017 post-prescribed burn GNSS sub-set mapping data. We completed data post-processing correction in Trimble Pathfinder Office to increase data accuracy. Differential positioning enhances the collected GNSS coordinates by referencing the positions to known ground positions from a local base-station (Chang 2006). The data were then exported form Pathfinder as shapefiles to be used in ArcGIS where we created feature data sets of the aspen and completed any edits needed. After we completed the edits on the polygons, we stratified the layers for canopy, regeneration, and shrubs, thus completing the 2016 pre-burn baseline map and the 2017 ground-truth polygons for the Eskerine Complex. We derived area statistics from these data (example displayed in Figure 6).

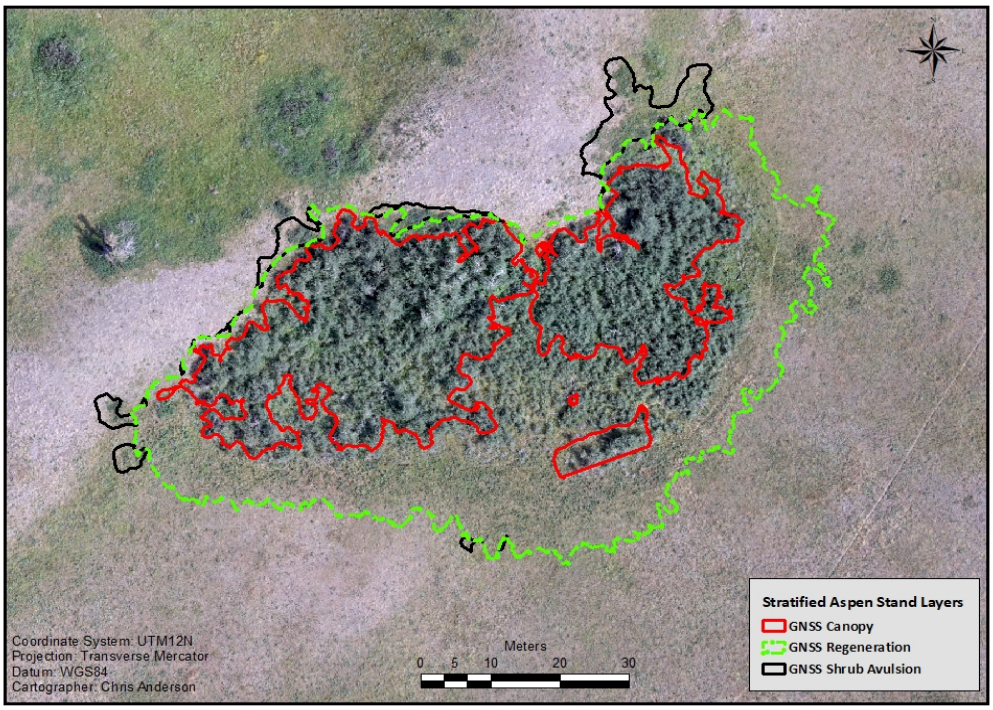

Figure 6. Example of the stratified classification layers created from the 2016 GNSS mapping data. The background imagery is a portion of the RGB imagery

2.2 Processing the Aerial Survey Data

Processing UAS imagery for a remote sensing study consists of several steps and can be time-consuming; image processing on a small project, ~ 1 - 5, ha can be completed in a single day, a large project, > 25 ha, (the area to processing time estimates listed here are considering specifications for this project) can take several months to process depending on computing capability. The process has two main phases, the creation of an orthomosaic, and image classification; each of these steps has many intermediate stages requiring quality assurance monitoring. The orthorectified mosaic (orthomosaic) is the resulting image from joining together all of the photos captured by the UAS (Cruzan et al. 2016) and vertically rectified using the digital elevation information. We utilized Trimble Business Center (TBC), and UASMaster for initial processing of the imagery. The process for each flight block begins in TBC and is completed in UASMaster (Figure

7). The processing steps for each Aircraft (UX5 and UX5HP) have slight variations but are generally (or can be) processed the same way. For example, data collected via UX5HP does not require GCPs for the imagery to be processed, but GCPs can improve photogrammetric results and were therefore used. All the products needed for data processing in UAS Master are imported from Trimble Business Center, including photos, base-station data, camera, and flight trajectory, coordinate system and GCPs (Figures 8 & 9). The orthomosaic is completed in UASMaster.

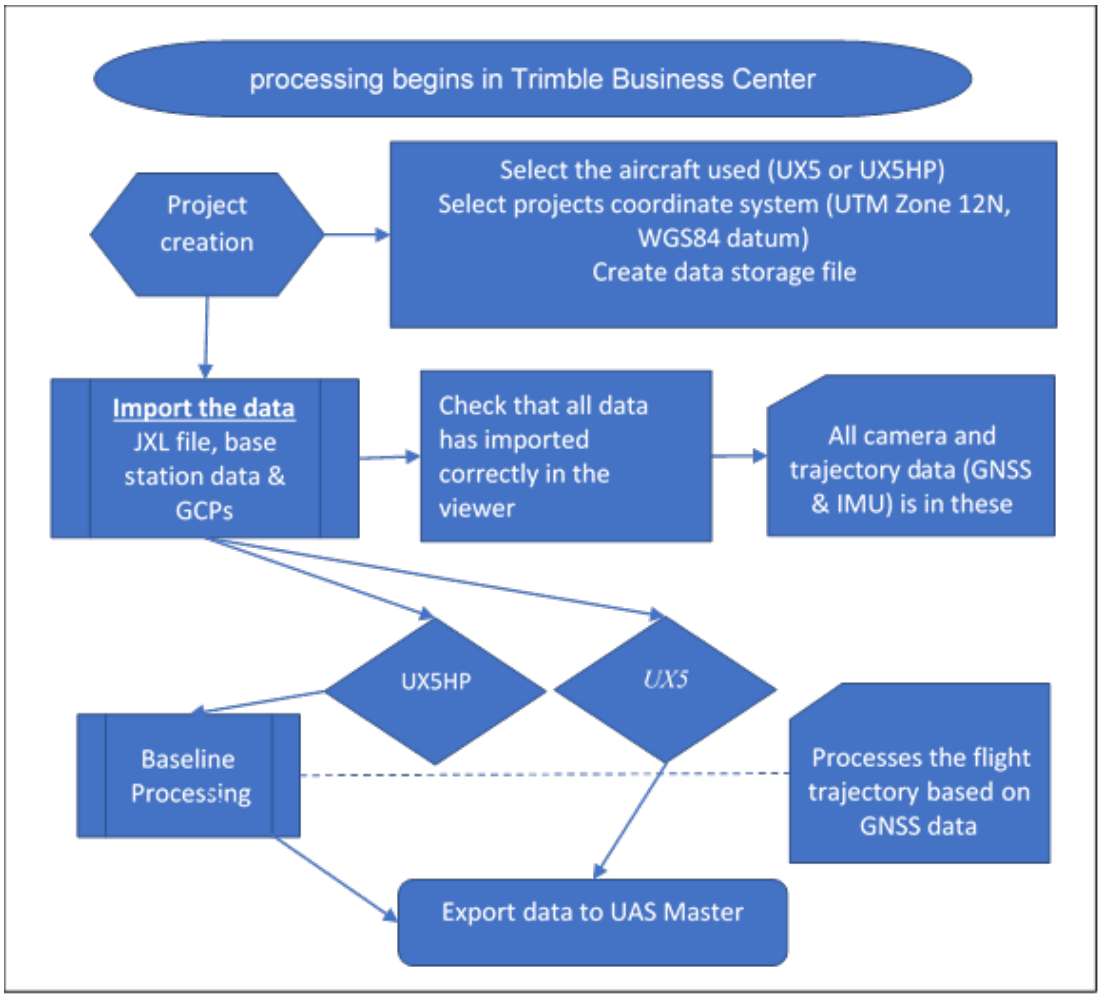

Figure 7. Trimble Business Center processing steps. The processing sequence for TBC is displayed on the items in the left column (rectangles with a margin) and are general steps to be completed, the center column signifies secondary checks and choices, and the right column gives descriptive notes.

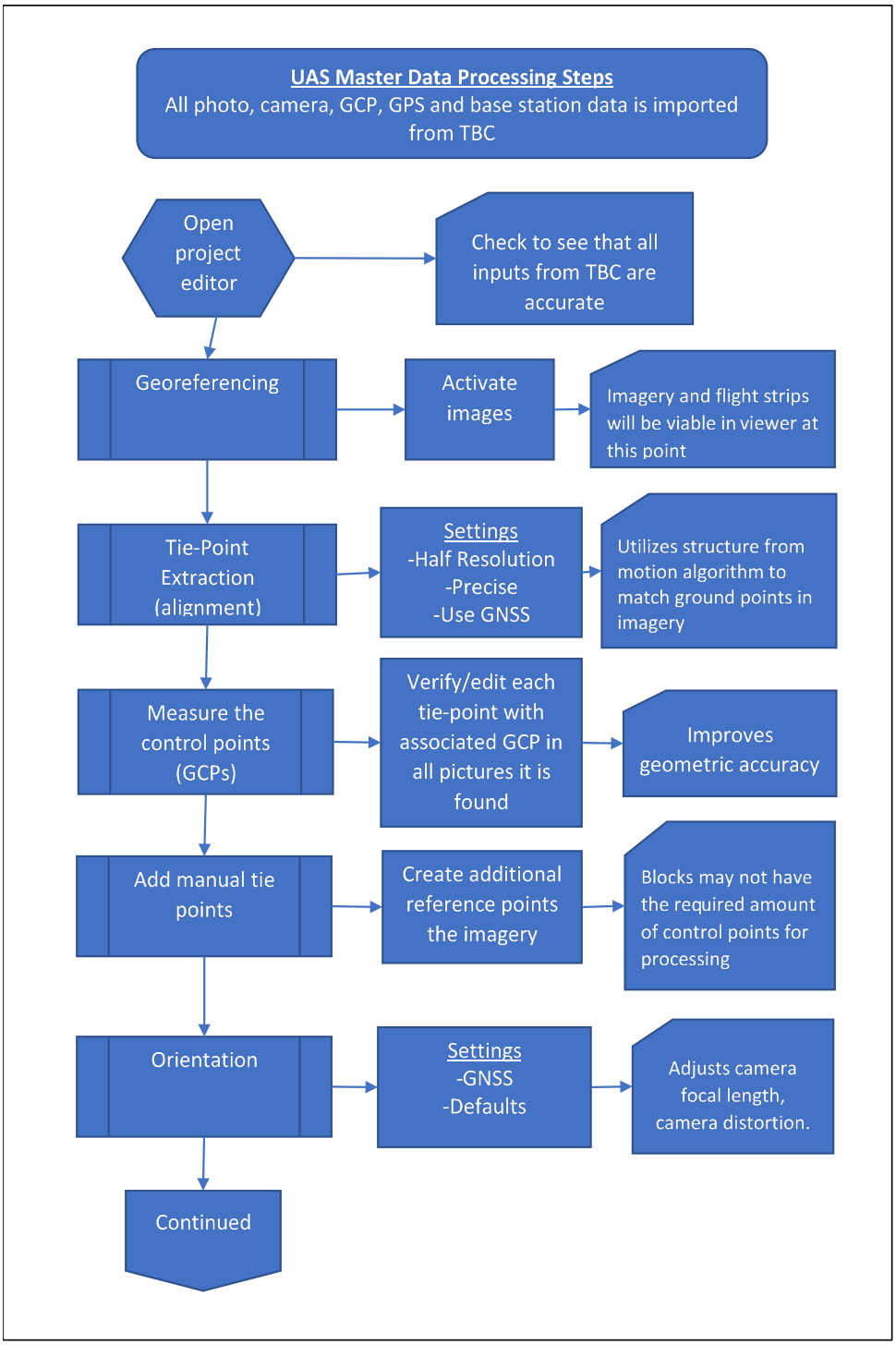

Figure 8. UASMaster processing steps. The left column signifies the general processing steps, the center column signifies specific settings that need to be selected for each processing segment, and the right column is either an informational note or the product that was created in that session.

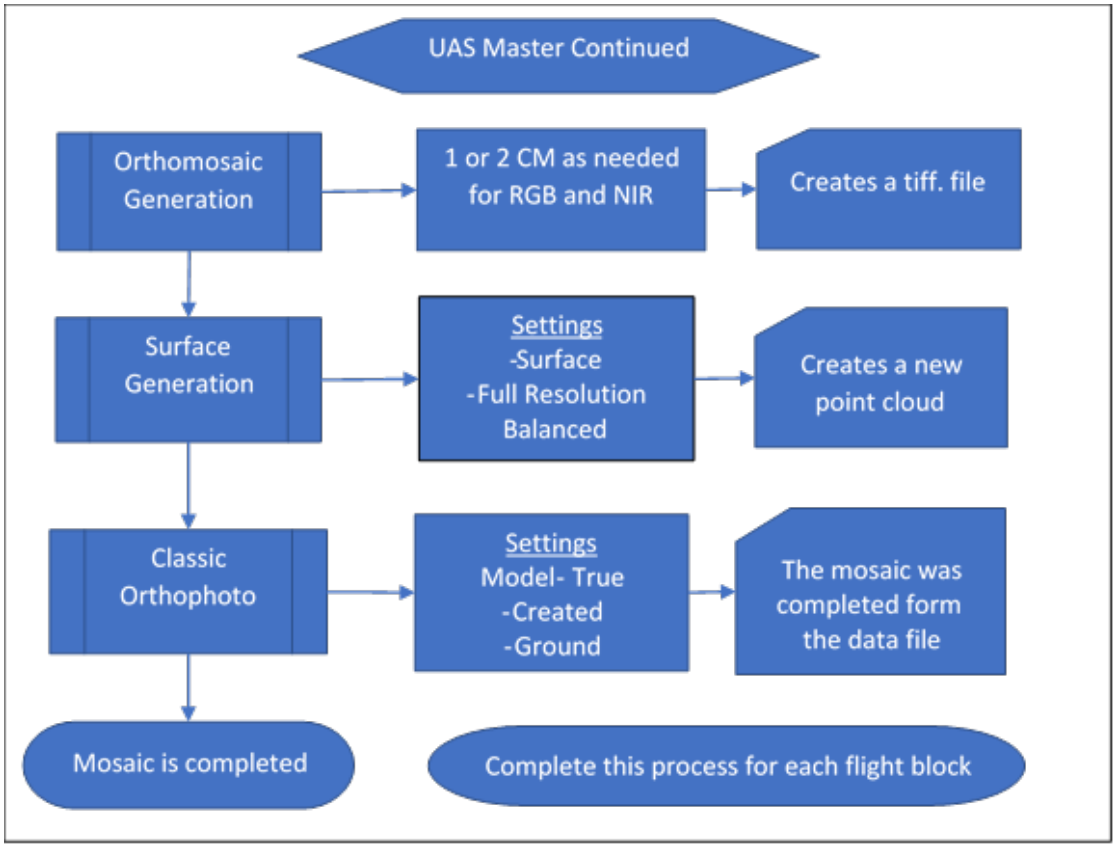

Figure 9.UASMaster processing steps continued. The left column signifies the general processing steps, the center column signifies specific settings that need to be selected for each processing segment, and the right column is either an informational note or the product that was created in that session

Creating a complete mosaic of the imagery in ERDAS Imagine Mosaic pro: After we completed a mosaic for each flight block we used Mosaic Pro (a tool used for geographically joining image flight block mosaics) to join flight blocks together. After loading the imagery into the tool for two completed flight blocks we set the image overlay. The overlay designates a seam line where the pixels from a portion of each block overlap and are merged for the creation of the new image. We set the overlap at different lengths, but between a range of 25 - 50 m depending on the size of the block. The lower overlay distance was used on the larger blocks to expedite the processing. We continued adding each flight block one by one to the accumulated image until all flight blocks were combined, creating a complete mosaic of the Eskerine Complex study area. The process was the same for the NIR and the RGB data sets. After examining the results of the NIR

and RGB mosaics we noticed the final mosaic contained gaps and other artifacts such as blurred imagery that may have caused significant problems with classification. Our solution was to repeat all the processing steps in Agisoft Photoscan with the new high-speed computers. This allowed processing of all blocks in the north of the study area o one session and then the southern half in a second session; this then gave us only two images that required mosaicking in Erdas Imagine. The resulting imagery created in Agisoft was a more complete mosaic with far less blur and blank spots in the imagery.

2.3 Classification

Image classification is the process of sorting pixel values into categories. In this study, we focused on 8-bit images that consist of three bands (red, green and blue). The NIR data is still being processed and we will analyze it upon completion. Each band has associated reflectance values with potential values ranging from 0-255, depending on the intensity of the spectral reflectance, e.g., if the red band in an RGB image has a value of 10, this means the pixel has little red reflectance associated with it, whereas if the pixel value is 220, this indicates a high red reflectance. In some cases, the full range of values may not be captured in the raw image and may require further image enhancement, e.g., contrast stretch. Each pixel has varying reflectance for each image band, and these values can be categorized into different land cover types based on spectral reflectance; the pixels are binned according to their values or statistical similarities. For example, a range of values is categorized as road, another as water, and all other classes specified in the data set. There are two basic forms of classification, supervised and unsupervised.

Unsupervised classification is an automated process completed by an image processing program after the analyst establishes the initial desired settings. The process is based on clustering groups of pixels whose spectral return values statistically fit together in the image data. There are two common algorithms used in the unsupervised classification, ISODATA (Iterative Self-Organizing Data Analysis Technique), and K-means. The ISODATA method uses the minimum spectral distance of pixels to form clusters based on a range in the data that is entered by the user, the algorithm refines these clusters over

many iterations. K-means also forms clusters but requires the user to enter the number of output clusters desired. The Pixels are classified into this number of clusters

Upon completion of this process, the data categories which are created by the algorithm need to be interpreted and placed into appropriate classes; select groups can be added, merged or deleted.

Supervised classification is controlled by the analyst and based on patterns recognized from prior knowledge. Training areas for specific classes are created by the user by selecting several groups of pixels in the image that belong in a category, and the technician, therefore "teaches" the software which pixel values belong to each category before the clustering algorithm is started. The algorithm uses the training areas to classify the data; classes can be edited upon completion. There are several algorithms, and the four most common are the nearest neighbor, closest distance to means, maximum likelihood and parallelepiped.

We completed the unsupervised classification for both the RGB and NIR Eskerine Complex mosaics. The process has several options to be considered, such as the number of classes to be created, and the number of iterations to be completed. The classes and iterations were set for different values depending on the classification event and the imagery being classified. Generally, the settings of 25 and 10 were used respectively. This means that the algorithm will repeat the classification process 10 times while creating 25 distinct classes. We used a class of 25 to be sure we are capturing all variation in the landscape, and upon completion of the classification we combined categories that had multiple assignments. We assigned each of the 25 classes to a landform or vegetation type. The possible categories for classification in our study site were aspen, shrubs, grass, rock, snag, water, road, barren ground, and conifer, while our main objective was to identify the aspen, shrubs, and grass.

We performed supervised classifications on the RGB and NIR imagery. The first step in performing the supervised classification is to complete a signature file. A signature data set defines the training pixels that will be accessed by the algorithm to classify the data.

Each signature can be a single pixel or a group of pixels. The sample areas are called feature spaces or an area of interest (AOI). Each AOI has several attributes that need to be created and is stored in the signature file (.sig). The signature file attributes are as follows; name (an identifier that is used in the output thematic raster), color (each signature is associated with a specific color that designates which class it belongs in), and value (each signature has a designated value that is determined by the pixels that make up the training area). The classes are identified while the signature file is created. The .sig files are completed by opening the raster in ERDAS IMAGINE and creating a set of AOIs for each class. For the NIR imagery, we created classes of aspen canopy and regeneration, shrubs, grass, rock, snag, water, road, trail, and conifer. The main classes of interest, aspen, shrub, and grass received a minimum of 50 AOI datasets whereas the non-target landscape features can have as few as 10 (This sequence was completed many times, and the number of AOIs created for each process was not always the same due to time constraints). We set the supervised classification method as maximum likelihood, which is a rules-based classification method that places pixels constituting a specified requirement into a class. The method assumes equal probability and a normal distribution of the data. Upon completion of the thematic raster (the classified data) we made any necessary edits, in some cases, we deleted signatures and classes, and additional signatures were created. After we completed the editing, we repeated the classification process to refine the thematic raster.

2.3.1.1 *Knowledge Engineer*

Knowledge Engineer (KE) is an expert classification tool in the Erdas imagine software. It utilizes a rules-based approach for multispectral image classification. The user creates a decision tree to refine information and place pixels into classes based on the rules. The decision tree employs several geospatial products to classify the data. We completed a principal components analysis on the RGB data which is a method of transformation where the data is compressed into fewer bands to create a form of the data that is easier to interpret. The bands are reduced to similar values during the transformation and then placed into land cover categories by an analyst. We completed an unsupervised

classification with the resulting principal components raster; the classification was then improved for aspen stand analysis through a rules-based approach in KE. We produced a classification by using a vegetation height model (canopy height model, CHM) and the classified raster data from the principal components analysis. We created the CHM from a digital elevation model (DEM) and a digital surface model (DSM). The DEM and DSM models were derived from the UAS RGB 2-cm resolution imagery using Agisoft Metashape software by Dr. Curtis Edson. The model allowed us to determine where the vegetation in the study site was ≥ 2.5 m in ht. It is important to note that a very high percentage of the vegetation in the study area that is living and is ≥ 2.5 m in height, was aspen canopy. The proportion of aspen stems ≥ 2.5 m in height greatly exceeded all other trees that are also of this height or taller (e.g., Douglas fir, *Pseudotsuga mensiezii,* which was rarely detected within aspen stands). There were so few canopy trees in the aspen stands that were not aspen that it was unnecessary to account for them in the analysis. Also, the pixel values of the conifer trees in the RGB classification were not consistent; they were often similar to shrubs or aspen. The red area in Figure 10 represents all vegetation ≥ 2.5 m in height and the green represents all vegetation that is between 0.2 - 2.49 m in ht. The red also represents areas that would need to be treated by prescribed burning to restore the grassland, while the green areas are accessible to browsing by elk.

The KE classification allowed us to classify all vegetation that was classified as aspen in the PCA based unsupervised classification (Figure 11) that is also ≥ 2.5 m in height as aspen canopy (Figure 12), refining the stand structure analysis and allowing us to examine the change in canopy area from before and after prescribed burning. The resulting classification assisted in determining the height division between the aspen regeneration and canopy layers. This process allowed us to differentiate between the classes and stratify the aspen stands on a more detailed level. Upon completion of the KE classification, we used the aggregate tool in ArcGIS to cluster all the pixels from one class together into a reduced resolution raster from 2 cm to 50 cm. The change in resolution was necessary to complete the raster to polygon data set for the regeneration layer in ArcGIS.

Upon completion of the stratified layers, we produced polygons of the aspen stands that we analyzed in ArcGIS to determine the change in aspen stand area from before to after prescribed burning.

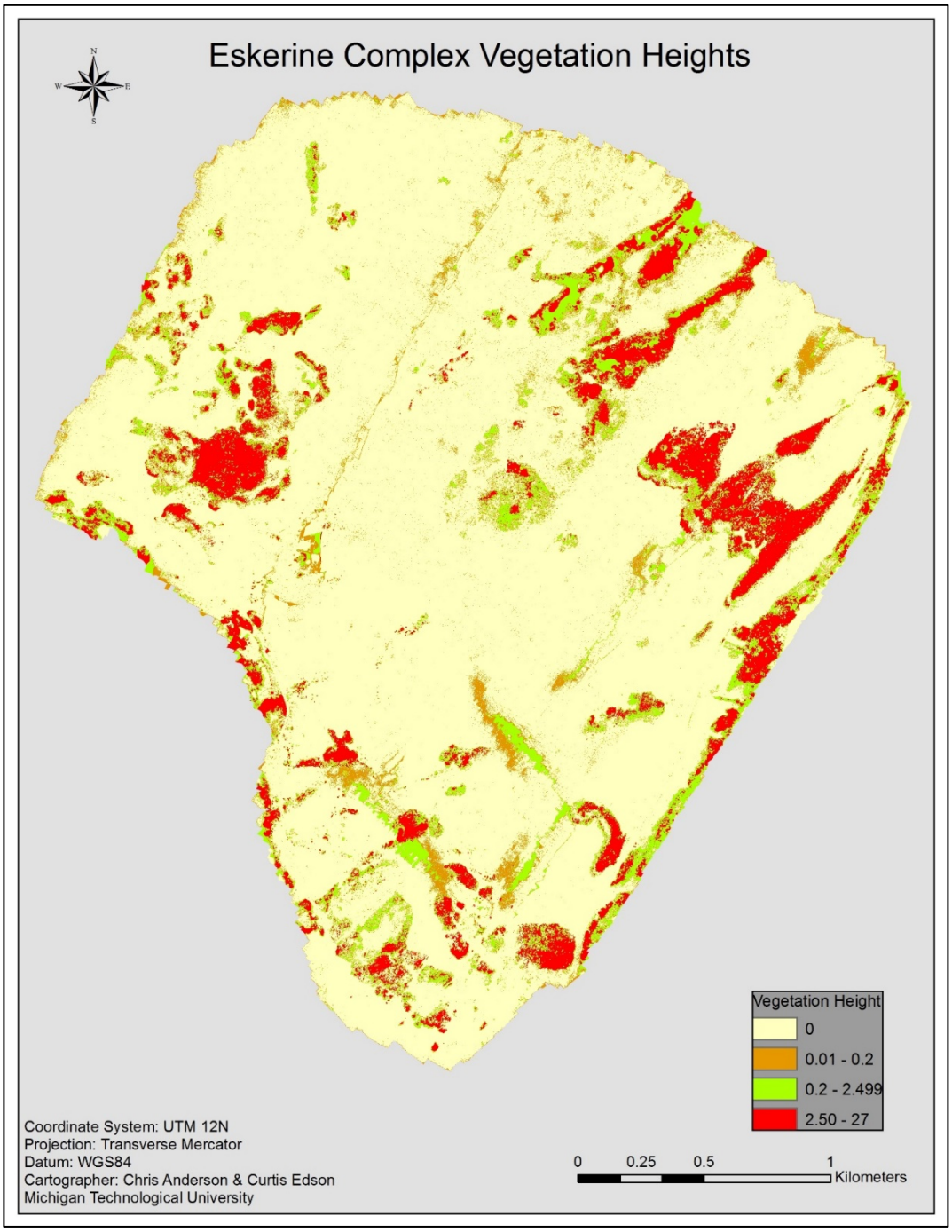

Figure 10. Vegetation height model. All vegetation between 0 – 0.2 was not used in the KE classification. Vegetation between 0.2 and 2.499 was used to distinguish between aspen regeneration and canopy. Vegetation ≥ 2.50 was used to identify canopy

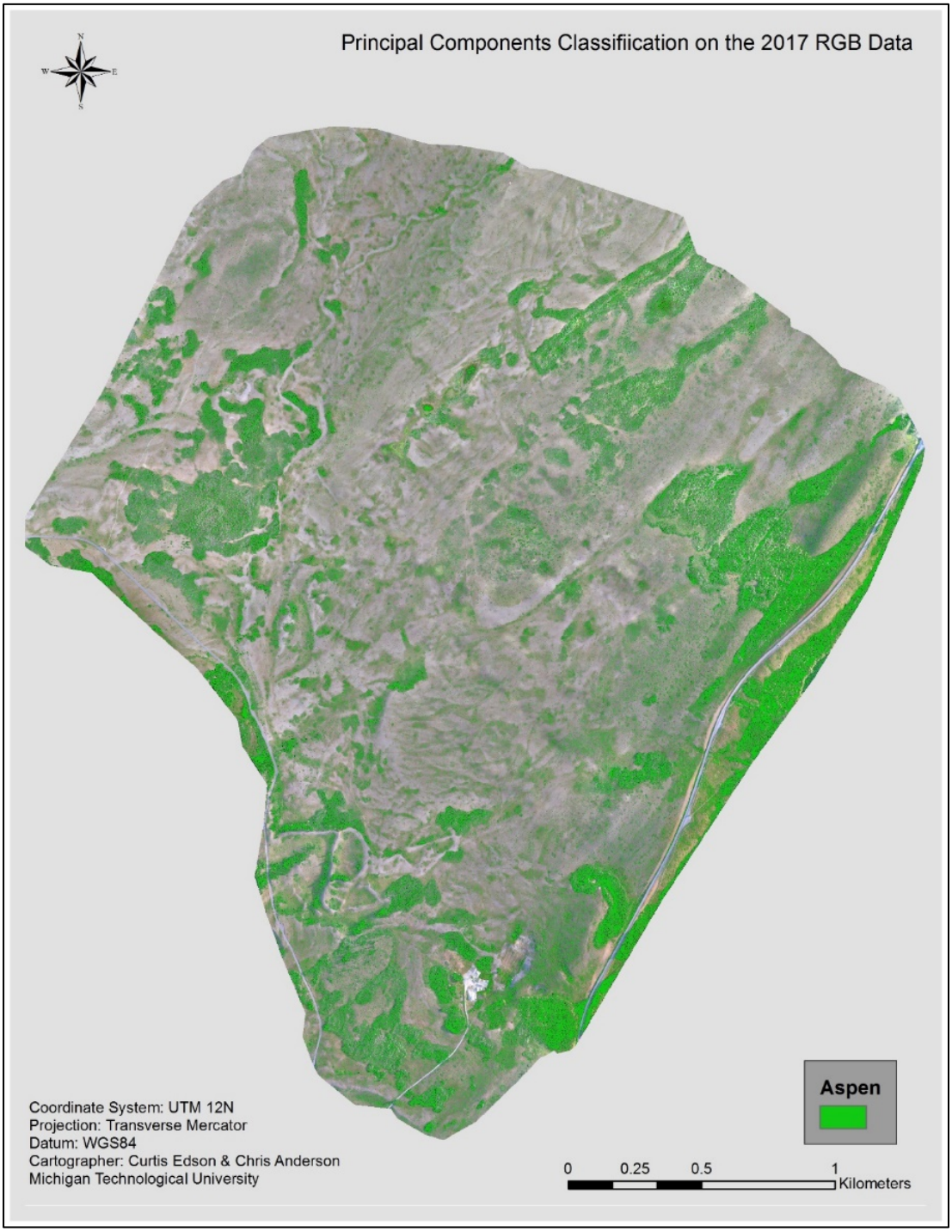

Figure 11. All vegetation classified as aspen during the unsupervised classification for the principal components analysis.

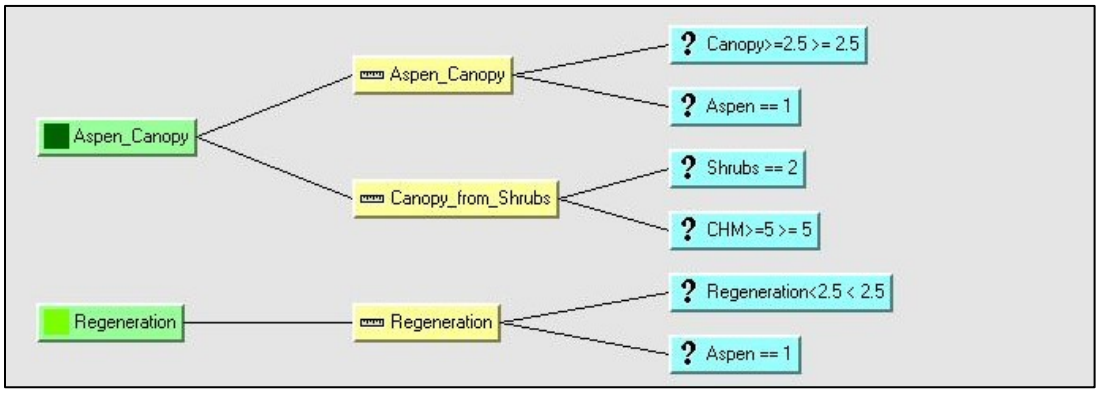

Figure 12. The decision tree used in KE for aspen stand classification.

2.3.1.2 *Additional Image Processing*

An additional classification method we attempted was to enhance the data through histogram equalization. In theory, this image enhancement technique makes the data more interpretable by creating an image where the pixel values are redistributed through a non-linear stretch, and there is the same number of pixels with each value near each other. We applied the histogram equalization on the NIR data and may use the imagery on future classifications.

We also attempted to perform a Fuzzy Classification, which is a method that can be used when an area of interest has many mixed classes; cells in the land cover classes are intermixed and have an overlapping range of values to the point where they are virtually indistinguishable to the one next to it. This means that each pixel could belong to more than one category. We completed the setup and pre-processing requirements for this step; but unfortunately, the process utilizes a considerable amount of temporary data. The classification could not be completed with the hardware available to us at the time of processing due to the size of our data.

2.4 Digitizing Polygons Introduction

A typical sequence of events would be to create a vector layer from the thematic raster to calculate the area of each aspen stand layer. We instituted a different approach for

analyzing the aspen stands because the high spatial resolution of the data caused difficulties with the classification; the pixel density was not sufficient for creating an aggregated vector for a specific layer without further processing. The aspen stands located in the Eskerine Complex contained a mixture of tall canopy stems, snags, regeneration and shrubs of various sizes creating a diverse mixture of classes. For example, many of the aspen stands contained shrubs that were of similar height as the regenerated aspen (aspen < 2.5 m); in some cases, the shrubs outnumbered the aspen. In this limited spectral resolution imagery, the pixel value for many of the shrubs was very similar to the pixel value of aspen; this overlap made it extremely difficult to decipher between these classes. When creating the training pixels for the regenerated aspen, and then running the classification, the resulting classification overlapped to a point where it was impossible to create a shrub polygon or an aspen regeneration polygon that consisted of one class. The alternative method we instituted to classify the area of post-prescribed burn aspen stand imagery was through heads-up digitization in ArcGIS. Heads-up digitization is the process of manually creating a vector layer on the computer monitor through a data source (Chang 2006). For this study, we digitized polygons from the raster layer created via the UAS RGB imagery (2 cm resolution) through manual image interpretation. The digitizing of each aspen stand layer was completed by interpreting the aspen stand imagery visually and drawing a polygon by following the category boundaries.

We applied the same rules of height and distance that were applied for the GNSS mapping methods to the digitization process, but as ocular estimates, therefore representing the 2016 GNSS mapping methods as closely as possible. We followed the perimeter of each layer and did not digitize gaps in the interior of the aspen stands, therefore following the same mapping methods used for the 2016 GNSS mapping data. All layers for each stand were digitized independently of one another.

We used the stratified aspen stand layers created from the subset of 2017 GNSS mapped stands to establish decisions for digitizing each landform during the heads-up approach, specifically, to establish what is and what is not aspen. We visually analyzed each layer's

imagery attributes such as color, texture and vegetation patterns for deciding where one-layer ends, and another begins in the GNSS polygons; we applied these attributes when digitizing polygons on the screen from the imagery (the subset layer boundary locations were mapped at a sub-meter level of accuracy). When creating the polygons, the zoom function was used extensively, and nodes were placed as often as possible while moving the mouse cursor along the outside edge of each layer. Upon completion of each layer, the boundary was examined and edits were performed where necessary by moving, adding or deleting nodes.

2.4.1.1 *Digitizing the Regeneration Layer*

The aspen regeneration layer in the 2017 ground-truthed data had a distinct pattern and color compared to the surrounding vegetation. We started digitizing the polygon in a location with a high probability of aspen based on the predetermined attributes of color, pattern, and texture. We continued digitizing the polygon from the starting point until returning to the starting point; thus, completing the polygon layer. The attributes used for digitizing the regeneration layer are represented in Figure 13.

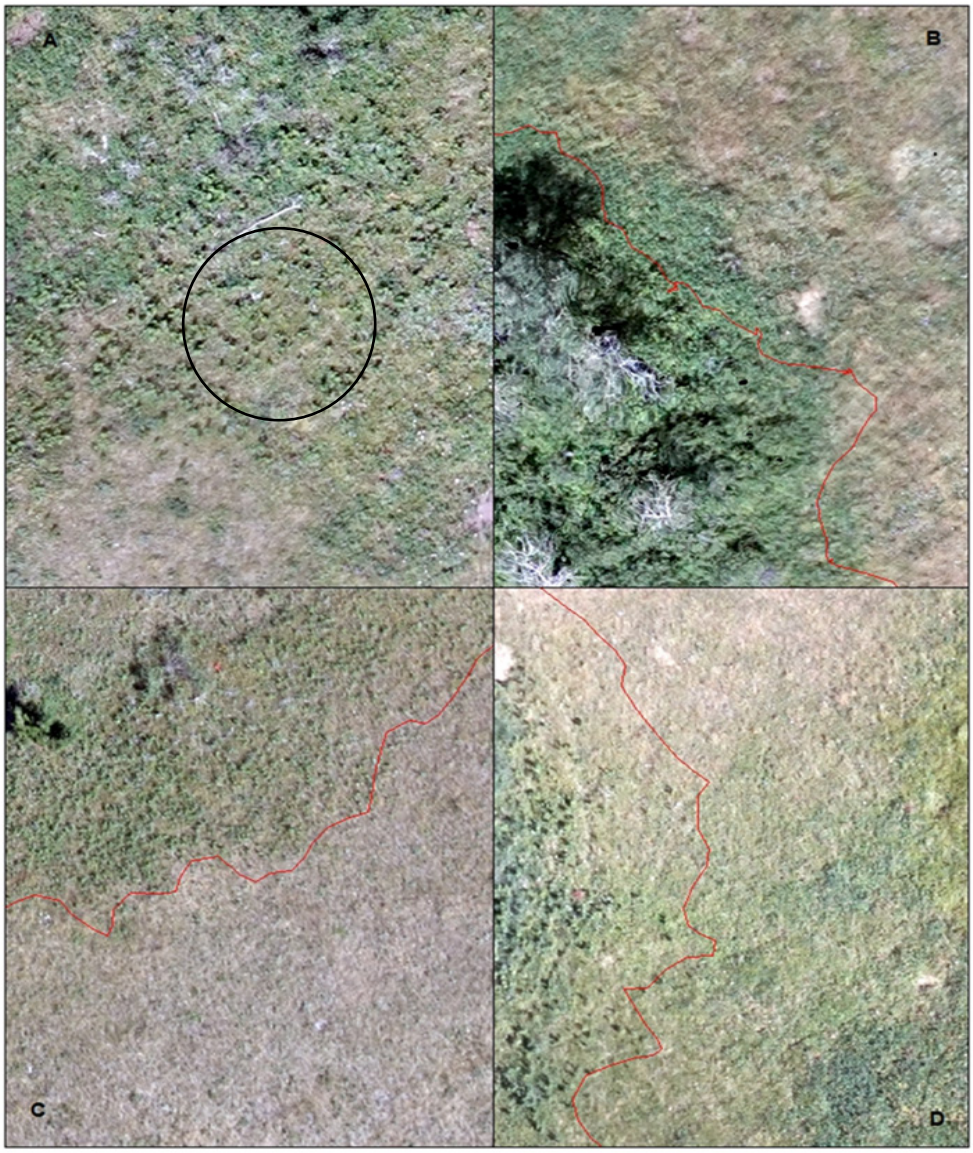

Figure 13. Attributes used for digitizing the aspen regeneration layer. Image (A) shows a pattern in the aspen (small aspen located in a relatively equal distance from each other (inside the circle). Image (B) displays a change in texture, left of the red line is aspen regeneration and to the right of the red line is not. Image (C) is an example of a distinct edge and change in color in the landscape, above the line is aspen, below the line is not. Image (D) displays the difficulties with digitizing, the red line is the actual edge between aspen regeneration and grass in the 2017 GNSS mapping data, which is difficult to see on the image as there is no obvious distinction between grass and aspen. Image D is an example of an area where an error of omission is likely.

2.4.1.2 *Digitizing the Canopy Layer*

Digitizing the canopy was very similar to the regeneration, we decided what is and what is not canopy, found a suitable starting point, and followed the edge of the canopy area until the canopy layer was completed. The canopy was a relatively consistent color; generally a darker green than the surrounding area, variance in color and texture were minimal, and there was very little or no space between trees. We scanned each stand for canopy throughout its entire area to be sure that we created a polygon for all parts of the canopy. A stand can have a section of the canopy that is discontinued from other portions, but still part of the same stand; this means there was regenerated aspen that is < 2.5 m in height between areas that were ≥ 2.5 m in height within the same stand. These areas were created as a multi-part canopy feature in ArcGIS. We also compared the 2017 canopy and imagery data to the areas that were canopy in the 2016 data, if sections were canopy in 2016, and we saw that the area did not burn in the 2017 prescribed burn, it is probable that the area was still canopy. Detailed attributes used for digitizing the canopy layer are displayed in Figure 14.

Figure 14. Attributes used for digitizing the canopy layer. Image (A) displays a change in color, pattern, and texture, the lower portion is aspen and the upper portion is grass. Image (B) shows consistent canopy throughout the image except for the small area in the upper left corner. Image (C) displays a multipart canopy feature (disconnected canopy segments in the same stand), the red polygons are aspen. Note: there are conifers of canopy height located within this stand that are not part of the recorded aspen canopy. Image (D) displays a change in pattern and texture, above the line, is aspen; below the line is not.

2.4.1.3 *Digitizing the Shrub Layer*

We mapped the shrubs in a similar manner as the regeneration; the primary objective of the shrub layer is to determine where the shrubs extend from the aspen. For digitizing the shrubs, we started creating the polygon in a spot where there is obvious consistent cover of shrubs or a mix of shrubs and aspen next to the grass. We then used the attributes of color pattern and texture to differentiate shrubs. Shrubs, in general, have a very dense structure in many areas and a color that contrasts from aspen and grass extending from the edge of the aspen a few m before the grass begins. The shrub layer was limited to extending no farther than 20 m from the stand edge; this means that if the shrubs extended beyond 20 m from the stand edge we did not include these shrubs as aspen stand expansion. When needed we used the measurement (ruler) tool in ArcGIS while editing the shrub layers to make changes where needed. Attributes used for mapping the shrub layer are displayed in Figure 15.

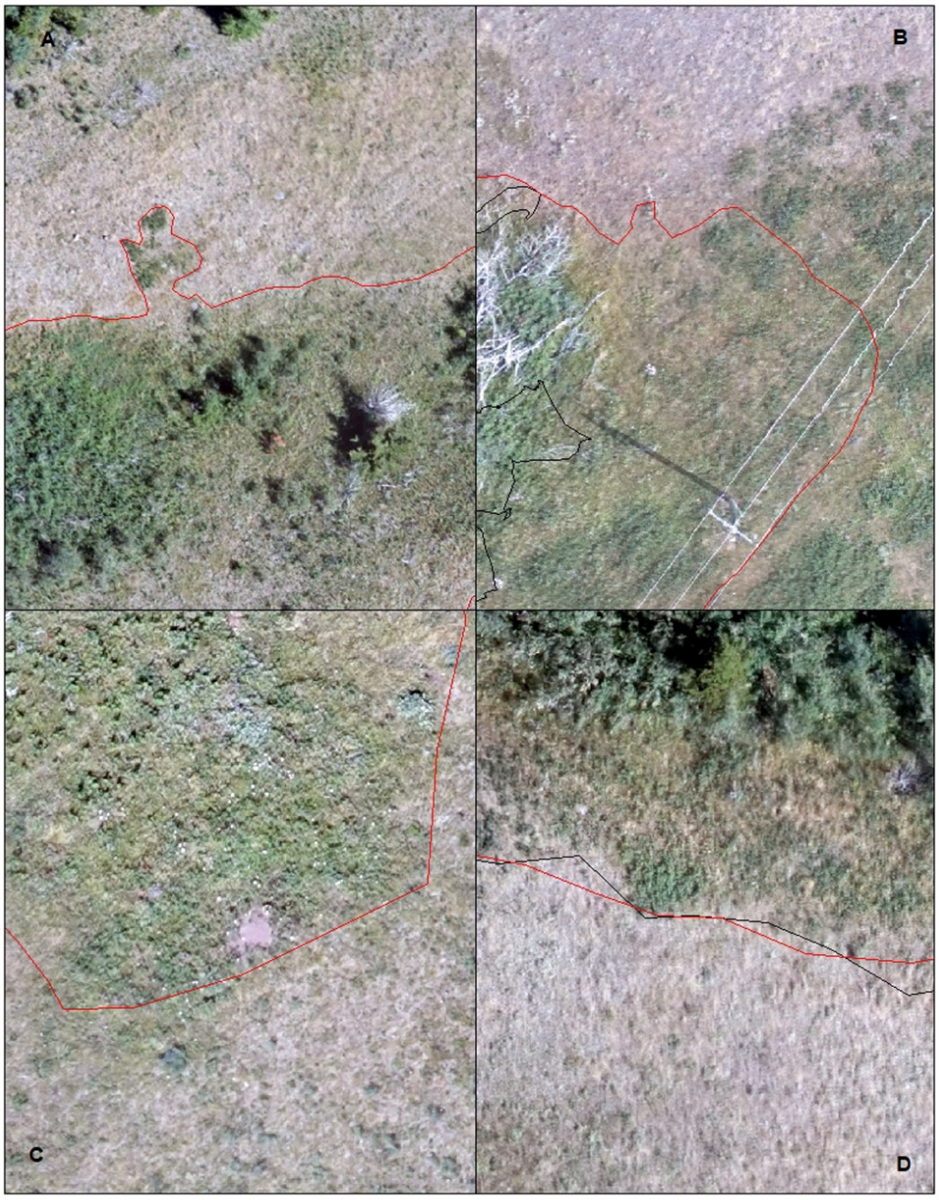

Figure 15. Attributes used for digitizing the shrub layer. Image (A) An example of a shrub patch extending from the aspen stand. Image (B) An area where 20 m shrub cutoff limit was used for shrub expansion (shrubs extend further than the red line but are not considered stand expansion beyond 20 m). Image (C) displays a change in texture pattern and color, above line is shrubs, below is grass and forbs. Image (D) represents the difficulties with digitizing the shrub layer, the red line is the shrub border, the black line is the regeneration layer for the GNSS mapping data, the layers are mixed to the point that they are impossible to decipher form one another during digitization.

2.5 Results

Assessing the aspen stand structure required several methods of geospatial data collection and processing which encompassed GNSS mapping and aerial imagery. These data include initial mapping to create a baseline dataset, UAS flights for post-prescribed burn mapping, limited post-prescribed burn GNSS mapping, the use of knowledge Engineer for aspen stand classification and the creation of digitized polygons for additional post-prescribed burn assessment.

We mapped 30 aspen stands in the Eskerine Complex in 2016 (Figure 19), and a subset of 5 five stands in 2017 (Figure 27) via Trimble Geo7x mapping grade GNSS. We collected imagery via UAS in both NIR and RGB in 2017 encompassing the same 30 aspen stands of the Eskerine Complex that were mapped in 2016. The processing of this imagery resulted in two complete mosaicked images of the Eskerine Complex; NIR, (Figure 28), and RGB (Figures 16 - 26). We used the RGB data set to create the digitized polygons, (Figure 20).

To test the response of aspen to prescribed burn, we compared the 2016 GNSS mapping area data (ha) to the 2017 digitized polygon area data (ha), and the polygons created from the KE classification (ha), by implementing a two-sample t-test assuming equal variances on each layer, total aspen, canopy, regeneration, and shrubs. A change in aspen stand area was not significant on any level when comparing the 2016 GNSS mapping data to the 2017 UAS digitized data (Table 1).

2.5.1 Digitized Polygon Results

Total ha of aspen area (all canopy plus regeneration) from pre-burn (2016 GNSS data) to post-burn (2017 digitized polygons) increased by 1.27, from 94.96 with a 95% confidence interval of ±1.26 to 96.23 ±1.29 *(t* = - .007, 58 df, $p = 0.497$). Mean aspen stand size (in ha) increased slightly from 3.17 ±2.58, range = 29.34 to 3.21 ±2.64, range =30.00. Aspen canopy (in ha) throughout the study area decreased by 17.90, from 57.10 ±0.94 to 39.20 ±0.73 ($t = 0.54$, 54 df, $p = 0.295$). The average area in ha of aspen canopy

per stand when all the aspen stands were averaged decreased from 2.04 ±1.93, range = 19.72 to 1.46 ±1.50 ha, range = 18.24, a decrease of 33.37% (this change was not statistically significant). The proportion of regeneration (in ha) throughout the study area increased by 20.19, from 38.22 ±0.411 to 58.41 ±0.69 (t = - 0.76, 58 df, p = 0.224). The mean area in ha of regeneration increased from 1.27 ±0.84, range = 10.85 to 1.88 ±1.40, range = 16.21. The shrub area (shrub avulsion in ha), increased by 1.0740, from 8.74 ±0.11 to 9.82 ±0.12 (t = - .225, 58 df, p = 0.411). The mean proportion for shrub avulsion throughout the study area incased from 0.29 ±0.21, range = 3.00 to 0.33 ±0.24, range = 3.22.

The overall aspen stand area in ha from before (2016) to after the prescribed burn (2017) was relatively unchanged. Although the difference was not significant, there was a noticeable difference between the canopy and regeneration area as the proportion of canopy decreased by 31.34%, and the proportion of regeneration area increased by 52.83%.

2016 mapping Data – pre-burn: We mapped 30 aspen stands and calculated the area in ha of each stand on all stratified levels, canopy, the extent of regeneration, shrub expansion, and total aspen. The largest overall aspen stand is E30 which had 29.435, and the smallest stand is E17 which had an area of 0.027, a range of 29.408. Two aspen stands E05 and E25 did not have any stems in the canopy layer, while two stands E24 and E25 did not have a shrub layer, E25 did not have a canopy or shrub avulsion layer.

2017 Digitized polygon data: We created stratified layers for all 30 aspen stands and calculated the area in ha of each stand on all levels, canopy, the extent of regeneration, shrubs expansion, and total aspen. The largest overall aspen stand, E30, was 30.034, and the smallest is E17, which was 0.031, a range of 30.003. Two aspen stands, E05 and E25, did not have any stems in the canopy layer, while two stands, E24 and E25, did not have a shrub avulsion layer, E25 did not have a canopy or shrub avulsion layer.

Table 1. Side-by-Side area comparison (ha) of the 2016 GNSS aspen stand mapping data to the digitized polygon aspen stand data created from the 2017 RGB UAS imagery.

Stand	2016 GNSS Canopy	2017 Digitized Canopy	2016 GNSS Regen	2017 Digitized Regen	2016 GNSS All Aspen	2017 Digitized All Aspen	2016 GNSS Shrubs	2017 Digitized Shrubs
E01	0.1383	0.1584	0.6733	0.6473	0.8117	0.8057	0.0908	0.1376
E02	1.2372	0.4355	1.3378	2.2928	2.5750	2.7283	0.3478	0.4381
E03	19.7258	9.2186	5.2176	16.2447	24.9434	25.4633	1.0663	1.2720
E04	1.9188	1.8199	1.3365	1.3669	3.2553	3.1869	0.0993	0.2245
E05	0.0000	0.0000	0.4339	0.5001	0.4339	0.5001	0.1056	0.1048
E06	0.1281	0.0989	0.1726	0.1925	0.3007	0.2914	0.0286	0.0852
E07	1.2017	0.7881	2.9015	3.3569	4.1032	4.1450	0.2749	0.1714
E08	0.0540	0.0534	0.2485	0.3154	0.3025	0.3688	0.0541	0.0321
E09	0.8680	0.0099	0.7480	1.0924	1.6159	1.6021	0.4653	0.0376
E10	0.8076	0.1550	0.6612	0.4224	1.4688	0.5774	0.5766	0.0117
E11	0.2219	0.0851	0.2354	0.3825	0.4573	0.4676	0.2258	0.1241
E12	0.8775	0.7743	0.6761	0.7685	1.5536	1.5429	0.0373	0.0672
E13	0.2871	0.1407	0.8103	0.9423	1.0974	1.0830	0.0434	0.1258
E14	0.2522	0.1752	0.8437	0.9631	1.0959	1.1383	0.1335	0.1323
E15	6.6782	2.8121	5.6648	9.5004	12.3430	12.3126	0.6616	1.6530
E16	0.0099	0.0057	0.1139	0.1071	0.1238	0.1128	0.0154	0.0196
E17	0.0034	0.0007	0.0272	0.0302	0.0305	0.0308	0.0265	0.0437
E18	1.6078	1.5169	0.4880	0.5571	2.0953	2.0740	0.0646	0.2562
E19	0.1756	0.1600	0.2325	0.2197	0.4081	0.3797	0.0232	0.0725
E20	0.9486	0.7733	0.9482	1.0906	1.8968	1.8639	0.1376	0.3996
E21	0.0005	0.0000	0.1454	0.1166	0.1460	0.1166	0.1039	0.0466
E22	0.0696	0.0585	0.7743	0.7519	0.8439	0.8104	0.1447	0.1342
E23	0.0354	0.0371	0.2607	0.2507	0.2954	0.2879	0.0294	0.1081
E24	0.0273	0.0156	0.2756	0.2896	0.3029	0.3052	0.0000	0.0000
E25	0.0000	0.0000	0.0819	0.0780	0.0819	0.0780	0.0000	0.0000
E26	0.2416	0.2537	0.7643	0.7336	1.0056	0.9872	0.2351	0.2475
E27	0.4594	0.3214	0.4578	0.6229	0.9165	0.9443	0.0132	0.0572
E28	0.0255	0.0083	0.3416	0.3540	0.3671	0.3623	0.0136	0.0343
E29	1.1117	1.0790	0.5055	0.5482	1.6147	1.6272	0.7160	0.5571
E30	18.4915	18.2456	10.9432	11.7879	29.4393	30.0336	3.0071	3.2212
Total	**57.6041**	**39.2011**	**38.3214**	**56.5264**	**95.9258**	**96.2273**	**8.7412**	**9.8152**

We conducted a geospatial overlay analysis to calculate the geometric intersection on the 2016 GNSS mapping data and Digitized polygons. This intersection measurement calculates the physical area in ha that overlapped when the data was collected for each feature class (completed with the intersection tool in ArcGIS). Included with the analysis was an erase feature, which calculated in ha the area collected in ha for the 2016 GNSS

mapping data but was not collected when the digitization was completed for the 2017 data (completed with the erase tool in ArcGIS, GNSS mapping area was erased by the digitization area).

The proportion of intersected canopy (Figure 22) ranged from 0.00% – 94.93%, with a mean of 53.25% and a 95% confidence interval of ±11.07%. The intersection data represents the proportion of the aspen stand that did not succumb to the prescribed burn. The erase data is the proportion of each aspen stand that succumbed to the prescribed burn. The proportion of canopy erase ranged from 0% – 100%, with a mean of 35.99% with a 95% confidence interval of ±10.67 (Table 2). This means that 53.25% of canopy remained in the aspen stands after the prescribed burn and 35.99% of the canopy area found during the GNSS mapping of 2016 was not found while the digitization was completed (the area burned during the prescribed burn). The proportion of intersected regeneration (Figure 23) ranged from 31.99% – 96.59%, with a mean of 87.20% ±4.47%. The proportion of regeneration erase ranged from 0.01% – 10%, with a mean of 0.07 ±0.02% (Table 2). This means that 87.20% of regeneration remained in the aspen stands after the prescribed burn and 0.07% of the regeneration area that was found during the GNSS mapping of 2016 was not found while the digitization was completed. The proportion of total aspen intersected ranged from 34.76% – 98.31%, with a mean of 88.82 ±5.05%. The proportion of total aspen erase ranged from 4.64% – 115.50%, with a mean of 21.75 ±6.38% (Table 3). This means that 88.82% of the total aspen remained in the aspen stands after the prescribed burn and 22.66% of the area of tota5 aspen found during the GNSS mapping of 2016 was not found while the digitization was completed. The proportion of intersected shrubs (Figure 24) ranged from 4.01% – 98.35%, with a mean of 60.12 ±11.21%. The proportion of shrub erase ranged from 0.0005% – 67.72%, with a mean of 20.65 ±8.03% (Table 3). This means that 60.12% of the shrubs remained after the prescribed burn and 20.65% of the shrub area that was found during the GNSS mapping of 2016 was not found while the digitization was completed.

Table 2. Geospatial overlay data of the aspen canopy and regeneration for the 2016 GNSS mapping data (ha) and the 2017 digitized polygons.

	Canopy					Regeneration				
Stand	2016 GNSS	Intersection	Intersect Proportion	Erase	Erase Proportion	2016 GNSS	Intersection	Intersect Proportion	Erase	Erase Proportion
E01	0.1383	0.1168	84.40	0.0216	15.60	0.6733	0.6368	94.57	0.0365	0.05
E02	1.2372	0.4149	33.54	0.8223	66.46	1.3378	1.2257	91.62	0.1125	0.08
E03	19.7258	9.0546	45.90	10.6723	54.10	5.2176	4.8443	92.85	0.3727	0.07
E04	1.9188	1.7238	89.84	0.1950	10.16	1.3365	1.1384	85.18	0.1995	0.15
E05	0.0000	0.0000	0.00	0.0381	0.00	0.4339	0.3861	88.97	0.0479	0.11
E06	0.1281	0.0899	70.23	0.0000	0.00	0.1726	0.1460	84.55	0.0267	0.15
E07	1.2017	0.7474	62.19	0.5093	42.38	2.9015	2.7421	94.50	0.1079	0.04
E08	0.0540	0.0466	86.26	0.0074	13.74	0.2485	0.2400	96.59	0.0088	0.04
E09	0.8680	0.4957	57.11	0.3723	42.89	0.7480	0.7052	94.28	0.0429	0.06
E10	0.8076	0.1195	14.79	0.1852	22.93	0.6612	0.2115	31.99	0.0044	0.01
E11	0.2219	0.0802	36.13	0.1417	63.87	0.2354	0.2051	87.15	0.0375	0.16
E12	0.8775	0.7477	85.21	0.1298	14.79	0.6761	0.6271	92.75	0.0491	0.07
E13	0.2871	0.1364	47.50	0.1508	52.50	0.8103	0.7632	94.19	0.0471	0.06
E14	0.2522	0.1700	67.38	0.0823	32.62	0.8437	0.7975	94.53	0.0462	0.05
E15	6.6782	2.6647	39.90	4.0135	60.10	5.6648	5.3298	94.09	0.3381	0.06
E16	0.0099	0.0041	41.63	0.0058	58.37	0.1139	0.0991	87.01	0.0148	0.13
E17	0.0034	0.0002	6.70	0.0031	93.30	0.0272	0.0193	71.19	0.0080	0.29
E18	1.6078	1.4770	91.87	0.1381	8.59	0.4880	0.4163	85.30	0.0723	0.15
E19	0.1756	0.1385	78.87	0.0371	21.13	0.2325	0.1897	81.57	0.0432	0.19
E20	0.9486	0.7074	74.57	0.2412	25.43	0.9482	0.8540	90.06	0.0951	0.10
E21	0.0005	0.0000	0.00	0.0005	100.00	0.1454	0.1119	76.96	0.0335	0.23
E22	0.0696	0.0377	54.11	0.0320	45.89	0.7743	0.6890	88.98	0.0853	0.11
E23	0.0354	0.0156	44.01	0.0198	55.99	0.2607	0.2306	88.45	0.0304	0.12
E24	0.0273	0.0135	49.38	0.0138	50.62	0.2756	0.2588	93.91	0.0168	0.06
E25	0.0000	0.0000	0.00	0.0865	0.00	0.0819	0.0738	90.16	0.0081	0.10
E26	0.2416	0.1550	64.18	0.0000	0.00	0.7643	0.7008	91.70	0.0637	0.08
E27	0.4594	0.2979	64.85	0.1615	35.15	0.4578	0.4182	91.36	0.0394	0.09
E28	0.0255	0.0052	20.17	0.0204	79.83	0.3416	0.3178	93.03	0.0238	0.07
E29	1.1117	1.0215	91.89	0.0902	8.11	0.5055	0.4557	90.14	0.0521	0.10
E30	18.4915	17.5535	94.93	0.9380	5.07	10.9432	10.5211	96.14	0.4286	0.04
Total	**57.6041**	**38.0351**	**66.03**	**19.1295**	**33.21**	**38.3214**	**35.3549**	**92.26**	**2.4927**	**0.07**
mean			51.50		36.54			87.20		0.10

Table 3. Geospatial overlay data for total aspen area and shrubs of the 2016 GNSS mapping data (ha) and the 2017 Digitized polygons.

	Total Aspen					Shrubs				
Stand	2016 GNSS	Intersection	Intersect Proportion	Erase	Erase Proportion	2016 GNSS	Intersection	Intersect Proportion	Erase	Erase Proportion
E01	0.8117	0.7751	95.50	0.0581	7.16	0.0908	0.0548	60.34	0.0360	39.66
E02	2.5750	2.4626	95.63	0.9348	36.30	0.3478	0.3196	91.89	0.0282	8.11
E03	24.9434	13.8989	55.72	11.0450	44.28	1.0663	0.9858	92.45	0.0805	7.55
E04	3.2553	3.0557	93.87	0.3945	12.12	0.0993	0.0770	77.58	0.0223	22.42
E05	0.4339	0.3861	88.97	0.0860	19.81	0.1056	0.0874	82.74	0.0182	17.26
E06	0.3007	0.2740	91.13	0.0267	8.87	0.0286	0.0271	94.77	0.0015	5.23
E07	4.1032	3.9954	97.37	0.6172	15.04	0.2749	0.1076	39.15	0.0633	23.02
E08	0.3025	0.2937	97.09	0.0162	5.36	0.0541	0.0236	43.70	0.0305	56.30
E09	1.6159	1.5731	97.35	0.4152	25.69	0.4653	0.0186	4.01	0.1473	31.65
E10	1.4688	0.5105	34.76	0.1896	12.91	0.5766	0.0297	5.15	0.0630	10.92
E11	0.4573	0.4198	91.81	0.1792	39.19	0.2258	0.1186	52.52	0.1072	47.48
E12	1.5536	1.5045	96.84	0.1789	11.51	0.0373	0.0189	50.70	0.0184	49.30
E13	1.0974	1.0503	95.71	0.1979	18.03	0.0434	0.0324	74.57	0.1258	0.01
E14	1.0959	1.0498	95.79	0.1284	11.72	0.1335	0.0535	40.05	0.0800	59.94
E15	12.3430	12.0050	97.26	4.3515	35.26	0.6616	0.5416	81.86	0.1205	18.21
E16	0.1238	0.1090	88.05	0.0206	16.63	0.0154	0.0066	43.08	0.0088	56.92
E17	0.0305	0.0226	73.95	0.0111	36.30	0.0265	0.0223	84.21	0.0042	15.79
E18	2.0953	2.0230	96.55	0.2105	10.04	0.0646	0.0610	94.43	0.0036	5.57
E19	0.4081	0.3649	89.40	0.0803	19.69	0.0232	0.0206	88.63	0.0026	11.37
E20	1.8968	1.8017	94.99	0.3363	17.73	0.1376	0.1334	96.95	0.0042	3.05
E21	0.1460	0.1125	77.04	0.0340	23.31	0.1039	0.0335	32.28	0.0704	67.72
E22	0.8439	0.7586	89.89	0.1173	13.90	0.1447	0.0766	52.95	0.0681	0.07
E23	0.2954	0.2650	89.70	0.0502	17.00	0.0294	0.0289	98.35	0.0005	0.00
E24	0.3029	0.2861	94.46	0.0306	10.11	0.0000	0.0000	0.00	0.0000	0.00
E25	0.0819	0.0738	90.16	0.0746	91.08	0.0000	0.0000	0.00	0.0000	0.00
E26	1.0056	0.9420	93.67	0.0637	6.33	0.2351	0.1626	69.16	0.0725	0.07
E27	0.9165	0.8771	95.70	0.2009	21.92	0.0132	0.0095	71.59	0.0572	0.00
E28	0.3671	0.3433	93.51	0.0442	12.04	0.0136	0.0086	63.31	0.0050	36.69
E29	1.6147	1.5626	96.77	0.1423	8.81	0.7160	0.4517	63.08	0.2643	36.92
E30	29.4393	28.9408	98.31	1.3666	4.64	3.0071	1.8507	61.54	1.1564	38.46
Total	**95.9258**	**81.7375**	**85.21**	**21.6022**	**22.52**	**8.7412**	**2.6603**	**30.43**	**2.6603**	**30.43**
Mean			88.83		21.75			60.12		20.65

2.5.1.1 *Accuracy Assessment of the Digitized polygons*

Completing a post-study accuracy assessment in the field was not possible as the entire study area burned during the Kenow wildfire in September of 2017.

We completed post-prescribed burn mapping on five aspen stands at the same stratified levels as the 2016 stands. The purpose of the mapping was to ground-truth the 2017 UAS aerial imagery data and is also used for ground-truthing the 2017 digitized polygons. The

five stands we mapped in 2017 were randomly selected from the 30 stands mapped in 2016 and the data collected is displayed in Table 4. The accuracy assessment was completed by comparing the digitized polygons to the GNSS ground-truth data collected in 2017 (stands 8,10,17,22 and 27, Table 5 and Figures 16, 17,18).

Table 4. Statistics for the stratified layers on the subset of GNSS mapping data collected in 2017.

Eskerine Complex Aspen Stands 2017 (Hectares)				
Stand	**Canopy**	**Regeneration**	**Avulsion**	**All Aspen**
E08	0.0483	0.2534	0.0910	0.3017
E10	0.0099	0.5974	0.0372	0.3722
E17	0.0015	0.0245	0.0059	0.0260
E22	0.0829	0.7427	0.0556	0.8256
E27	0.3503	0.5612	0.0882	0.9115
Total	**0.4929**	**2.1791**	**0.2779**	**2.4370**

We calculated the areas of omission and commission in ha (Table 5) for the canopy, regeneration, and shrub layers. The grass commission is the area that was digitized as grass but should not have been (grass representing general undescriptive grassland, which is the area outside of all the recorded class layers). The errors of omission consist of all area that belongs in the category but were not collected. The errors of commission included all areas that do not belong in the target category but were incorrectly placed in the target category. For example, while digitizing the regeneration layer, the finite edge of the actual aspen line must be accurately matched to avoid commission or omission. If the analyst veers to the outside of the stand and includes grassland, shrubs or any other landform that is not part of the aspen stand, this would be considered a commission. If the analyst does not include an area of aspen that should have been included in the layer, this is considered omission.

The total area in ha of omission for the canopy layer was 0.212 and the total commission area was 0.098. The total omission area of the regeneration was 0.234, and the total commission area was 0.245. The total omission area of the shrubs was 22.6, and the total

commission area was 0.429. (Table 5). The accuracy column in Table 5 is the total proportion that was digitized correctly for each layer. We digitized over 99% of the canopy correctly, 87% of the regeneration correctly and 34% of the shrubs correctly. The canopy and regeneration accuracies are acceptable when compared to satellite-derived data accuracy thresholds (85% is generally considered acceptable), while the shrub accuracy is not. The accuracies of the shrub layers omission and commission demonstrate significant errors in the digitization of the layer. The accuracy numbers do not account for the areas of omission but do account specifically for the total area that was digitized correctly in all layers.

Table 5. Accuracy assessment for the digitized polygons. The accuracy row represents the area of each layer that was digitized correctly.

Geospatial Analysis of the Digitized Aspen Subset Commission/Omission Data in Hectares

Layer	Data	E08	E10	E17	E22	E27	Total	Accuracy
Canopy	Ommision	-0.0111	-0.0745	-0.0011	-0.0430	-0.0822	-0.2119	
	Commission	0.0161	0.0091	0.0003	0.0186	0.0533	0.0975	**99.45%**
	Total	**0.0050**	**-0.0654**	**-0.0008**	**-0.0244**	**-0.0289**	**-0.1145**	
Regeneration	Ommision	-0.0206	-0.0147	-0.0043	-0.1012	-0.0936	-0.2343	
	Commission	0.0674	0.0298	0.0080	0.0675	0.0723	0.2449	**87.30%**
	Total	**0.0468**	**0.0151**	**0.0037**	**-0.0337**	**-0.0213**	**0.0106**	
Shrub	Ommision	-0.0161	-0.0989	-0.0261	-0.0743	-0.0109	-0.2262	
	Commission	0.1022	0.0233	0.0226	0.0067	0.0244	0.1791	**34.56%**
	Total	**0.0861**	**-0.0756**	**-0.0035**	**-0.0676**	**0.0135**	**-0.0471**	

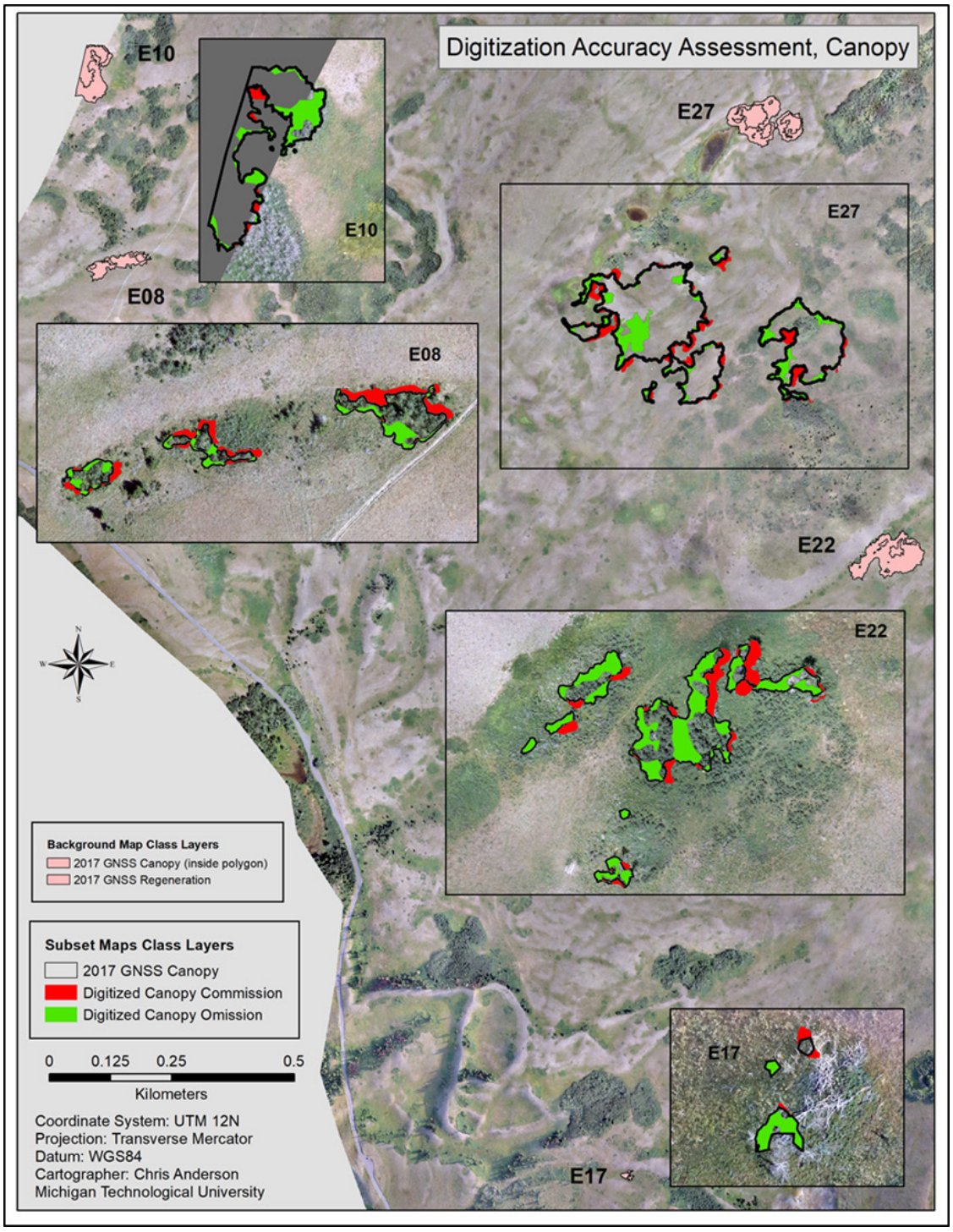

Figure 16. Digitized canopy commission – omission assessment. Background polygons identify the stands location in the study area, inset maps display omission and commission. Red = area that was included but should not have been. Green = area that was not included but should have been.

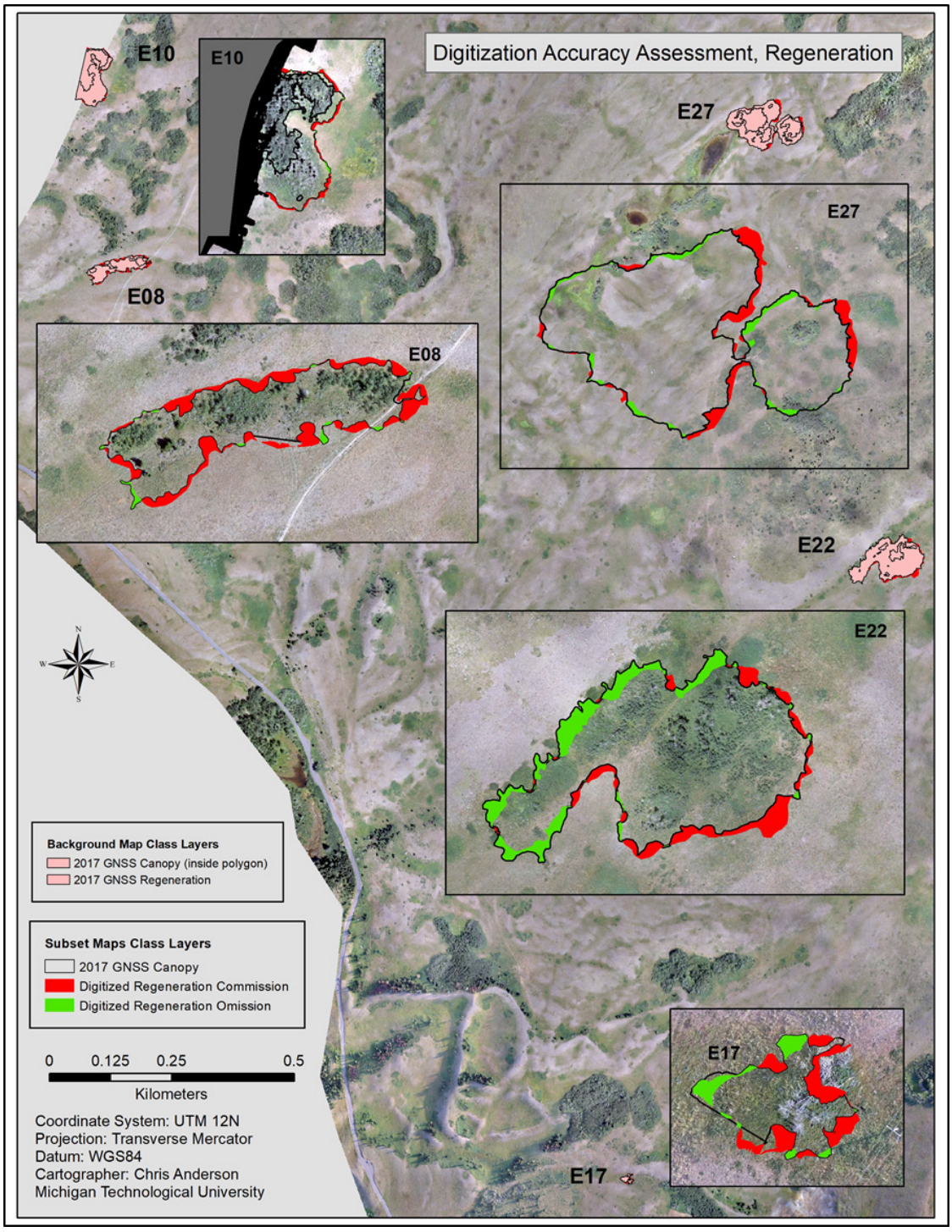

Figure 17. Digitized regeneration commission – omission assessment. Background polygons identify the stands location in the study area, inset maps display omission and commission. Red = area that was included but should not have been. Green = area that was not included but should have been.

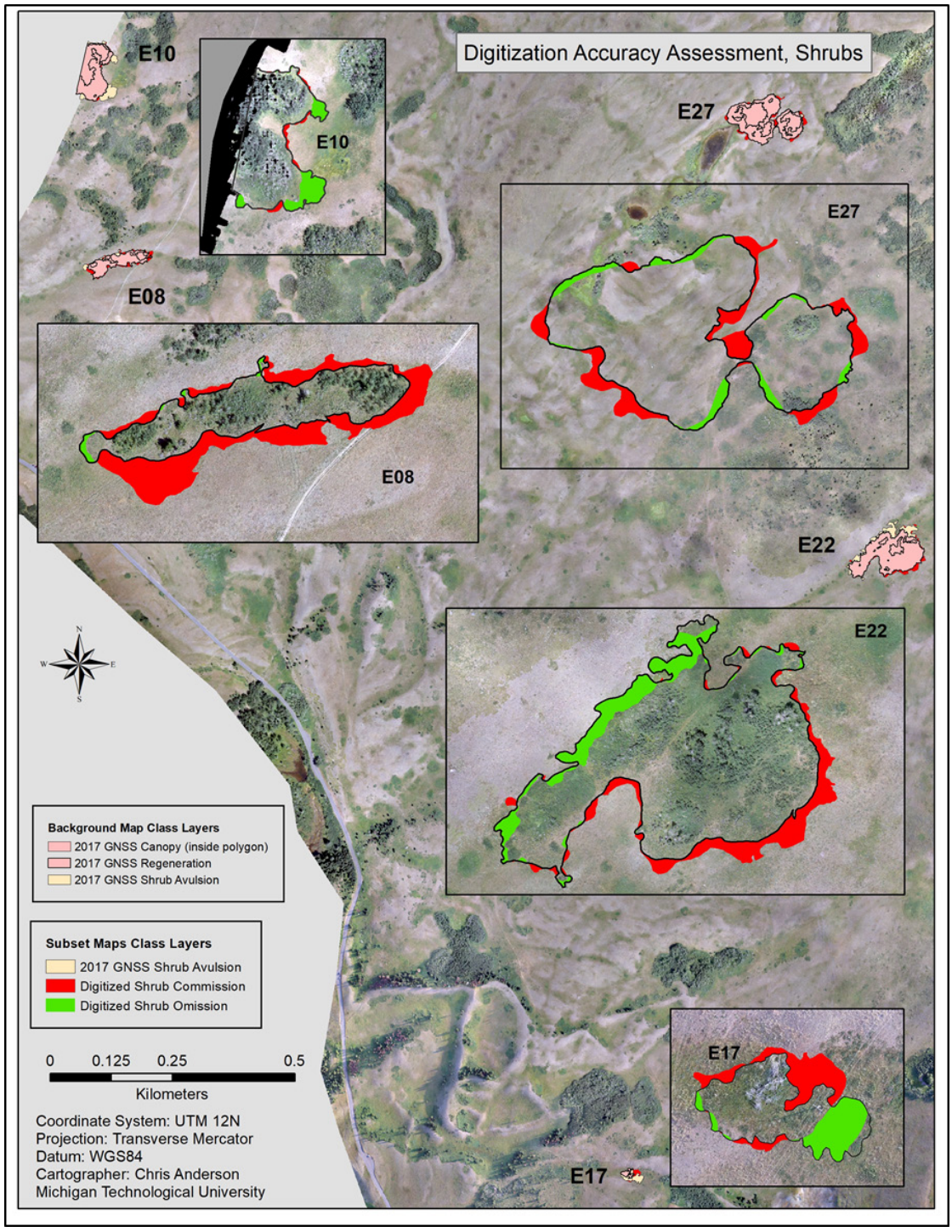

Figure 18. Digitized shrub commission – omission assessment. Background polygons identify the stands location in the study area, inset maps display omission and commission. Red = area that was included but should not have been. Green = area that was not included but should have been.

2.6 Knowledge Engineer Results

For the 2016 GNSS and 2017 KE polygon comparison, total aspen area in ha (canopy and regeneration) decreased by 36.47, from 95.94 with a 95% confidence interval of ± 1.26 to 59.47 ± 0.89, (t = 0.784, 58 df, p = 0.217). Mean aspen stand area decreased from 3.17 ±2.58, range = 29.40 to 1.98 ±2.61, range = 22.00. Aspen canopy in ha throughout the study area decreased by 17.90, from 57.10 ±0.94 to 39.20 ± 0.73 (t = 0.54, 54 df, p = 0.295). Mean canopy area decreased from 2.04 ±1.80, range = 19.72 to 1.30 ±1.42, range = 18.19 (this change was not statistically significant). The area in ha of aspen regeneration decreased from 38.22 ±0.781 to 31.23 ±1.09 (t = 0.419, 58 df, p = 0.338). Mean regeneration area in ha decreased from 1.27 ±0.84, range = 10.91 to 1.04 ±0.78, range = 8.12.

The overall aspen stand area from before (2016) to after the prescribed burn (2017) remained relatively unchanged. Although the difference is not significant, it is important to note that the image classification accounted for gaps within the aspen stands, whereas the GNSS data collection does not.

2017 KE data: We created stratified layers for all 30 aspen stands and calculated the area of each stand in ha for the canopy and regeneration levels and accounted for total aspen. The largest overall aspen stand, E30, was 22.006 ha, and the smallest was E25, which was 0.001 ha. Two aspen stands, E05 and E25, did not have any stems in the canopy layer (Figure 21).

Table 6. Side by Side comparison of the 2016 GNSS aspen stand mapping area (ha) to the KE classification

Stand	2016 GNSS Canopy	2017 UAS Canopy	2016 GNSS Regen	2017 UAS Regen	2016 GNSS All Aspen	2017 UAS All Aspen
E01	0.1383	0.1898	0.6733	0.2421	0.8117	0.3309
E02	1.2372	0.6404	1.3378	0.4149	2.5750	0.8945
E03	19.7258	11.4393	5.2176	8.1210	24.9434	16.3751
E04	1.9188	1.3508	1.3365	1.2228	3.2553	2.1663
E05	0.0000	0.0000	0.4339	0.0036	0.4339	0.0036
E06	0.1281	0.0237	0.1726	0.1680	0.3007	0.1685
E07	1.2017	0.6994	2.9015	1.7362	4.1032	1.9980
E08	0.0540	0.0060	0.2485	0.0930	0.3025	0.0934
E09	0.8680	0.5091	0.7480	0.6187	1.6159	0.8643
E10	0.8076	0.0673	0.6612	0.0955	1.4688	0.1392
E11	0.2219	0.1974	0.2354	0.1136	0.4573	0.2734
E12	0.8775	0.1389	0.6761	0.9773	1.5536	0.9794
E13	0.2871	0.1117	0.8103	0.3849	1.0974	0.4516
E14	0.2522	0.0814	0.8437	0.3194	1.0959	0.3237
E15	6.6782	2.5632	5.6648	5.5709	12.3430	6.6097
E16	0.0099	0.0047	0.1139	0.0555	0.1238	0.0587
E17	0.0034	0.0011	0.0272	0.0424	0.0305	0.0424
E18	1.6078	1.0819	0.4880	1.0349	2.0953	1.8176
E19	0.1756	0.0277	0.2325	0.2502	0.4081	0.2506
E20	0.9486	0.5004	0.9482	0.7562	1.8968	0.9630
E21	0.0005	0.0000	0.1454	0.0041	0.1460	0.0041
E22	0.0696	0.0199	0.7743	0.2685	0.8439	0.2719
E23	0.0354	0.0323	0.2607	0.0327	0.2954	0.0537
E24	0.0273	0.0021	0.2756	0.0538	0.3029	0.0539
E25	0.0000	0.0001	0.0819	0.0007	0.0819	0.0008
E26	0.2416	0.1952	0.7643	0.1652	1.0056	0.3040
E27	0.4594	0.1184	0.4578	0.4851	0.9165	0.5445
E28	0.0255	0.0001	0.3416	0.0317	0.3671	0.0317
E29	1.1117	1.0839	0.5055	0.5349	1.6147	1.3929
E30	18.4915	18.1927	10.9432	7.4276	29.4393	22.0064
Total	**57.6041**	**39.2788**	**38.3214**	**31.2253**	**95.9258**	**59.4678**

We conducted a geospatial overlay analysis to calculate the geometric intersection on the 2016 GNSS mapping data and the KE classification data. The proportion of intersected canopy (Figure 25) ranged from 0.00% – 86.22%, with a mean of 33.81% and a 95% confidence interval of ±10.03%. The intersection data represents the proportion of the aspen stand that did not succumb to the prescribed burn. The erase data is the proportion of each aspen stand that succumbed to the prescribed burn. The proportion of canopy erase ranged from 0.00% – 99.99%, with a mean of 57.54% ±11.02% (Table 7). This means that 33.81 % of canopy remained in the aspen stands after the prescribed burn and 57.54% of the canopy area found during the mapping of 2016 was not found while the KE classification was completed (this area burned during the prescribed burn). The proportion of intersected regeneration (Figure 26) ranged from 0.73% – 94.58%, with a mean of 20.97% ±6.61%. The proportion of regeneration erase ranged from 5.41% – 99.26%, with a mean of 76.45 ±7.69 (Table 7). This means that 20.97% of regeneration remained in the aspen stands after the prescribed burn and 76.45% of the regeneration area that was found during the GNSS mapping of 2016 was not found while the KE classification was completed. The proportion of total aspen intersected ranged from 0.73% – 95.17%, with a mean of 43.16 ±9.52. The proportion of total aspen erase ranged from 4.82% – 99.26%, with a mean of 54.65% (Table 8). This means that 43.16% of the total aspen remained in the aspen stands after the prescribed burn and 54.65% of the area of total aspen found during the GNSS mapping of 2016 was not found while the KE digitization was completed.

Table 7. Geospatial overlay data of the aspen canopy and regeneration for the 2016 GNSS mapping data (ha) and the 2017 KE classification polygons (displayed in Figures 25 and 26).

	Canopy					Regeneration				
Stand	2016 GNSS	Intersection	Intersect Proportion	Erase	Erase Proportion	2016 GNSS	Intersection	Intersect Proportion	Erase	Erase Proportion
E01	0.1383	0.0832	60.12	0.0552	39.88	0.6733	0.1945	28.89	0.4788	71.11
E02	1.2372	0.6019	48.65	0.6353	51.35	1.3378	0.0931	6.96	1.2450	93.06
E03	19.7258	11.3439	57.51	8.3830	42.50	5.2176	0.6364	12.20	4.5795	87.77
E04	1.9188	1.3008	67.80	0.6179	32.20	1.3365	0.2680	20.05	1.0692	80.00
E05	0.0000	0.0000	0.00	0.0000	0.00	0.4339	0.0032	0.74	0.4307	99.26
E06	0.1281	0.0221	17.23	0.1060	82.77	0.1726	0.0466	26.99	0.1260	73.01
E07	1.2017	0.5659	47.09	0.6908	57.48	2.9015	0.9466	32.62	1.9021	65.56
E08	0.0540	0.0000	0.00	0.0518	95.97	0.2485	0.0441	17.77	0.2047	82.37
E09	0.8680	0.4839	55.76	0.3840	44.24	0.7480	0.1200	16.04	0.6281	83.97
E10	0.8076	0.0611	7.57	0.2380	29.47	0.6612	0.0217	3.29	0.1225	18.52
E11	0.2219	0.1673	75.38	0.0546	24.62	0.2354	0.0443	18.84	0.1976	83.93
E12	0.8775	0.1362	15.52	0.7413	84.48	0.6761	0.1638	24.23	0.5123	75.77
E13	0.2871	0.0946	32.94	0.1925	67.06	0.8103	0.1953	24.11	0.6149	75.89
E14	0.2522	0.0766	30.37	0.1756	69.63	0.8437	0.1207	14.31	0.7230	85.69
E15	6.6782	2.4679	36.96	4.2102	63.04	5.6648	1.1525	20.35	4.5144	79.69
E16	0.0099	0.0024	24.22	0.0075	75.78	0.1139	0.0434	38.09	0.0705	61.91
E17	0.0034	0.0004	11.48	0.0030	88.52	0.0272	0.0257	94.58	0.0015	5.42
E18	1.6078	1.0542	65.57	0.6053	37.65	0.4880	0.2011	41.22	0.2868	58.77
E19	0.1756	0.0263	15.00	0.1493	85.00	0.2325	0.0795	34.18	0.1531	65.82
E20	0.9486	0.4594	48.43	0.4892	51.57	0.9482	0.1381	14.56	0.8102	85.44
E21	0.0005	0.0000	0.00	0.0005	100.00	0.1454	0.0040	2.73	0.1415	97.27
E22	0.0696	0.0131	18.83	0.0565	81.17	0.7743	0.2155	27.84	0.5587	72.16
E23	0.0354	0.0088	24.86	0.0266	75.14	0.2607	0.0230	8.81	0.2376	91.17
E24	0.0273	0.0020	7.18	0.0253	92.82	0.2756	0.0289	10.49	0.2467	89.51
E25	0.0000	0.0000	0.00	0.0000	0.00	0.0819	0.0007	0.89	0.0812	99.11
E26	0.2416	0.1180	48.86	0.1235	51.14	0.7643	0.0754	9.87	0.6888	90.12
E27	0.4594	0.1158	25.21	0.3436	74.79	0.4578	0.1267	27.67	0.3310	72.31
E28	0.0255	0.0000	0.15	0.0255	99.85	0.3416	0.0228	6.67	0.3188	93.33
E29	1.1117	0.9585	86.22	0.1532	13.78	0.5055	0.1184	23.43	0.3869	76.55
E30	18.4915	15.8004	85.45	2.6911	14.55	10.9432	2.2826	20.86	8.6605	79.14
Total	**57.6041**	**35.9648**	**62.43**	**21.2365**	**36.87**	**38.3214**	**7.4369**	**19.41**	**30.3226**	**0.79**
mean			33.81		57.55			20.98		76.45

Table 8. Geospatial overlay data of the aspen canopy and regeneration for the 2016 GNSS mapping data (ha) and the 2017 KE polygons continued.

Total Aspen					
Stand	2016 GNSS	Intersection	Intersect Proportion	Erase	Erase Proportion
E01	0.8117	0.3308	40.76	0.4808	59.24
E02	2.5750	0.8843	34.34	1.6907	65.66
E03	24.9434	16.2882	65.30	8.6252	34.58
E04	3.2553	2.1606	66.37	1.0947	33.63
E05	0.4339	0.0032	0.74	0.4307	99.26
E06	0.3007	0.1670	55.55	0.1337	44.45
E07	4.1032	1.9877	48.44	2.1155	51.56
E08	0.3025	0.0891	29.47	0.2133	70.53
E09	1.6159	0.8641	53.47	0.7519	46.53
E10	1.4688	0.1391	9.47	0.3758	25.59
E11	0.4573	0.2510	54.88	0.2063	45.12
E12	1.5536	0.9788	63.00	0.5748	37.00
E13	1.0974	0.4514	41.13	0.6460	58.87
E14	1.0959	0.3235	29.52	0.7724	70.48
E15	12.3430	6.5728	53.25	5.7702	46.75
E16	0.1238	0.0480	38.79	0.0758	61.21
E17	0.0305	0.0291	95.18	0.0015	4.82
E18	2.0953	1.7865	85.26	0.3088	14.74
E19	0.4081	0.2503	61.32	0.1579	38.68
E20	1.8968	0.9570	50.45	0.9398	49.55
E21	0.1460	0.0041	2.78	0.1419	97.22
E22	0.8439	0.2715	32.17	0.5724	67.83
E23	0.2954	0.0503	17.01	0.2452	82.99
E24	0.3029	0.0535	17.67	0.2494	82.33
E25	0.0819	0.0008	0.96	0.0811	99.04
E26	1.0056	0.2900	28.84	0.7157	71.16
E27	0.9165	0.5423	59.17	0.3742	40.83
E28	0.3671	0.0313	8.52	0.3359	91.48
E29	1.6147	1.2496	77.39	0.3651	22.61
E30	29.4393	21.7113	73.75	7.6580	26.01
Total	**95.9258**	**58.7672**	**61.2632**	**36.1048**	**37.64**
Mean			43.17		54.66

2.6.1.1 *Knowledge Engineer Accuracy Assessment*

We compared the total area collected in 2017 for each type of data collection (UAS and GNSS) in a subset of 5 stands. The accuracy column in Table 9 is the proportion of each UAS layers area compared to the GNSS layer, canopy 30.39%, regeneration 25.30%, and total aspen 41.69%. All three proportions for layer area collected were unsatisfactory. (The threshold for accuracy is compared to satellite data, 85% is generally considered acceptable) The accuracy standards for UAS derived studies are not well defined. The UAS area data accounts for gaps within the aspen, the GNSS data does not.

Table 9. Direct area comparison of the subset of aspen collected by UAS and GNSS.

Direct Area Comparison by Hectare

Layer	E08	E10	E17	E22	E27	Total Area	Accuracy
GNSS Canopy	0.0483	0.2170	0.0015	0.0829	0.3503	0.7001	
UAS Canopy	0.0060	0.0673	0.0011	0.0199	0.1184	0.2127	30.39%
	0.12	**0.31**	**0.73**	**0.24**	**0.34**	**0.30**	
GNSS Regeneration	0.2534	0.3360	0.0245	0.7427	0.5612	1.9177	
UAS Regeneration	0.0930	0.0955	0.0424	0.2685	0.4851	0.4851	25.30%
	0.37	**0.28**	**1.73**	**0.36**	**0.86**	3.6089	
GNSS All Aspen	0.3017	0.5530	0.0260	0.8256	0.9115	2.6178	
UAS All Aspen	0.0934	0.1392	0.0424	0.2719	0.5445	1.0913	41.69%
	0.31	**0.25**	**1.63**	**0.33**	**0.60**	**0.42**	

Commission and omission assessment.

Total area in ha of omission for the canopy layer was -0.386, and commission was 0.083. Total area in ha of omission for the regeneration layer was -0.249 and commission was 0.434. Total area in ha of omission for all aspen was -1.259, and commission was 0.025. (Table 10).

The accuracy proportions in Table 10 account for all area measured for each layer that was the same geospatially, all layers were unsatisfactory. For example, the KE

classification only measured 18.48% of the canopy accurately when compared to 2017 ground-truth data.

Table 10. Geospatial analysis of the UAS collected aspen subset commission/omission data in ha. The accuracy lists the total proportion of each layer that was classified correctly.

Geospatiol Analysis of the UAS Collected Aspen Subset Commission/Omission Data in Hectares

Layer	Data	E08	E10	E17	E22	E27	Total	Accuracy
Canopy	Ommision	-0.0461	-0.0147	-0.0012	-0.0701	-0.2544	-0.3865	18.48%
	Commission	0.0038	0.0491	0.0008	0.0072	0.0225	0.0833	
	Total	**-0.0424**	**0.0344**	**-0.0004**	**-0.0630**	**-0.2319**		
Regeneration	Ommision	-0.2059	-0.1359	-0.0015	-0.5450	-0.3614	-1.2497	28.68%
	Commission	0.0456	0.0134	0.0194	0.0709	0.2853	0.4345	
	Total	**-0.1603**	**-0.1225**	**0.0179**	**-0.4742**	**-0.0761**		
All Aspen	Ommision	-0.2120	-0.1118	-0.0015	-0.5554	-0.3696	-1.2502	40.70%
	Commission	0.0037	0.0000	0.0179	0.0017	0.0025	0.0258	
	Total	**-0.2083**	**-0.1118**	**0.0164**	**-0.5538**	**-0.3671**		

2.6.1.2 *Total Areas for All Layers measured*

The post-burn canopy area in ha was very similar for both the 2017 digitization data and the KE classification data, 39.2011 and 39.2788, respectively (Table 11). The total area in ha of the regeneration layer was very different for digitization and the KE classification, 56.5264 and 31.2253, respectively (Table 11). The difference is due primarily to the KE classification accounting for the gaps in the aspen, whereas the digitization data does not.

Table 11. Total areas (in ha) for all classes measured for all data collection types.

Total	Canopy	Regeneration	Total Aspen	Shrubs
2016 GNSS Polygons	57.6041	38.3214	95.9258	8.7412
2017 DIgitization	39.2011	56.5264	96.2273	9.8152
2017 KE Classification	39.2788	31.2253	59.4678	N/A

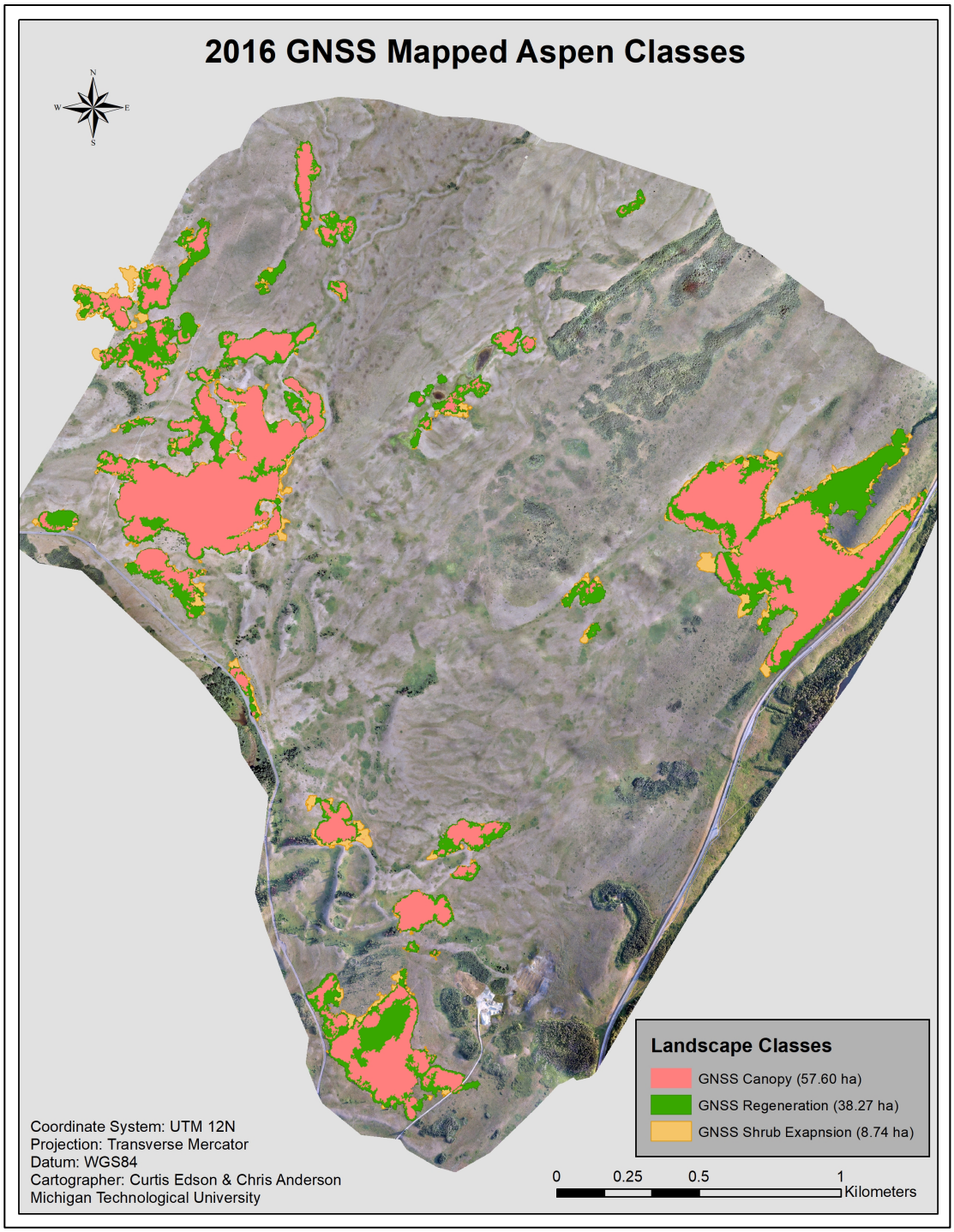

Figure 19. All aspen stand classes mapped in 2016 with GNSS (before prescribed burn), background imagery is UAS imagery flown in 2017.

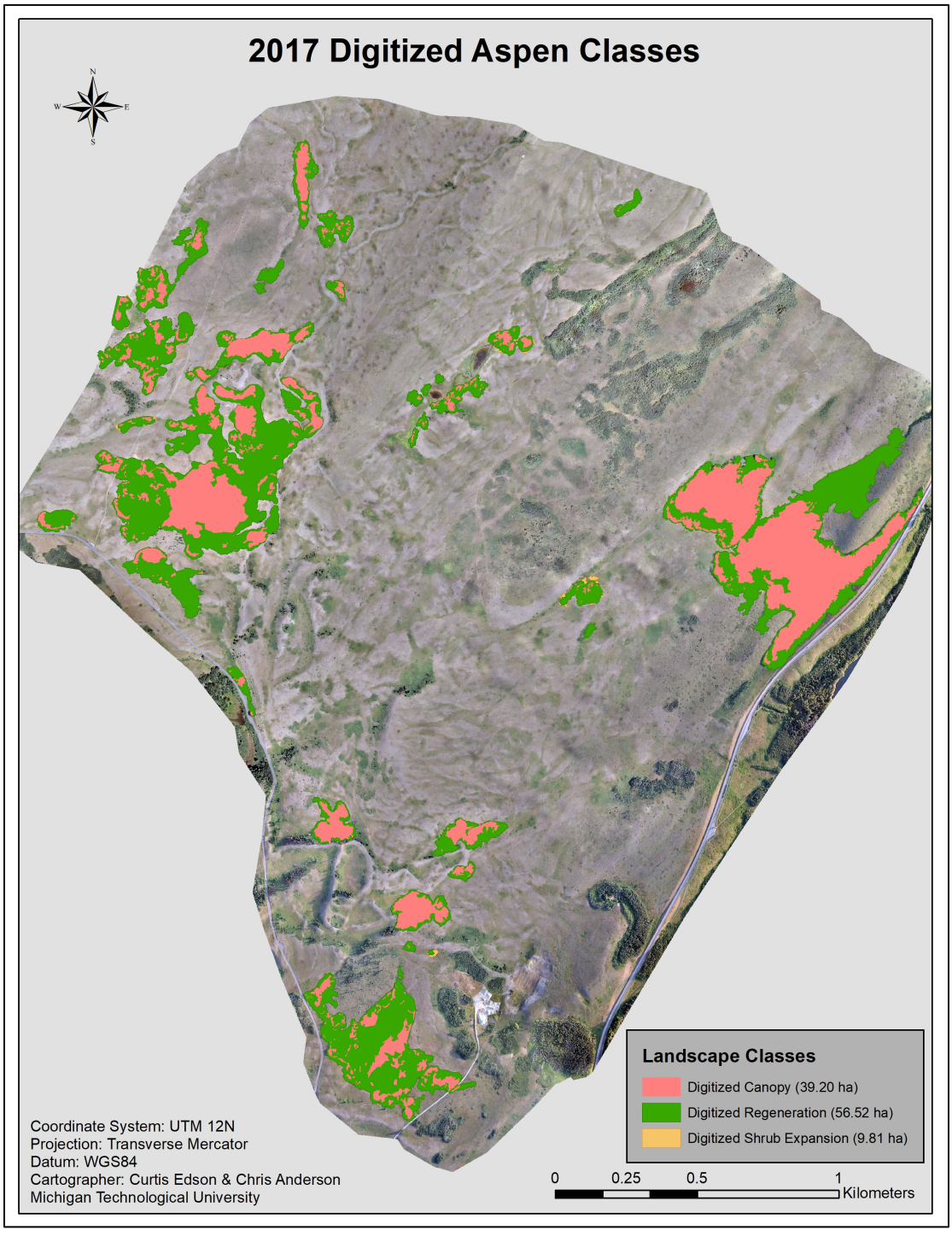

Figure 20. All aspen stands with classes digitized in 2017 with the heads-up method (post-prescribe burn), Background imagery is UAS imagery flown in 2017.

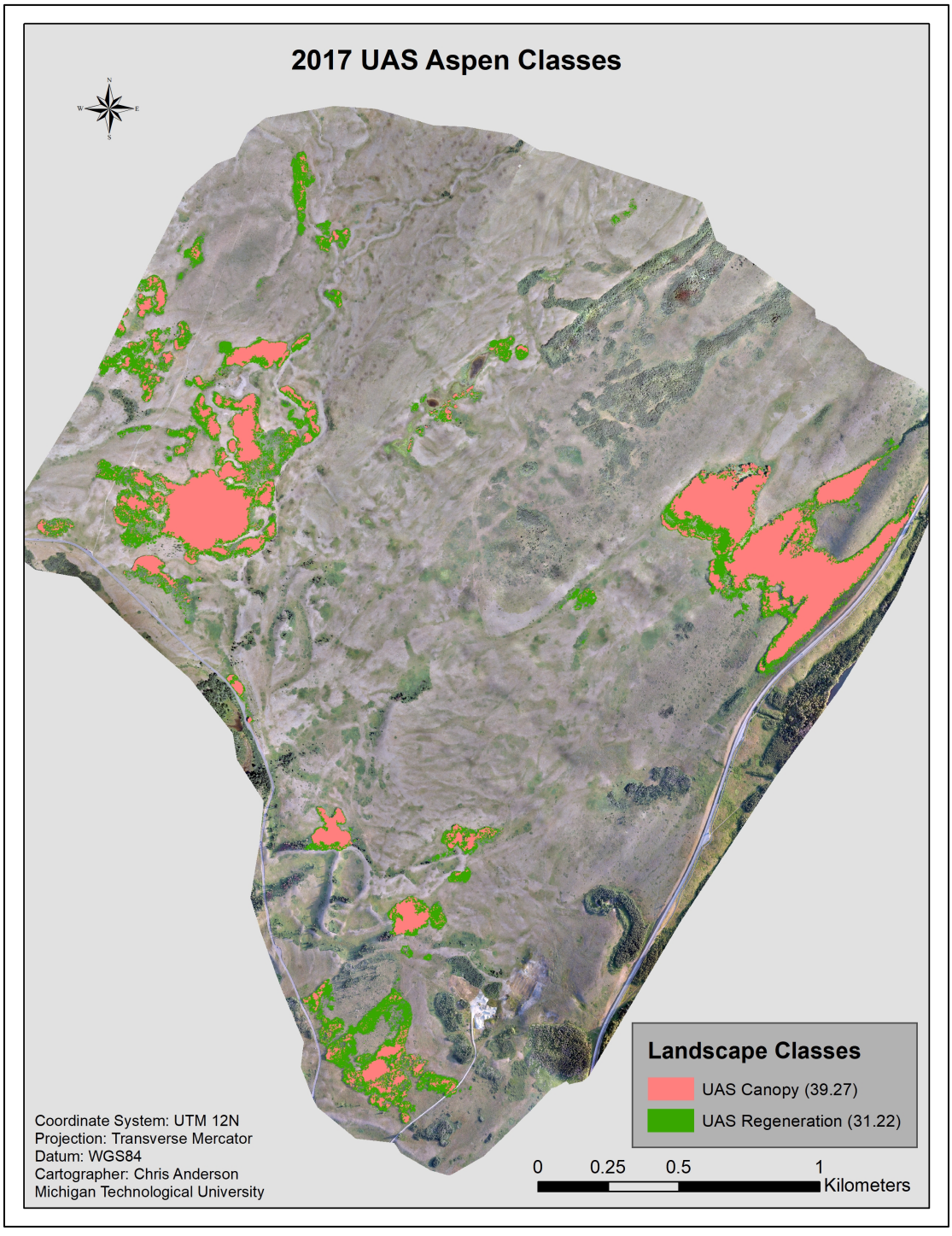

Figure 21. All aspen stands with classes classified with knowledge Engineer from the UAS imagery (post prescribe burn). Background imagery is UAS imagery flown in 2017.

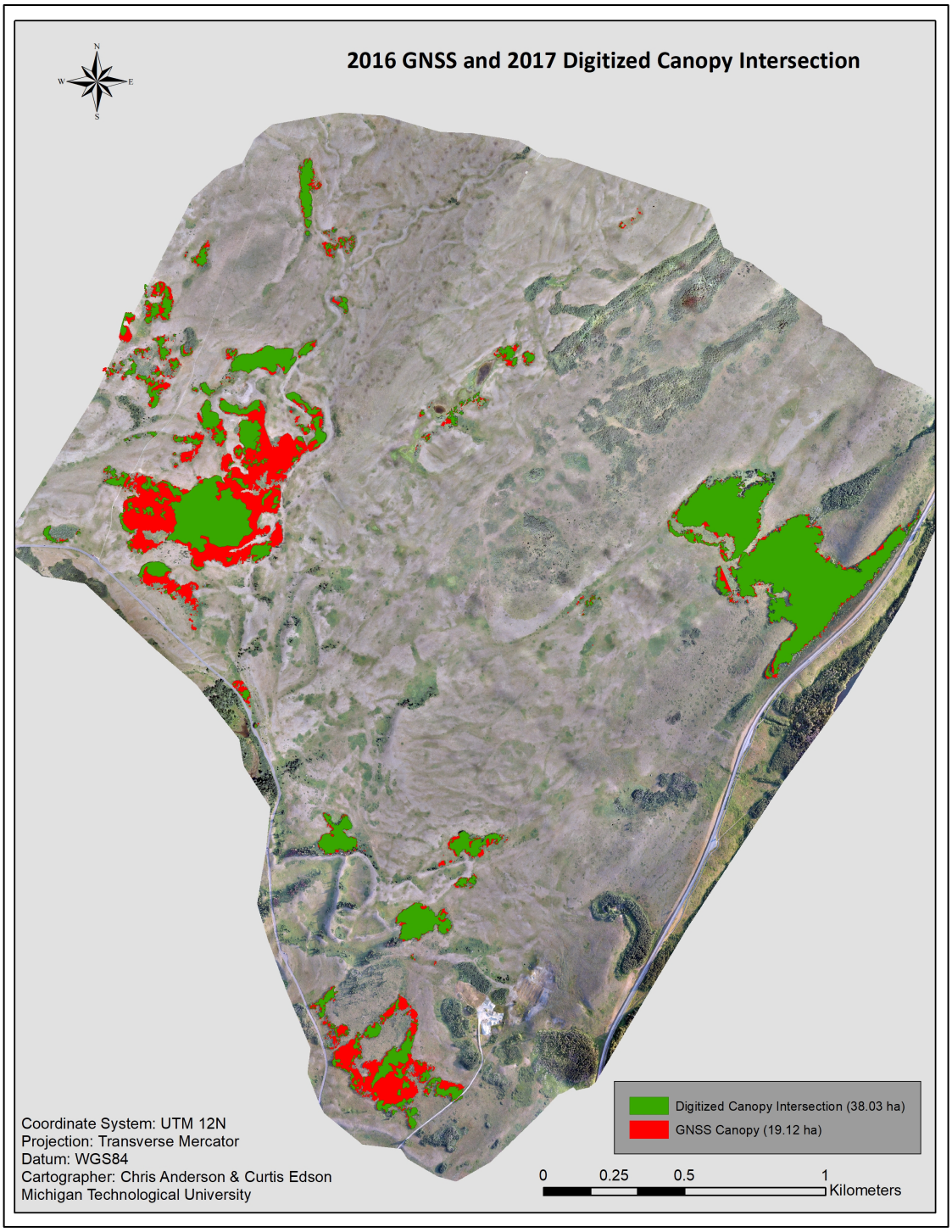

Figure 22. Canopy intersection and erase of the 2016 GNSS and 2017 digitized data. Green = area that was canopy in 2016 and 2017 (intersection). Red = area that was canopy in 2016 but is not in 2017 (erase). Red area = canopy that was burned in the 2017 prescribed burn

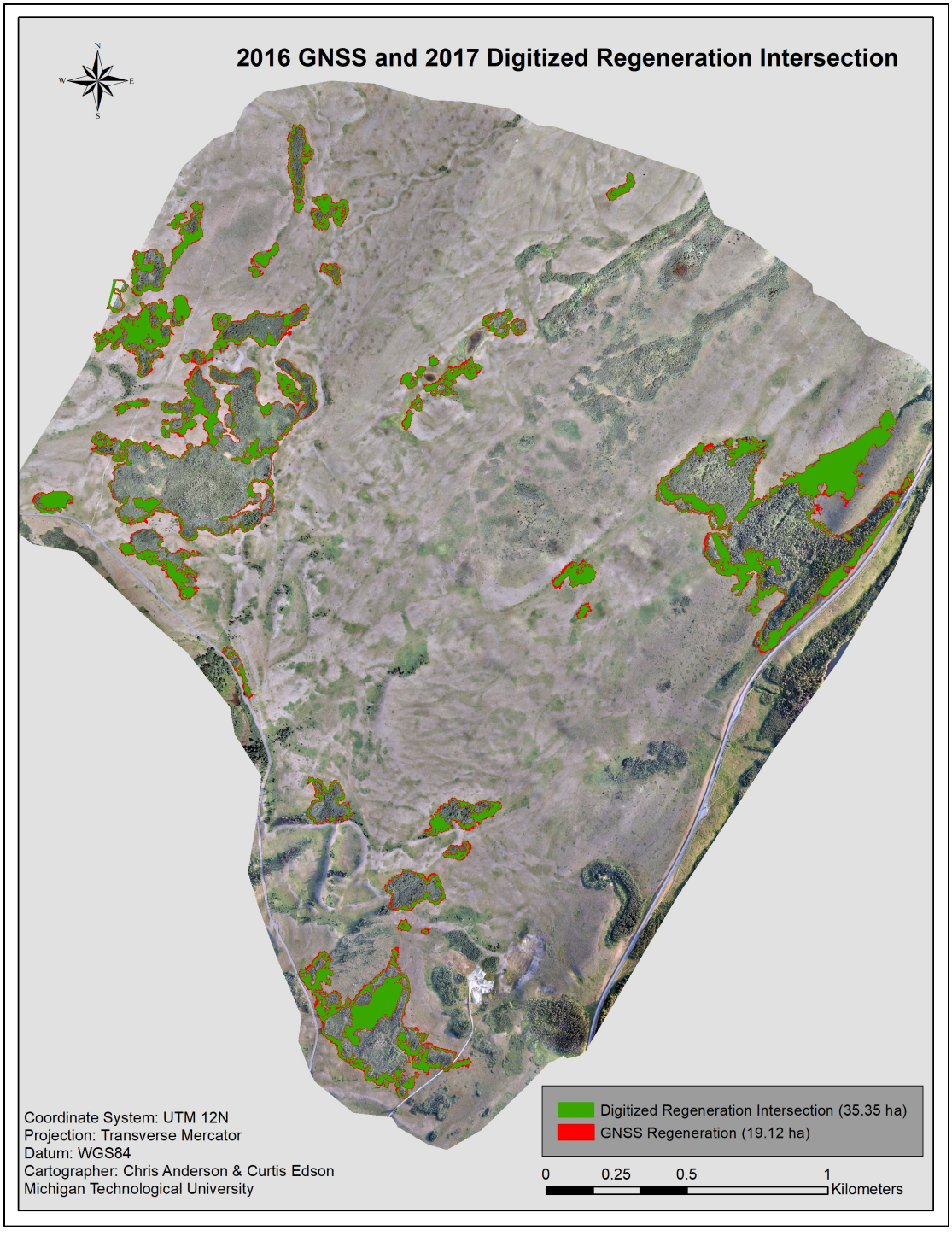

Figure 23. Regeneration Intersection and erase of the 2016 GNSS and 2017 digitized data. Green = area that was regeneration in 2016 and 2017 (intersection). Red = area that was regeneration in 2016 but not in 2017 (erase). Red area = regeneration that was burned in the 2017 prescribed burn

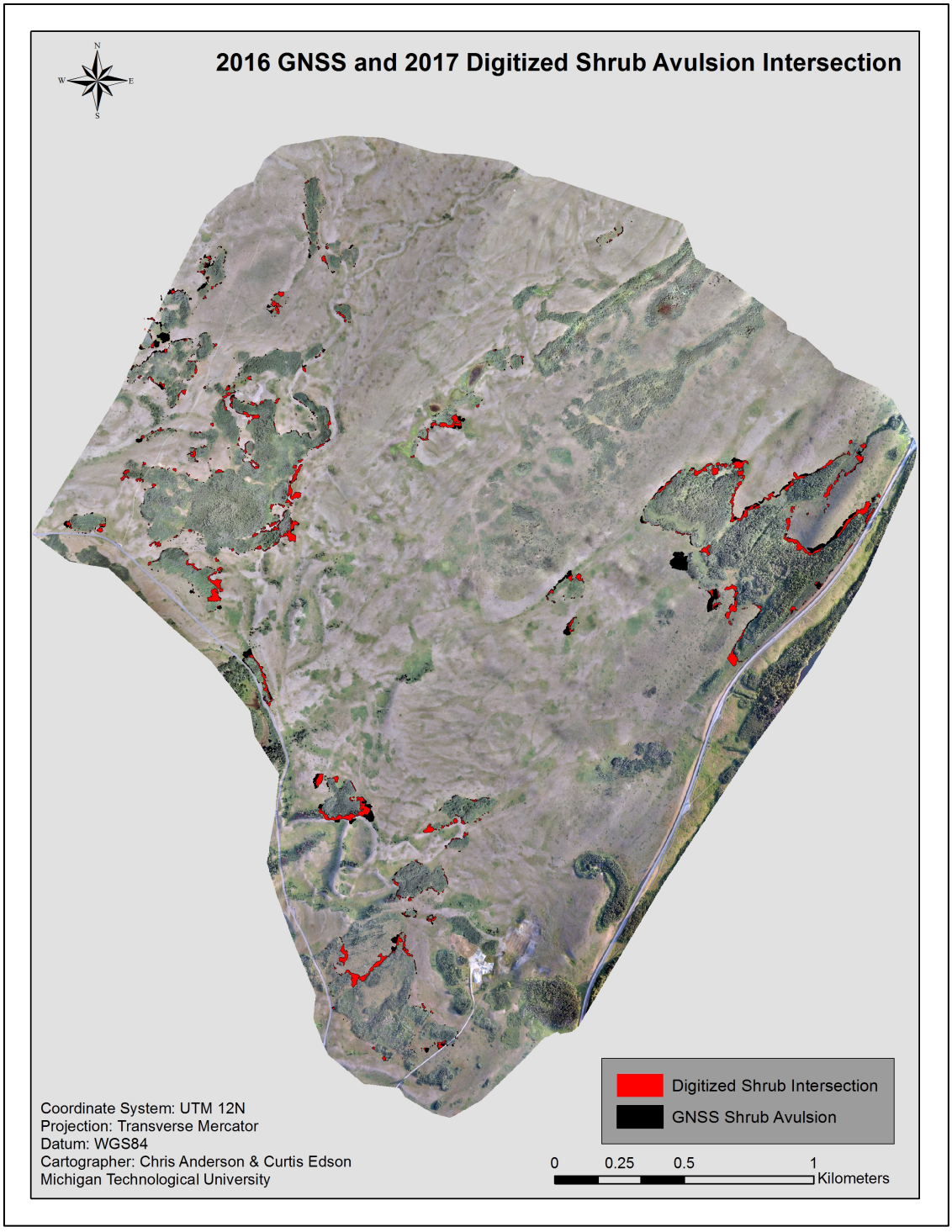

Figure 24. Shrub intersection and erase of the 2016 GNSS and 2017 digitized data. Green = area that was shrubs in 2016 and 2017 (intersection). Red = area that was shrubs in 2016 but not in 2017 (erase). Red area = shrubs that burned in the 2017 prescribed burn

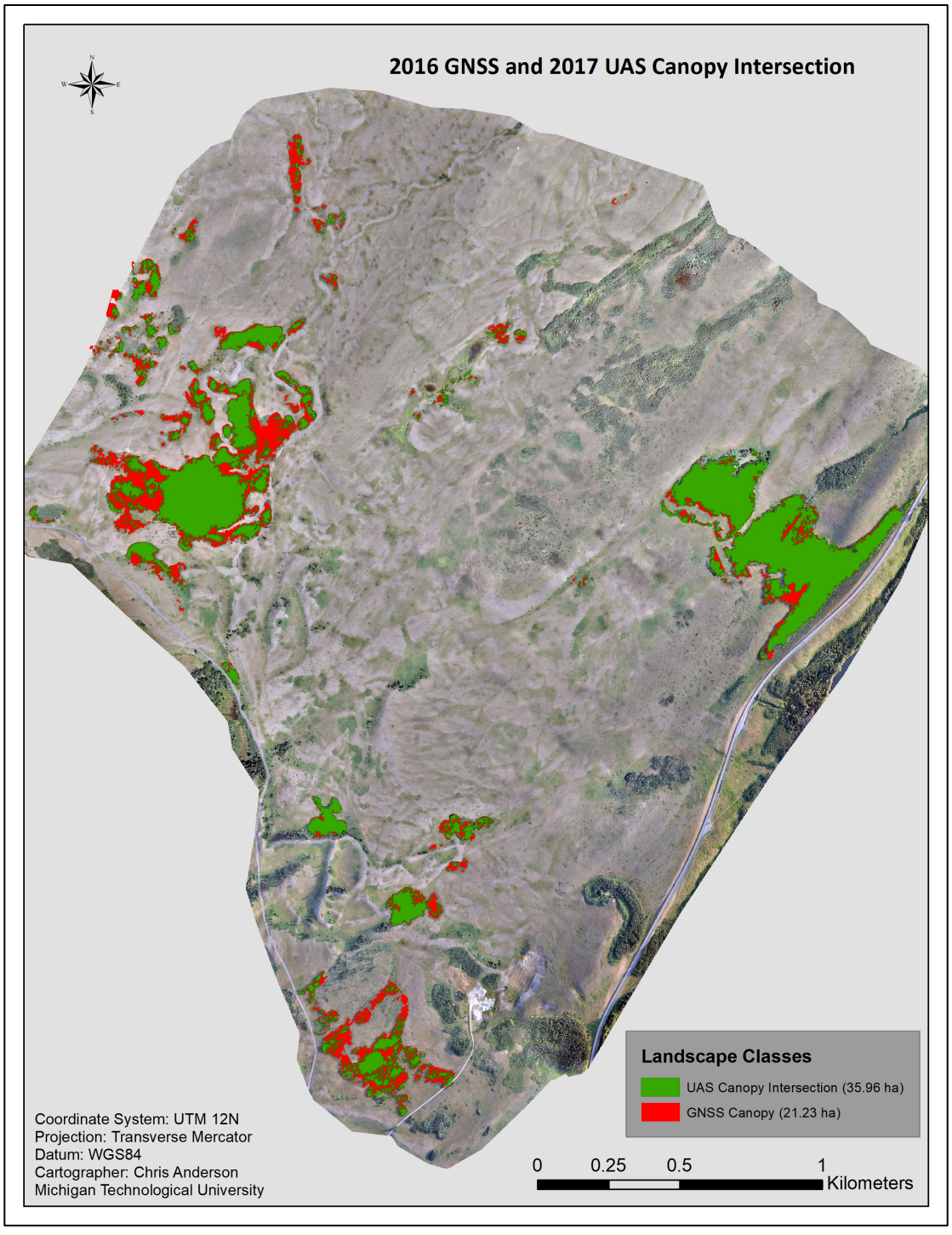

Figure 25. Canopy intersection and erase of the 2016 GNSS mapping and the KE classification of the 2017 UAS imagery. Green = area that was canopy in 2016 and 2017 (intersection). Red = area that was canopy in 2016 but not in 2017 (erase). Red = area that was no longer canopy after the 2017 prescribed burn.

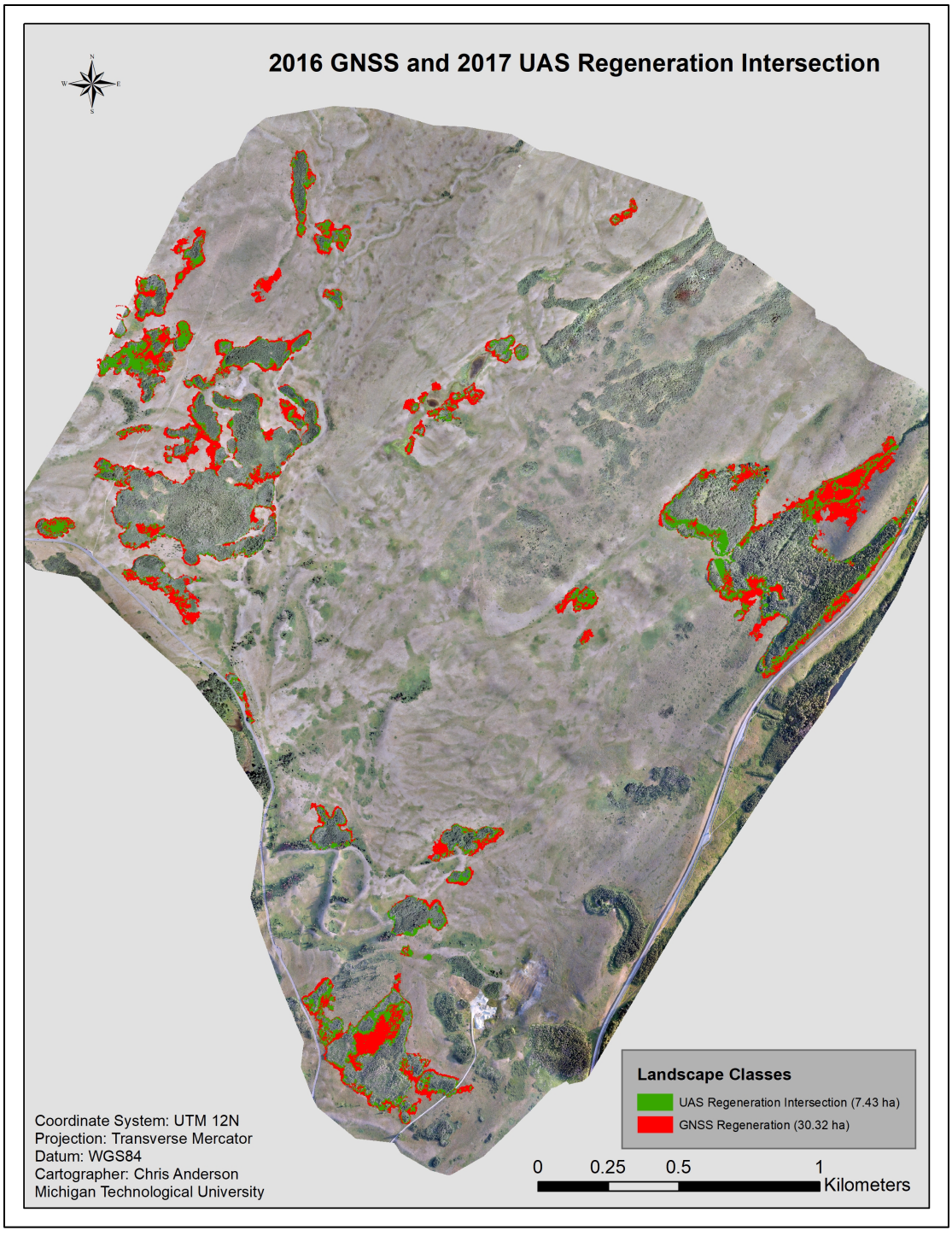

Figure 26. Regeneration intersection and erase of the 2016 GNSS mapping and the KE classification of the 2017 UAS imagery. Green = area that was regeneration in 2016 and 2017 (intersection). Red = area that was regeneration in 2016 but not in 2017 (erase). Red = area that was no longer regeneration after the 2017 prescribed bur

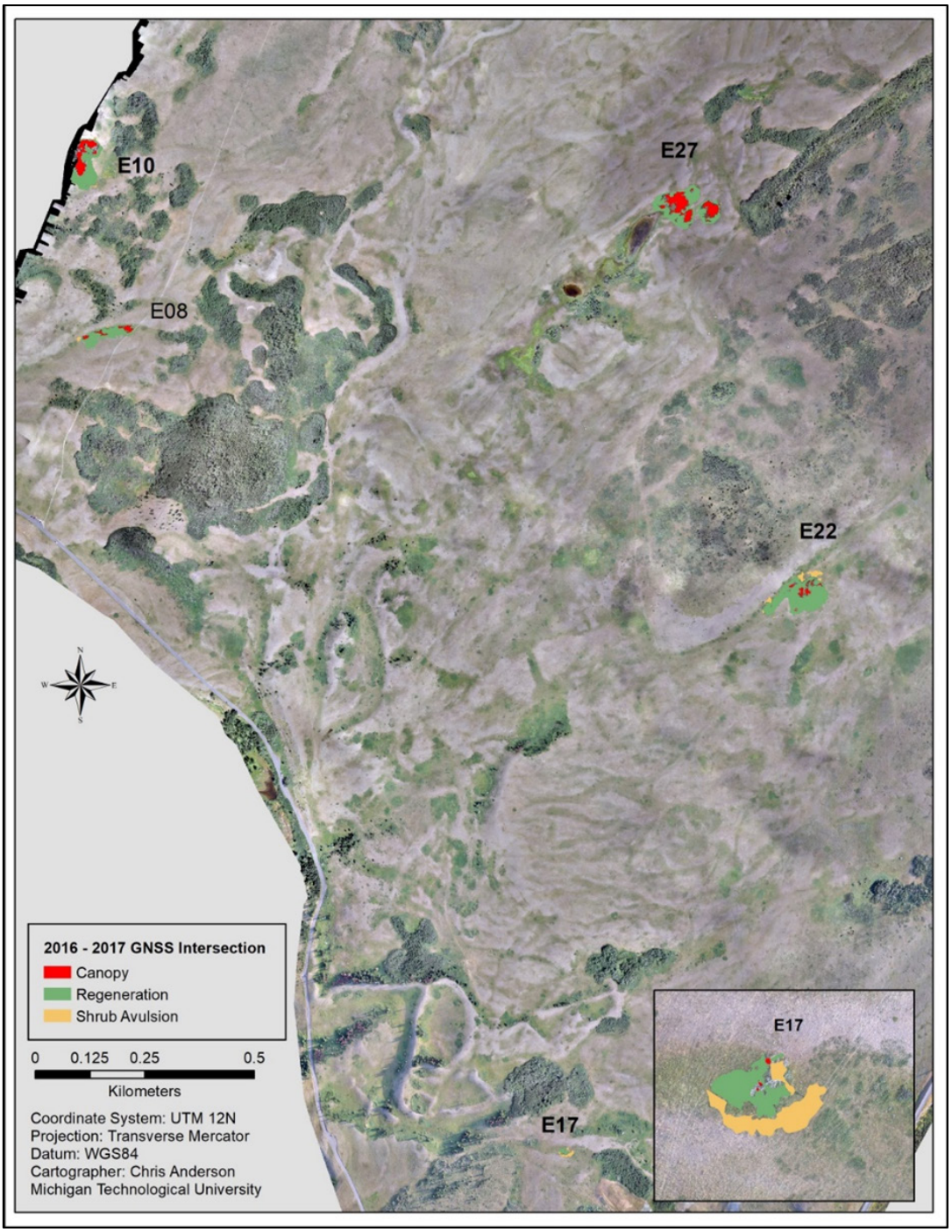

Figure 27. The overlap (intersection) of all stratified classes measured through GNSS mapping in 5 of 30 stands during 2016 and 2017.

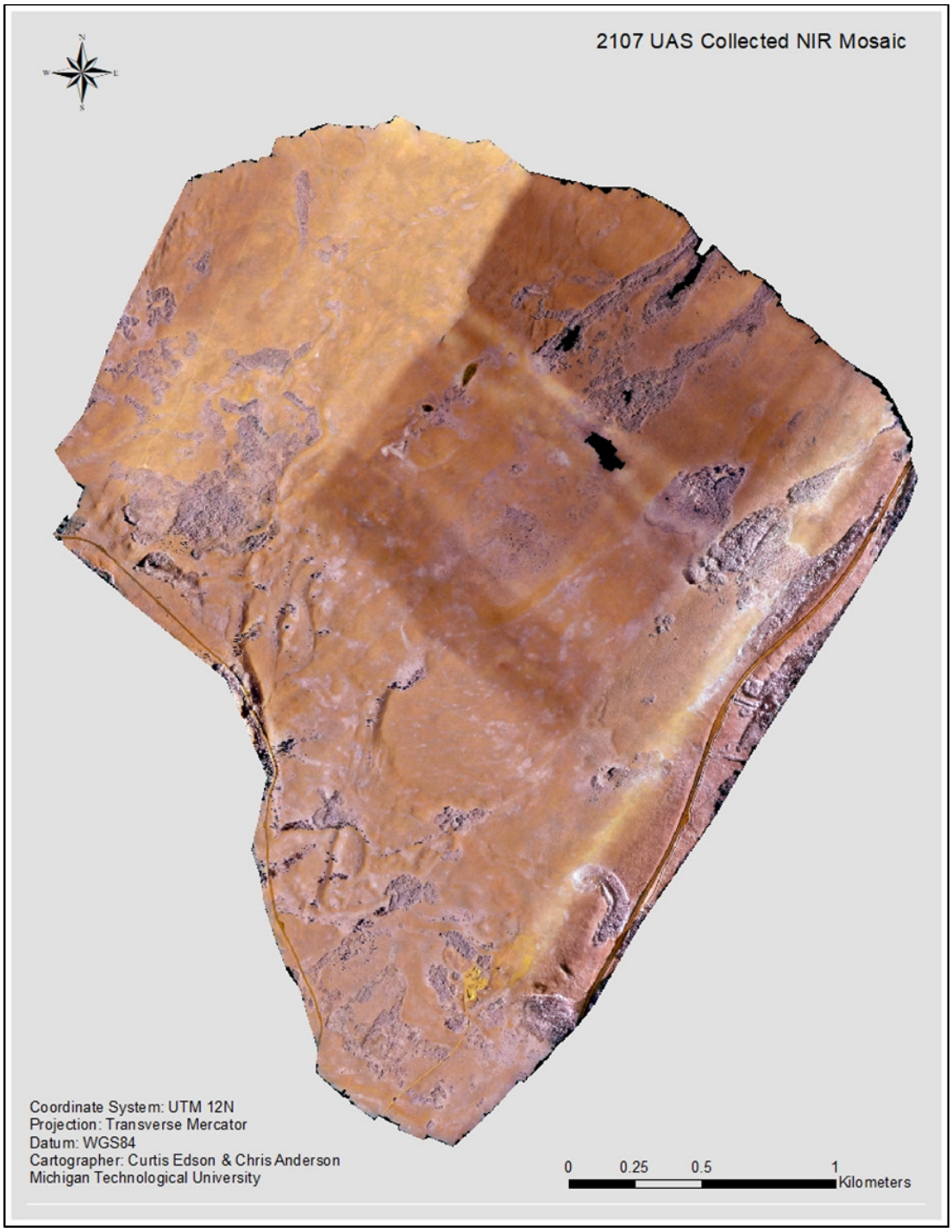

Figure 28. Full mosaic of UAS NIR data, flown in 2017 (UX5HP). The darker red area is the area processed in Agisoft Photoscan compared to TBC & UASMaster

3 Discussion

Our research exemplifies how the implementation of the UAS as a data collection tool is on the technological cutting edge and has strong potential in environmental applications. This technology complements the techniques ecologists use to conduct research and adds to the base of ecological knowledge and available data and methods inventory for natural resource managers (Koh and Wich 2012, Schiffman 2014, Wich and Koh 2018). Overall, the execution of this study and the resulting analysis achieved many of our goals. Although evaluating the imagery had its challenges, the imagery is of excellent quality and can benefit environmental and ecological research at many levels. Throughout the process of collecting, processing, and analyzing data we learned which techniques are beneficial for a project of this geographical size and resolution, and which are not. We have shown that habitat information can be collected over a large study area at one and two-centimeter resolutions. We assessed change in aspen stand spatial heterogeneity from before to after prescribed burning and provided imagery of the Eskerine Complex. The quantity of data collected is an example of how vast amounts of data can be collected via UAS in a relatively short time frame; we collected the imagery for both data sets (NIR & RGB) over three weeks with two field technicians. Future possibilities for data analysis within this data set are very diverse. For example, we could assess animal movement in the study area, as game trails are visible throughout the imagery, and we can analyze specific forest attributes in aspen stands, such as the deadfall in the aspen stands that have burned with extreme severity.

From a management perspective the imagery is beneficial as it allows the identification of aspen stand features that are difficult to accurately identify from traditional field surveys, or from what we encounter while walking the perimeter during the GNSS survey. These attributes include the gaps in the aspen stands or the trails that run through the aspen. Identifying gaps in the aspen is important because the creation of gaps enhances stand spatial heterogeneity: This heterogeneity (e.g., more snags and diverse ages of aspen) improves habitat for songbirds and other species such as the dusky grouse

(*Dendragapus obscurus*), ruffed grouse (*Bonasa umbellus)*, and different plant species that prefer different levels of vegetation or sunlight (Lee 1998, Keyser et al. 2005).

The objectives of our study were to answer the following research questions and demonstrate how UAS could be used to answer them effectively: Specifically, is the combination of prescribed burning and elk browse decreasing woody vegetation and increasing grassland area? Is aspen recruitment decreasing? Is there any change in aspen stand area from before to after prescribed burning? Has prescribed burning affected the structure of the aspen stand? How well can we define the edge of each aspen stand?

We found using UAS technology that the combination of prescribed burning and elk browse did not decrease woody vegetation significantly as the total stand area remained relatively unchanged. Is aspen recruitment decreasing? The results show that the total area consisting of canopy according to the aspen digitization data decreased, therefore this metric suggests that recruitment is decreasing. The digitization data does not tell us if there is recruitment in the interior of the stand. From a statistical point of view, we cannot confidently say that aspen recruitment is decreasing as the results were not statistically significant. The decrease in canopy observed in the aspen digitization data simply means that some canopy area was burned by the to the prescribed burn, it does not tell us if aspen recruitment in the canopy has decreased. Has stand area changed from before to after the prescribed burn? We concluded from the results that the overall aspen area remained relatively unchanged, although the spatial heterogeneity of the stand did change as the regeneration increased and canopy area decreased, but not at a statistically significant level. Has the prescribed burning affected the structure of the aspen stand? The structure of the stand did not change significantly from a statistical point of view. The area consisting of canopy decreased from an observational point of view, and the stand structure did change; but not significantly. For example, the area comprised if canopy decreased by 31.34% as a result of the prescribed burning. How well can we define the edge of each aspen stand by means of the UAS classification? The edge of the stand was difficult to define but not impossible. The total commission for the 5 ground-truthed stands was 0.0833 ha and the total omission was 0.2502 ha. This means that we

included area as aspen that should not have been included more often than we did not include area that we should have. The average size of the ground-truthed stands was 0.4874 ha, which means that we added on average .05 ha or 10% to each stand that should not have been added.

Along with the ecological results, the data collection process emphasizes the importance of how and when to collect data. These are the critical component for any UAS based remote sensing project. For example, two of the critical quality issues in the imagery were oblique photos, wind, and shadows. Although the Trimble aircraft could fly in winds up to 55 km hour, the occasional wind gust would turn the camera to an oblique position. The 80% overlap within the photos prevented the oblique photos from becoming a significant issue in the imagery, but several of the photos were unusable. The wind was also an issue when obtaining imagery of the aspen canopy; on the relatively windy days, taller aspen stems sway in the wind. The aircraft passed over the swaying stem several times, capturing an image correlated with a GNSS coordinate each time it passed overhead. Each photograph was taken when the tree is in a slightly different location, thus receiving a different coordinate on each pass. Areas of dense canopy were also an issue for the sensor. As the images were taken on each pass of the same ground location, but from different angles, obstructions such as branches blocked camera form capturing the exact location as the previous picture. Each of these issues presented a problem when the pictures were mosaicked in Trimble Master and to a lesser extent in Agisoft. The resulting imagery had a blurry spot or a small gap in the imagery as the photogrammetry process could not correlate the many images of that stem with a single coordinate, or the canopy itself obstructed the software from associating images with one another. Figure 29 displays the processing problem areas in the imagery.

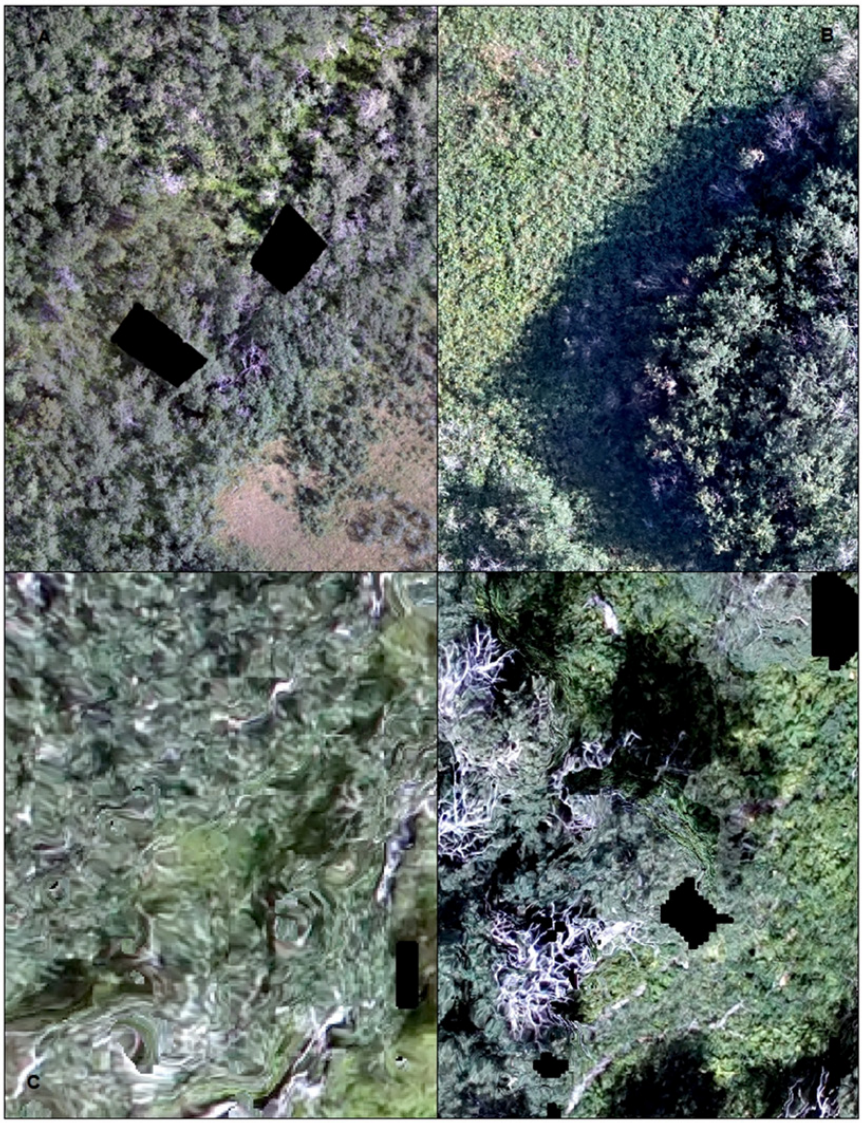

Figure 29. Examples of imagery that that did not process well. Image (A) shows blank areas in the aspen canopy that could not be processed. Image (B) displays shadows in the imagery that caused difficulties while processing the data. Image (C) is an example of a zoommed in view of blurry imagery caused by wind or obstuctions. Image (D) displays both zoomed in view of blurry imagery and blank spots in the same image.

After we examined the results of the Trimble UASMaster processing, we processed the data in AgiSoft following similar steps. The ensuing imagery and classification possess the same complications, but the result was a more satisfactory and complete overall image with fewer areas of blurred imagery or no data. Therefore, the imagery processed

with AgiSoft was the data that was used for further processing and data analysis. A possible way to prevent this from becoming an issue in future research may be to implement a crisscross flight pattern across the study area, or gain permission to fly higher, thus reducing the severity of oblique images. The addition of a flight block that is perpendicular to the current block successfully improved the data processing for other UAS based studies (Oumer et al. 2017), although this may be difficult to implement over a large area due to time constraints.

3.1.1 Pixel Values

The pixel values are a critical aspect of the classification process. We found that in this high-resolution data set of a complicated landscape, several of the landscape classes have very similar pixels, making it difficult for the classification software to decipher between these classes. For example, aspen snags received similar pixel value as rocks and trails, and small aspen had a similar pixel value as shrubs; creating problems when dividing the landscape features into neatly defined layers in the classification. (When stratifying the aspen canopy layer from all other vegetation we are separating a mix of snags shadows and shrubs mixed in with live aspen). Therefore, the resulting aspen stand classification is a mix of pixels representing aspen, shadows, shrubs, and snags that resembles a checkerboard or a splattering of colors, when what we need for the methods we instituted is a dense cluster for each layer. A cluster of live aspen pixels for the canopy area of a specific aspen stand would allow us to create a vector layer for each stand.

When we attempted to create a vector data set consisting of the class associated polygons from the classified raster data, because the resolution is so fine and neighboring pixels were different; ArcGIS would create thousands of small polygons for the many aspen pixels within the canopy area. Our goal was to create one polygon that included all the aspen from that class. We could have aggregated all the small polygons into one multipart feature, but this would not have accounted for the area amongst the polygons that were misclassified as a class other than aspen. i.e., shadows or shrubs. We also attempted the same processing steps with the NIR histogram equalization imagery and

had improved products, but the result was the same, we could not create a vector layer from the thematic raster. Therefore, we could not assess area data for each stratified layer or conduct other aspen stand statistical analyses from the classifications alone. A resolution would have been to use multispectral data that included RGB and NIR in the same photography. These data would have assisted in differentiating between classes as it would have assigned different values to pixels based on a more refined spectral reflection than the RGB or NIR data by itself. (We solved this problem using KE which is discussed in the following paragraph.) The "checkerboard pattern" classification result was not a detrimental processing result when looked at individually, as the data exemplified details within the aspen stand. The classification result was difficult to utilize in this project because of the method we were applying; which was the comparison of two different types of data collection, the GNSS mapping data, and the UAS based data collection.

A better approach would have been an image change detection method of collecting UAS imagery in 2016 and in 2017, which would have enabled a direct comparison of digital data types. Furthermore, this study exemplifies how the best use of UAS data is to directly compare UAS data sets to one another over specific time periods. We also would have benefited from collecting the data at a lower resolution. If the pixel size of the data was 10 cm for example, the data would have matched more closely with the GNSS data and had less variation in pixel values. For example, at the one cm resolution a pixel value may register a branch on a tree or a small gap between two trees in the canopy, at the 10 cm resolution it is likely the pixel value will be related to the entire tree. Therefore, most images of the canopy would have had pixel values related to the canopy. Furthermore, it would have been more economic to simply measure the stands in 2017 with a handheld GNSS like we did in 2016

The thematic map created from the classification combined with the imagery does give a resource manager a landscape assessment tool for comparing specific areas from before and after disturbance. For example, the proportion of snags in an area that is completely burned (no live canopy is standing and the dead stems remain upright) can be estimated

by pure deduction. Furthermore, when using the elevation data produced from the UAS imagery, many features could be eliminated by height. Rocks and snags may have the same or similar pixel value, but the rocks are below a certain height; therefore, there is a high probability that pixels within the rock/snag value in the canopy are snags and not rocks. An analyst could run a classification targeting snags in the burned aspen by using these parameters. This deduction gives the analyst an estimate of standing dead trees on the landscape after an extreme fire. We did not run a snag classification as most of the stands in the Eskerine Complex did not burn with extreme severity and therefore much of the canopy remained intact. When the majority of the canopy remains post-prescribed burn many of the snags are not visible from the air as the living canopy overtakes them.

3.1.2 Digitized Polygons

An alternative way of creating a raster data set from imagery is to digitize vector data for each landscape feature. We digitized the aspen canopy, regeneration, and shrubs. We used this vector data to compare the area for all 30 aspen stands from before and after the prescribed burn for all layers and found there was no significant difference on any level. Although we had a high accuracy rate, this technique had its limitations. For example, it was difficult to decipher between the canopy and regeneration layers when choosing where to place the line between the taller regenerated stems, and the shorter canopy stems. This area was a dense intermixing of aspen (and occasional shrubs) of various sizes; it was impossible through visual inspection of a raster layer to decipher between aspen that was ~ 2.3 m tall and aspen that was ~ 2.7 m tall. We encountered similar complications while digitizing the regeneration layer. Many of the shrubs in the study site grew to a similar height and had a similar leaf structure and reflectance as regenerated aspen. Several of these species such as snowberry (*Symphoricarpos* spp.) and serviceberry (*Amelanchier alnifolia*) grew among each other on the cusp of the aspen stand/grassland edge, providing a mix of vegetation that was difficult to assess. Although pattern, color, and texture were satisfactory attributes for digitizing the aspen stand layers in most cases, these dynamics did present difficulties, as several vegetation signatures were difficult to place in one category over the other. The difficulties were apparent in

the accuracy assessment as the shrubs had the largest area of commission (0.4219 ha) which means that this committed area did not consist of shrubs but was included in the shrub layer.

The difficulties of classifying vegetation in a complex environment are not new, as analysts have wanted a resource to measure the imprecise nature of the natural landscape for some time (Filippi and Jensen 2006). This classification issue of categorizing the mixture of plants into homogeneous classes was the same issue we had in the supervised and unsupervised classification processes. The fuzzy classification, which is a version of supervised classification with an algorithm that is more acute to the complexity of the natural world (Chen 2005, Filippi and Jensen 2006), may be a way to enhance the classification process. The fuzzy classification is used in image processing when a pixel can be easily placed in more than one category, the process chooses the best fit for the pixel. We attempted a fuzzy classification on the complete mosaic of the imagery, but after spending several days preparing and processing that data, the available hardware did not have the necessary temporary memory capacity (the machine in use had a 2.9 TB memory capacity) to complete the process, and the fuzzy classification was abandoned.

3.1.3 Knowledge Engineer

We stratified the regeneration and canopy layers for the aspen stands of the Eskerine Complex using KE. The process utilized a vegetation height model created from the DEM and the DSM, and aspen pixel values from the unsupervised classification created from the PCA. The height model informs the analyst of the vegetation height of features (including plants) on the landscape. KE enabled us to create a thematic raster of all pixels classified as aspen in the principal components analysis that are ≥ 2.5 m in ht as canopy. The KE allows us to add multiple decisions to the algorithm; we additionally classified all shrubs > 5 m in ht as aspen canopy because we have not identified any shrubs in the study site that reach a height of 5 m. Also, there is very little vegetation in general on the landscape > 5 m in ht that is not aspen. Therefore, there is a high probability that any vegetation that reached a height > 5 m and was not classified as aspen in the principal

components analysis is a misclassification. For the regeneration layer which was processed in KE, we classified aspen as all vegetation that had a ht > 0.20 m and < 2.5 m and was classified as aspen in the supervised classification created from the PCA. The minimum ht of 0.20 m was chosen as a minimum aspen ht to eliminate small variations in the landscape and to minimize misclassified shrubs, 2.5 m is the lower limit of the canopy. Therefore, the regeneration layer does not include the very young stems but does depict variation in the aspen stand edge. We did not run a classification for the shrub layer in the KE due to shrub consistency across the landscape and further complications plus time constraints; shrubs were continuous across the landscape in the unsupervised classification that was based on the PCA. Which means that the consistency of shrubs across the study site made it difficult to separate the shrubs that belonged to one aspen stand from the next.

A direct comparison of the digitized perimeter using the UAS imagery to the KE classification was difficult due to the very different types of data collection. The GNSS data was collected by walking the perimeter of a layer and creating a simple closed polygon of which we calculated the area; these data did not account for gaps or snags in the aspen. The KE classification performed on the UAS imagery accounted for all living aspen of a stand and excluded gaps and visible snags, therefore when same stands were compared for the same year, the UAS derived area calculation generally had a smaller area. An additional reason that needs mentioning is that the GNSS error could have contributed slightly to a slightly smaller stand calculation as the spatial accuracy of the UAS imagery is expected to be better, < 30 cm for the GNSS and ~ 2 cm for the UAS.

The GNSS data gives the user an overall area based on perimeter measurement of which aspen are encompassed on the landscape; this information is useful as a manager will know where the aspen are located and to what extent. For example, if an ecological restoration project is focused on the area that consists of aspen of any age structure or is not concerned about gaps or structural heterogeneity within the stand, an analyst can compare the areas from year to year. The manager would then know where aspen are located and how the area and location (the edge of the stand) of these stands change over

time. The UAS derived data will give the user the depiction of stand dynamics and structure, especially when the surface model and elevation models are included. The thematic raster and resulting class related polygons will allow the manager to assess stand structure and gain information such as the number of gaps and their size. In general, the combination of UAS derived data and geospatial analysis tools such as image enhancements, KE, and GIS allow an analyst to conduct a more complex landscape analysis.

3.1.4 The Future of UAS data Collection

Data collection capabilities of the UAS will increase; batteries will become smaller, lighter, with greater storage capacity, and the aircraft will be able to fly longer as technology improves (Wich and Koh 2018). Improvements in the capabilities of storing and processing big data are improving the time and processing capabilities of UAS based remote sensing projects and reducing the cost. Data capacity of computers and external hard drives were a major limitation for our project but were addressed as the project progressed and may not be an issue for projects with a sufficient budget or access to computing technology. The advent of cloud computing by companies such as IBM https://www.ibm.com/cloud/solutions and Azure Microsoft cloud computing https://azure.microsoft.com/en-ca/ are also possibilities for big data processing and will allow analysts access to higher powered computers to conduct data processing. These inevitabilities will enable data to be obtained that is now generally unavailable with current data collection methods. Improvements made by developers are leading to UAS that are capable of hovering next to a cliff or over a nest in a tree (Chabot and Bird 2015, Weissensteiner et al. 2015), with obstacle avoidance technologies allowing ecologist to capture data that in the past would have been either extremely difficult to obtain or impossible. The developing avoidance detection systems can also be used (Chabot and Bird 2015) for UAS surveys of waterbirds in tight places. These surveys are currently completed by traditional winged aircraft but may be assisted with the use of a UAS; as many of the locations are in hard to reach places making data collection difficult.

3.1.5 Additional Processing Options

The added benefits of UAS based data collection should not be understated. (The post-prescribed burn aspen stands could have been completed via GNSS ground-based mapping and would have required less processing time). The imagery and KE classification provide detail of the stand interior giving researchers a basis for analyzing stand dynamics and spatial heterogeneity in the future. If we had measured the stand with hand-held GNSS post-prescribed burn, we would have had an accurate assessment of stand area, but we would not have the ability to assess gaps, snags or any other attribute we have not thought of at this time. The high-resolution data (1- 2 cm) provides the possibility of in-depth analyses on all levels of the study site. There are techniques we can apply to make the data more useable or to assess specific attributes within the data. We could downgrade the data to a lower spatial resolution through down-sampling which would enable us to process the data more quickly and provide a less complicated classification process for computing and the analyst alike. For example, the heterogeneity of pixels (classes) amongst the canopy would be reduced. We can also use object-based image analysis (OBIA) to analyze specific features within the data such as openings in the aspen stands. OBIA is a process of extracting meaningful information from imagery to group features together. Pixels are grouped into objects based on their similarities such as shape, size perimeter and spectral resolution (Blaschke 2009). A more extensive option would be to perform a topographic normalization, which corrects for radiometric distortion, before the mosaic process. Radiometric distortion is a topographic effect formed by differing illuminations from the angle of the sun and terrain. The effect causes variances in the brightness values of the image. The process normalizes the imagery to make it appear as if it were a flat surface. Another option would have been to collect the data at a lower spatial resolution, although a lower resolution would limit what we could assess form the imagery in the future. The current resolutions of 1 and 2 cm allow flexibility, as it gives us the availability to resample the data and to analyze attributes going forward in detail and on a fine spatial scale.

3.2 Ecological Discussion – Geospatial Assessment of Aspen Habitat within the Eskerine Complex

The intact aspen-parkland of the Eskerine Complex is ecologically important because much of this habitat-type in the Intermountain Canadian Rockies has been impacted by some type of disturbance (Vujnovic et al. 2002). From an observational point of view, much of the landscape adjacent to the park between the mountains and the rangeland to the east is dominated by aspen. The aspen dynamics outside of the park may be an indicator of ecological change within the park if management steps are not taken to prevent further aspen expansion in the Eskerine.

The current ecological restoration plan of prescribed burning and elk browsing has not yet resulted in a significant decrease in the aspen stand area over the short period of this analysis. The overall change in stand area from before to after the 2016 prescribed burn is statistically insignificant and we have not seen a decrease in area of regeneration. The change in aspen stand structure is also statistically insignificant, but there is an observed difference between the area that is canopy and the area that is regeneration. The proportion of the aspen stands that are canopy decreased by 31.34% while the proportion that is regeneration increased by 52.83% (digitized data comparison). The proportion of canopy increased by 0.06% and the regeneration decreased by 0.03% when comparing the KE based classification to the 2016 GNSS derived polygon data, but the UAS based data accounts for gaps inside the aspen stands and the GNSS and heads up digitization data do not. This means that the digitization data provides a better head to head aspen stand area comparison with the 2016 GNSS data. The increase in regeneration proportion compared to the canopy in a stand that has not increased in overall size provides evidence that aspen sprouts have regenerated within the burned canopy. The stand is replacing itself and is regenerating after disturbance (DeByle and Winokur 1985, Bartos et al. 1994, Wan et al. 2014). This change in proportion (although not statistically significant) is a change in stand structure and provides information and further questions for project managers. Will the aspen continue regenerating if repeated burning is sustained over many years? Other research has found that aspen does not respond to continues burning

with consistent, vigorous growth (Keyser et al. 2005). Are the combination of fire and elk browse sufficient ecological forces to return a western fescue grassland to pre-European contact conditions? Is habitat type inertia (aspen forest inertia) capable of fueling further aspen expansion; are bottom-up resources such as nutrients and moisture able to sustain aspen growth and continued expansion?

To determine the next steps in the restoration process, continued monitoring of aspen dynamics post-prescribed burn is important, as peak regeneration response of aspen to fire happens in years two and three post-fire (prescribed burn or wildfire) (Bartos and Meuggler 1981, Keyser et al. 2005). The evidence acquired through this project (insignificant change in stand size) suggests that continued burning plus an additional component may need to be included with elk browse to prevent aspen from continuing their current rate of expansion.

Continual research is of particular concern because per microhistological analysis in our study site; aspen was a negligible component of elk diet. Between January and April in 2017, the proportion of grass in WLNP elk diet ranged between 81.8% and 87.7% (Eisenberg and Hibbs 2018 unpublished data). Elk only consumed aspen in 2 months, February and April, with the highest proportion being 1.4% of their diet (Eisenberg and Hibbs 2018, unpublished data). Grass was by far the preferred food of elk over this period. The grassland ecological restoration plan did not account for the low herbivory of aspen by elk. Reasons for the low herbivory may be due to complex top-down effects that are interacting with bottom-up effects in the ecosystem (Vucetich and Peterson 2004, Eisenberg et al. 2014, Creel and Christianson 2015). Wolves are present in WLNP and may be affecting the way elk behave on the landscape. The prescribed burning created an increased amount of dead and downed wood in the interior of the aspen. This coarse woody debris creates obstacles that are escape impediments for an elk avoiding a wolf. Although aspen is generally an important food source for elk while on their winter range, they may be avoiding the aspen stands as the likelihood of predation is much higher in an area that possesses escape impediments. The result is less browsing of aspen by elk, which is a result that has been observed in other studies which investigate relationships

between aspen, fire, elk and wolves as well (Brown et al. 1999, Kuijper et al. 2013, Eisenberg et al. 2015). In ecosystems where fire is used for ecological restoration and there are no wolves, aspen is browsed to extreme severity and very few aspen recruit into the canopy, which results in a decline of aspen (Bartos and Meuggler 1981, Canon et al. 1987, Baker et al. 1997).

The unforeseen top-down effects may not be the only factor that needs to be considered for its impact on aspen expansion in the Eskerine complex. Aspen can produce secondary metabolites that are sometimes seen post-fire to deter herbivory. These defense-compounds may play an essential role in aspen expansion as the aspen may be less desirable as a result of a high level of metabolites (Erwin et al. 2001, Lindroth and St. Clair 2013). Each aspen clone can produce a different level of defense compounds; therefore there is a possibility that aspen in one area may be more palatable for elk than aspen in another area (Lindroth and St. Clair 2013). The combination of plant metabolites and the wolf effect (ecology of fear) in WLNP illustrates the complexity of top-down and bottom-up interactions. Trophic interaction such as these are challenging to define, let alone conclude which has a more significant influence on the system (Peterson et al. 2014), more than likely a combination of the two factors are impacting aspen expansion.

An apparent third variable for implementing a long-term solution to aspen expansion is the addition of bison. Bison have a relationship with fire. Evidence from studies in the Konza Prairie and Yellowstone National Park have found that bison preferentially graze in burned areas (Knapp et al. 1999). Therefore, when a grassland burns (wildfire or prescribed burn) bison migrate to the burned area to feed on the new growth. If bison return to WLNP post-prescribed burn we would expect aspen regeneration to decline, destruction of adult woody biomass to increase, and a change in the grass and forb composition. The combination of bison and fire may be what the WLNP grassland needs to continue its resilience into the future, as native grassland has a positive response when exposed to fire (Vujnovic et al. 2002).

If the return of bison is not a possibility, continued prescribed burning and monitoring of the Eskerine Complex is a logical choice to restore the fescue grasslands in WLNP. The importance of the fescue grassland is evidence by the elk's preferred food between January and April of 2017, which was rough fescue (*Festuca. campestris)* and encompassed between 21.8% and 28.6% of their diet, (Eisenberg and Hibbs 2018 unpublished data). The combination of aspen expansion, the lack of elk browsing on aspen (due to plant defense compounds or wolves), and food preference of elk extenuate the importance of grassland health in WLNP.

3.2.1 Kenow Wildfire

The consequences of repeated burning and post-prescribed burn monitoring took an unexpected turn. After the post-prescribed burn data was collected on the 2017 prescribed burn, the Kenow wildfire consumed all aspen stands in the Eskerine Complex. Roughly one month after we collected the UAS imagery the entire study area burned in an extreme-severity wildfire that consumed nearly all the vegetation in the study site. Research and management will take a different approach to measure and monitor the effect of fire, as the focus will be turned to assessing the Eskerine Complex after the Kenow wildfire. We may also gain new insight as to how the aspen responds to repeated burning. The data we collected can now be used as a pre-Kenow wildfire baseline for assessing the response of this fire. Our remotely sensed data provide an invaluable tool for examining this landscape before and after prescribed burning and the Kenow wildfire for years to come. The Kenow wildfire is one example of the value of UAS data. Park management and researchers have an opportunity to use these data as a reference for future post-Kenow wildfire studies. This wildfire reinforces that the most valuable part of high spatial resolution UAS imagery is its perpetuity, as the baseline imagery is frozen in time, allowing many possible uses of the data.

3.3 Limitations

It cannot be understated that computing power, data storage, equipment cost, and processing time are the most significant limitations of a UAS project. We attempted

several different types of data processing to analyze the data we collected; in some cases, on a trial and error basis. These processing attempts might have resulted in several more completed GIS products at this time, and in a shorter time-frame, if we had more computing power available to us throughout the processing stages (Computer specifications are located in the data processing methods section). The complications of data processing on this project were a catalyst for the purchase of new "data processing" computers for the remote sensing department in the School of Forest Resources and Environmental Science. The data processing requires several different forms of data to be created before the next step can be completed. Each of these forms needs to be stored until the final mosaic is complete. This process results in the creation of many terabytes of data that cannot be deleted before the conclusion of the project. For example, the Eskerine Complex data consists of two 750 ha images (RGB and NIR), the NIR data set has a resolution of 1 cm, which means that the software processes each cm of the 750-ha data set to complete a classification. The software must process (400 billion (+)) pixels in the NIR imagery 1 cm at a time. In any digital image processing, the computer must analyze and conduct computation using all of these pixel values (digital numbers). Time is always a factor as many of the individual processing segments can take several days to be completed, on a project with 40 - 50 flight blocks the needed time amounts quickly. Also, data processing is occasionally interrupted or has failed. For example, the georeferencing can take three days for the process to complete and the process may not fail until near the end of day three; the unforeseen problem needs to be accounted for and the process restarted. The issues described would be of much less concern for a smaller data set of ~ 10 ha or less, as the processing time required for each session would be much shorter. Therefore, an economic analysis should be conducted prior to using UAS. In some cases, it might be more economically feasible to fly a project using human piloted aircraft with the requisite sensor.

Although as the cost of sensor and software equipment is reduced these difficulties will become less relevant, we must stress the importance of considering the size and cost of the desired study before a UAS remote sensing project is confirmed. Processing time can

add to the overall time requirements committed to the project significantly and become costly as needed storage and computing requirements are added in. Although all these limitations will be less concerning as the related technology cost is reduced, a remote sensing project of a large geographical scale and high spatial resolution is not recommended for researchers who cannot accept these time, cost and data constraints. For example, a project of ~ 25 ha can be completed in a reasonable time frame, most likely within a month of collecting the data.

3.4 From a Management Perspective

The UAS application in natural-resources monitoring has great potential but will benefit from reduced cost and accessible processing software before it is applied on a broad scale; at this time one of the largest detriments is the cost of the equipment. The imagery produced from the tool is an excellent baseline for assessing ecological change over a large area, but managers will need an undetermined amount of time, computing power and a qualified technician or scientist on staff to collect, analyze and manage the data. to assess this data. We have found, in this project, that differentiation of saplings and shrubs is difficult over a large area (> 700 ha). Similarly, it is challenging to differentiate between species of shrubs. This makes it difficult to determine where one cover type or species dominates as opposed to another. Furthermore, it is difficult for a manager to quickly determine, by use of the classification alone, where snags are present in the landscape; as there is a possibility the area classified as snags in the thematic raster are rocks or gravel, and many snags cannot be seen from the air.

Also, the high spatial resolution gave us more detail than what was needed for this project and caused difficulties while processing the data. For the aspen, a 10 – 20 cm resolution would have been adequate. With a high resolution the imagery is providing pixel values of all features on the landscape, including a branch that is part of a canopy tree that can be seen through the canopy, or a small shadow from a tree, branch, or a rock. Our goal was to obtain information as to where the aspen was located, we did not need a pixel value for every small variation on the landscape. This variation is what causes the

complex collection of classified pixels in the thematic raster, which is a representation of all the features on the landscape. If we did not have the fine spatial resolution, the pixel value of the area would be associated with the main features within the larger area (10 – 20 cm). If we surveyed the area with hyperspectral, or multispectral data the pixel values of the higher resolution imagery would be more refined, as the spectral reflectance in the imagery would be based on a broader electromagnetic spectrum than the RGB or NIR alone.

The benefits of a large data set, such as the data collected for this study, is the imagery itself. The imagery, or the classification data, is useful for locating an area of interest a manager wishes to examine in more detail; after the manager records the locations for a target area found in the imagery, researchers may enter the field to investigate the feature and collect the desired data at that location. Also, the UAS is an available tool for on-demand data collection (weather permitting) for hard to reach or hazardous areas, such as a recently burned forest (Anderson and Gaston 2013, Wich and Koh 2018). The UAS as a data collection tool is under development and experimentation for the natural the resources field. However, as managers, technicians, and software developers discover new and creative ways to apply the UAS for monitoring, broad-scale approaches over a large area may become possible.

3.5 Conclusion

The fescue grassland of the Eskerine Complex is currently intact but is a declining ecotype that benefits from ecological restoration and preservation. The comparison of the pre- and post-burn data collected demonstrate that aspen expansion continued to persist in the system and was at best held to a stand-still by the prescribed burn. The complex combination of top-down and bottom-up effects play an integral role in the aspen dynamics as the presence of wolves and plant defense compounds may prevent elk from browsing the aspen. The grassland will benefit from continued burning and a possible addition of bison on the landscape.

The continued use of UAS derived data collection of the Eskerine Complex is recommended as a tool to assess the aspen growth in the future. Continual surveys of the Eskerine will provide WLNP with a direct data type comparison. The 2017 UAS imagery was collected less than two months before the Kenow wildfire. The 2017 data provide an invaluable baseline data set to assess the aspen stand (plus many other vegetation types) response to the Kenow wildfire. The 2017 data also includes gaps in the canopy and openings in the aspen. This data can be directly compared with any future UAS data that is collected.

Although the data processing portion of this project had its challenges and was extensive, we were able to exemplify high-resolution imagery collection in an *on-demand* capacity as the data was collected at peak phenology during satisfactory weather conditions; and through our experimentation, we were able to develop and improve our lab for future work. This tool is not without its limitations, such as data processing time and environmental complications (shadows, oblique photos, and wind). In time, the utilization of the UAS will increase as cost decreases, computing power is more accessible, and data processing time is decreased

The Eskerine Complex project has given us valuable insight into aspen stand dynamics from an observational standpoint (assessment of stand dynamics via the digitized polygons) and given us multiple avenues to add to the overall base of ecological knowledge. The knowledge is added through the data we have processed and any future development from the imagery, as the data encompasses the entire Eskerine study area and lasts into perpetuity. The pre-Kenow wildfire KE classification could be a valuable tool for comparing aspen stand structure from before to after the wildfire and assess how repeated burning impacts the regeneration and recruitment of the aspen in this complex system.

Works Cited

Anderson, K., and K. J. Gaston. 2013. Lightweight unmanned aerial vehicles will revolutionize spatial ecology. Frontiers in Ecology and the Environment 11:138–146.

Baker, W. L. 2009. Fire Ecology in Rocky Mountain Landscapes. Island Press, Washington, D.C:

Baker, W. L., J. A. Munroe, and A. E. Hessl. 1997. The Effects of Elk on Aspen in the Winter Range in Rocky Mountain National Park 20:155–165.

Barrett, S. W. 1996. The historic role of fire in Waterton Lakes National Park, Alberta. Waterton Lakes National Park.

Bartos, D. L., J. K. Brown, G. D. Booth, D. L. Bartos, J. K. Brown, and G. D. Booth. 1994. Twelve Years Biomass Response in Aspen Communities following Fire. Society for Range Management 47:79–83.

Bartos, D. L., and W. F. Meuggler. 1981. Early succession in aspen communities following fire in western Wyoming. The Journal of Range Management 34:315-318 ST-Early succession in aspen communitie.

Blaschke, T. 2009. Object based image analysis for remote sensing. ISPRS Journal of Photogrammetry and Remote Sensing 65:2–16.

Brown, J. S., J. W. Laundre, and M. Gurung. 1999. The Ecology of Fear: Optimal Foraging, Game Theory, and Trophic Interactions. Journal of Mammalogy 80:385–399.

Brown, K., A. J. Hansen, R. E. Keane, and L. J. Graumlich. 2006. Complex interactions shaping aspen dynamics in the Greater Yellowstone Ecosystem. Landscape Ecology 21:933–951.

Campbell, C., I. Campbell, and C. Blyth. 1994. Bison Extirpation May Have Caused Aspen Expansion in Western Canada. Ecography 19:360–362.

Canon, A. S. K., P. J. Urness, and N. V Debyle. 1987. Habitat Selection, Foraging Behavior, and Dietary Nutrition of Elk in Burned Aspen Forest Published by : Society for Range Management Linked references are available on JSTOR for this article : Habitat Selection , Foraging B. Journal of Range Management 40:433–438.

Chabot, D., and D. M. Bird. 2015. Wildlife research and management methods in the 21st century: Where do unmanned aircraft fit in? Journal of Unmanned Vehicle Systems 3:137–155.

Chang, K.-T. 2006. Introduction to Geographic Information Systems. Page Introduction to Geographic Information Systems.

Chen, N. 2005. Fuzzy Classification Using Self-Organizing Map and Learning Vector Quantization. Pages 41–50 Data Mining and Knowledge Management. First edition. Springer, Berlin.

Creel, S., and D. Christianson. 2015. Wolf Presence and Increased Willow Consumption by Yellowstone Elk : Implications for Trophic Cascades Published by : Ecological Society of America Wolf presence and increased willow consumption Yellowstone by for trophic cascades implications elk : Ecology 90:2454–2466.

Creel, S., and J. A. Winnie. 2005. Responses of elk herd size to fine-scale spatial and temporal variation in the risk of predation by wolves. Animal Behaviour 69:1181–1189.

Cruzan, M. B., B. G. Weinstein, M. R. Grasty, B. F. Kohrn, E. C. Hendrickson, T. M. Arredondo, and P. G. Thompson. 2016. Small Unmanned Aerial Vehicles (Micro-Uavs, Drones) in Plant Ecology. Applications in Plant Sciences 4:1–11.

DeByle, N. V., and R. P. Winokur. 1985. Aspen: Ecology and Managment in the Western United States. Fort Collins, Colorado.

Eisenberg, C., A. Anderson, Christopher L. Collingwood, R. Sissons, C. J. Dunn, G. W. Meigs, D. E. Hibbs, S. Murphy, S. D. Kuipe, J. SpearChief-Morris, L. Little Bear, B. Johnston, and C. B. Edson. 2019. Effects of Extreme Wildfire, Prescribed Burns, and Indigenous Burning on Ecosystems. Page Frontiers in Ecology and the Environment.

Eisenberg, C., and D. E. Hibbs. 2018. Elk , Fire and Wolf Ecology in Aspen and Grassland Communities in Waterton Lakes National Park of Canada Prepared by : Investigators' Annual Progress Report 2018.

Eisenberg, C., D. E. Hibbs, and C. B. Edson. 2017. Elk, Fire and Wolf Ecology in Aspen and Grassland Communities in Waterton Lakes National Park of Canada.

Eisenberg, C., D. E. Hibbs, and W. J. Ripple. 2015. Effects of predation risk on elk (*Cervus elaphus*) landscape use in a wolf (*Canis lupus*) dominated system. Canadian Journal of Zoology 93:99–111.

Eisenberg, C., D. E. Hibbs, W. J. Ripple, and H. Salwasser. 2014. Context dependence of elk (*Cervus elaphus*) vigilance and wolf (*Canis lupus*) predation risk. Canadian Journal of Zoology 92:727–736.

Eisenberg, C., S. T. Seager, and D. E. Hibbs. 2013. Wolf, elk, and aspen food web relationships: Context and complexity. Forest Ecology and Management 299:70–80.

Erwin, E. A., Monica G. Turner, R. L. Lindroth, and W. H. Romme. 2001. Secondary Plant Compounds in Seedling and Mature Aspen (Populus Tremuloides) in Yellowstone National Park, Wyoming. The American Midland Naturalist 145:229–308.

Estes, J. A., J. Terborgh, J. S. Brashares, M. E. Power, J. Berger, W. J. Bond, S. R. Carpenter, T. E. Essington, R. D. Holt, J. B. C. Jackson, R. J. Marquis, L. Oksanen, T. Oksanen, R. T. Paine, E. K. Pikitch, W. J. Ripple, S. A. Sandin, M. Scheffer, T. W. Schoener, J. B. Shurin, A. R. E. Sinclair, M. E. Soulé, R. Virtanen, and D. A. Wardle. 2011. Trophic downgrading of planet earth. Science 333:301–306.

Filippi, A. M., and J. R. Jensen. 2006. Fuzzy learning vector quantization for hyperspectral coastal vegetation classification. Remote Sensing of Environment 100:512–530.

Flores, D. 1991. Bison Ecology and Bison Diplomacy: The Southern Plains from 1800 to 1850. The Journal of American History 78:465.

Frey, B. R., V. J. Lieffers, S. M. Landhäusser, P. G. Comeau, and K. J. Greenway. 2003. An analysis of sucker regeneration of trembling aspen. Canadian Journal of Forest Research 33:1169–1179.

Getzin, S., K. Wiegand, and I. Schöning. 2012. Assessing biodiversity in forests using very high-resolution images and unmanned aerial vehicles. Methods in Ecology and Evolution 3:397–404.

Gini, R., D. Passoni, L. Pinto, and G. Sona. 2014. Use of unmanned aerial systems for multispectral survey and tree classification: A test in a park area of northern Italy. European Journal of Remote Sensing 47:251–269.

Hobbs, T. N., D. L. Baker, J. E. Ellis, and Da. M. Swift. 1981. Composition and Quality of Elk Winter Diets in Colorado. The Journal of Wildlife Management 45:156–171.

Hogg, E. H. (Ted), J. P. Brandt, and M. Michaelian. 2008. Impacts of a regional drought on the productivity, dieback, and biomass of western Canadian aspen forests. Canadian Journal of Forest Research 38:1373–1384.

Hollenbeck, J. P., and W. J. Ripple. 2007. Aspen patch and migratory bird relationships in the northern Yellowstone ecosystem. Landscape Ecology 22:1411–1425.

Johnson, B. 2018. Butterfly. Waterton Lakes National Park.

Jones, M. B., and A. Donnelly. 2004. Carbon sequestration in temperate grassland ecosystems and the influence of management, climate and elevated CO2. New Phytologist 164:423–439.

Kashian, D. M., W. H. Romme, and C. M. Regan. 2007. Reconciling Divergent Interpretations of Quaking Aspen Decline on the Northern Colorado Front Range. Ecological Applications 17:1296–1311.

Kerr, J. T., and M. Ostrovsky. 2003. From space to species: Ecological applications for remote sensing. Trends in Ecology and Evolution 18:299–305.

Keyser, T. L., F. W. Smith, and W. D. Shepperd. 2005. Trembling aspen response to a mixed-severity wildfire in the Black Hills, South Dakota, USA. Canadian Journal of Forest Research 35:2679–2684.

Knapp, A. K., M. John, L. Scott, L. C. Johnson, E. G. Towne, D. C. Hartnett, A. K. Knapp, J. M. Blair, M. John, S. L. Collins, and D. C. Hartnett. 1999. North Keystone Role of Bison in American Tallgrass Prairie Bison increase habitat heterogeneity and alter a broad array of and ecosystem processes. BioScience 49:39–50.

Koh, L. P., and S. A. Wich. 2012. Dawn of drone ecology: Low-cost autonomous aerial vehicles for conservation. Tropical Conservation Science 5:121–132.

Kuijper, D. P. J., C. de Kleine, M. Churski, P. van Hooft, J. Bubnicki, and B. Jedrzejewska. 2013. Landscape of fear in Europe: Wolves affect spatial patterns of ungulate browsing in Bialowieża Primeval Forest, Poland. Ecography 36:1263–1275.

Laliberte, A. S., M. A. Goforth, C. M. Steele, and A. Rango. 2011. Multispectral remote sensing from unmanned aircraft: Image processing workflows and applications for rangeland environments. Remote Sensing 3:2529–2551.

Laundré, J. W., L. Hernández, and K. B. Altendorf. 2001. Wolves, elk, and bison: reestablishing the “landscape of fear” in Yellowstone National Park, U.S.A. Canadian Journal of Zoology 79:1401–1409.

Lee, P. 1998. Dynamics of snags in aspen-dominated midboreal forests. Forest Ecology and Management 105:263–272.

Levesque, L. M. 2005. Investigating Landscape Change and Ecological Restoration: University of Victoria.

Lillesand, T. M., R. W. Kiefer, and J. W. Chipman. 2015. Remote sensing and image interpretation -- 7th ed. Page John Wiley and Sons, Inc., New York. Seventh. John Wiley & Sons, Hoboken, NJ.

Lindroth, R. L., and S. B. St. Clair. 2013. Forest Ecology and Managemen t Adaptations of quaking aspen (Populus tremuloides Michx .) for defense against herbivores. Forest Ecology and Management 299:14–21.

Livingstone, S. J., R. D. Storrar, J. K. Hillier, C. R. Stokes, C. D. Clark, and L. Tarasov. 2015. An ice-sheet scale comparison of eskers with modelled subglacial drainage routes. Geomorphology 246:104–112.

Martin, D. M. 2017. Ecological restoration should be redefined for the twenty-first century 25:668–673.

Michez, A., H. Piégay, L. Jonathan, H. Claessens, and P. Lejeune. 2016a. Mapping of riparian invasive species with supervised classification of Unmanned Aerial System (UAS) imagery. International Journal of Applied Earth Observation and Geoinformation 44:88–94.

Michez, A., H. Piégay, J. Lisein, H. Claessens, and P. Lejeune. 2016b. Classification of riparian forest species and health condition using multi-temporal and hyperspatial imagery from unmanned aerial system. Environmental Monitoring and Assessment 188:1–19.

Oumer, A. S., A. Shemrock, D. Chabot, C. Dillon, G. Williams, R. Wasson, and S. E. Franklin. 2017. Hierarchical land cover and vegetation classification using multispectral data acquired from an unmanned aerial vehicle. International Journal of Remote Sensing 38:2037–2052.

Paine, R. T. 1980. Food Webs: Linkage, Interaction Strength and Community Infrastructure. The Journal of Animal Ecology 49:666–685.

Pedynowski, D. 2003. Prospects for Ecosystem Management in the Crown of the Continent Ecosystem, Canada-United States: Survey and Recommendations. Conservation Biology 17:1261–1269.

Perala, D. A. 1980. Quaking aspen series. Page North Central Forest Ex- periment Station. St. Paul Minnesota.

Peterson, R. O., J. A. Vucetich, J. M. Bump, and D. W. Smith. 2014. Trophic Cascades in a Multicausal World: Isle Royale and Yellowstone. Annual Review of Ecology, Evolution, and Systematics 45:325–345.

Pope, I., D. Bowen, J. Harbor, G. Shao, L. Zanotti, and G. Burniske. 2015. Deforestation of montane cloud forest in the Central Highlands of Guatemala: Contributing factors and implications for sustainability in Q'eqchi' communities. International Journal of Sustainable Development and World Ecology 22:201–212.

Romme, W. H., M. S. Boyce, R. Gresswell, E. H. Merrill, G. W. Minshall, C. Whitlock, and M. G. Turner. 2011. Twenty Years After the 1988 Yellowstone Fires: Lessons About Disturbance and Ecosystems. Ecosystems 14:1196–1215.

Romme, W. H., L. Floyd-Hanna, D. D. Hanna, and E. Bartlett. 2001. Aspen 's Ecological

Role in the West. Pages 243–260 Sustaining Aspen In Wstern Landscapes. U.S. Department of Agriculture, Rocky Mountain Research station, Fort Collins, Colorado.

Roos, C. I., M. N. Zedeño, K. L. Hollenback, and M. M. H. Erlick. 2018. Indigenous impacts on North American Great Plains fire regimes of the past millennium. Proceedings of the National Academy of Sciences 115:8143–8148.

Samson, F., and F. Knopf. 1994. Prairie Conservation in North America. American Institute of Biological Sciences 44:418–421.

Schiffman, R. 2014. Wildlife conservation: Drones flying high as new tool for field biologists. Science 344:459.

Seager, S. T., C. Eisenberg, and S. B. St. Clair. 2013. Patterns and consequences of ungulate herbivory on aspen in western North America. Forest Ecology and Management 299:81–90.

Shepperd, W. D. 2001. Manipulations to Regenerate Aspen Ecosystems. Page Sustaining Aspen in Western Landscapes. Technical Report RMRS-P-18.2001. Fort Collins, Colorado.

Simonson, J. T., and E. A. Johnson. 2005. Development of the cultural landscape in the forest-grassland transition in southern Alberta controlled by topographic variables. Journal of Vegetation Science 16:523–532.

Singer, F. J. 1979. Habitat Partitioning and Wildfire Relationships of Cervids in Glacier National Park , Montana. Journal of Wildlife Managment 43:437–444.

Skovlin, J. M., P. Zager, B. K. Johnson, D. E. Toweill, and J. W. Thomas. 2002. North American elk: Ecology and Management. Smithsonian Institute Press, Washington D.C.

Spence, C., and S. Mengistu. 2016. Deployment of an unmanned aerial system to assist in mapping an intermittent stream. Hydrological Processes 30:493–500.

Tang, L., and G. Shao. 2015. Drone remote sensing for forestry research and practices. Journal of Forestry Research 26:791–797.

Tang, L., G. Shao, Z. Piao, L. Dai, M. A. Jenkins, S. Wang, G. Wu, J. Wu, and J. Zhao. 2010. Forest degradation deepens around and within protected areas in East Asia. Biological Conservation 143:1295–1298.

Thompson, I. D., S. C. Maher, D. P. Rouillard, J. M. Fryxell, and J. A. Baker. 2007. Accuracy of forest inventory mapping: Some implications for boreal forest management. Forest Ecology and Management 252:208–221.

Turner, M. G., R. A. Reed, W. H. Romme, G. A. Tuskan, and O. A. K. R. Tn. 1998. Distribution, Morphology, Survival, and Genetics of Aspen (Populus tremuloides) Seedlings Following the 1988 Yellowstone Fires. University Of Wyoming.

Vucetich, J. A., and R. O. Peterson. 2004. The influence of top-down , bottom-up and abiotic factors on the moose (Alces alces) population of Isle Royale 271:183–189.

Vujnovic, K., R. W. Wein, and M. R. . Dale. 2002. Predicting plant species diversity in response to disturbance magnitude in grassland remnants of central Alberta. Canadian Journal of Botany 80:504–511.

Wan, H. Y., A. C. Olson, K. D. Muncey, and S. B. St. Clair. 2014. Legacy effects of fire size and severity on forest regeneration, recruitment, and wildlife activity in aspen forests. Forest Ecology and Management 329:59–68.

Weissensteiner, M. H., J. W. Poelstra, and J. B. W. Wolf. 2015. Low-budget ready-to-fly unmanned aerial vehicles: An effective tool for evaluating the nesting status of canopy-breeding bird species. Journal of Avian Biology 46.

White, C. A., M. C. Feller, and S. Bayley. 2003. Predation risk and the functional response of elk-aspen herbivory. Forest Ecology and Management 181:77–97.

Whitehead, K., and C. H. Hugenholtz. 2014. Remote sensing of the environment with small unmanned aircraft systems (UASs), part 1: a review of progress and challenges. Journal of Unmanned Vehicle Systems 02:69–85.

Wich, S., and L. P. Koh. 2018. Conservation drones; Mapping and Monitoring Biodiversity. First edition. Oxford University Press, Oxford, United Kingdom.

Wulder, M. A., C. C. Dymond, J. C. White, D. G. Leckie, and A. L. Carroll. 2006. Surveying mountain pine beetle damage of forests: A review of remote sensing opportunities. Forest Ecology and Management 221:27–41.

www.Trimble.com. 2017. Trimble Business Center Office Software.

Zhang, J., J. Hu, J. Lian, Z. Fan, X. Ouyang, and W. Ye. 2016. Seeing the forest from drones: Testing the potential of lightweight drones as a tool for long-term forest monitoring. Biological Conservation 198:60–69.